RADC-TR-87-3
Final Technical Report
July 1987

SIGNAL-FILTER DESIGN AND SYSTEM PERFORMANCE FOR POLARIMETRIC RADAR

ORINCON Corporation

Richard A. Altes, Stephen F. Connelly, James R. Miller,
Kishan G. Mehrotra and H. Liu

ROME AIR DEVELOPMENT CENTER
Air Force Systems Command
Griffiss Air Force Base, NY 13441-5700

This report has been reviewed by the RADC Public Affairs Office (PA) and is releasable to the National Technical Information Service (NTIS). At NTIS it will be releasable to the general public, including foreign nations.

RADC-TR-87-3 has been reviewed and is approved for publication.

APPROVED: Vincent C. Vannicola

VINCENT C. VANNICOLA
Project Engineer

APPROVED: Frank J. Rehm

FRANK J. REHM
Technical Director
Directorate of Surveillance

FOR THE COMMANDER: John A. Ritz

JOHN A. RITZ
Directorate of Plans & Programs

If your address has changed or if you wish to be removed from the RADC mailing list, or if the addressee is no longer employed by your organization, please notify RADC (OCTS) Griffiss AFB NY 13441-5700. This will assist us in maintaining a current mailing list.

Do not return copies of this report unless contractual obligations or notices on a specific document requires that it be returned.

UNCLASSIFIED
SECURITY CLASSIFICATION OF THIS PAGE

AD-A189 257

REPORT DOCUMENTATION PAGE

Form Approved OMB No. 0704-0188

1a. REPORT SECURITY CLASSIFICATION UNCLASSIFIED	1b. RESTRICTIVE MARKINGS N/A
2a. SECURITY CLASSIFICATION AUTHORITY N/A	3. DISTRIBUTION/AVAILABILITY OF REPORT Approved for public release; distribution unlimited
2b. DECLASSIFICATION/DOWNGRADING SCHEDULE N/A	
4. PERFORMING ORGANIZATION REPORT NUMBER(S) OCR-84 184041-A002	5. MONITORING ORGANIZATION REPORT NUMBER(S) RADC-TR-87-3
6a. NAME OF PERFORMING ORGANIZATION ORINCON Corporation 6b. OFFICE SYMBOL (If applicable)	7a. NAME OF MONITORING ORGANIZATION Rome Air Development Center (OCTS)
6c. ADDRESS (City, State, and ZIP Code) 3366 No. Torrey Pines Court Suite 320 LaJolla CA 92037	7b. ADDRESS (City, State, and ZIP Code) Griffiss AFB NY 13441-5700
8a. NAME OF FUNDING/SPONSORING ORGANIZATION Rome Air Development Center 8b. OFFICE SYMBOL (If applicable) OCTS	9. PROCUREMENT INSTRUMENT IDENTIFICATION NUMBER F30602-84-C-0017
8c. ADDRESS (City, State, and ZIP Code) Griffiss AFB NY 13441-5700	10. SOURCE OF FUNDING NUMBERS PROGRAM ELEMENT NO. 62702F; PROJECT NO. 4506; TASK NO. 11; WORK UNIT ACCESSION NO. 81

11. TITLE (Include Security Classification)
SIGNAL-FILTER DESIGN AND SYSTEM PERFORMANCE FOR POLARIMETRIC RADAR

12. PERSONAL AUTHOR(S)
Richard A. Altes, Stephen F. Connelly, James R. Miller, Kishan G. Mehrotra*, H. Liu*

13a. TYPE OF REPORT	13b. TIME COVERED	14. DATE OF REPORT (Year, Month, Day)	15. PAGE COUNT
Final	FROM Feb 84 TO Feb 86	July 1987	140

16. SUPPLEMENTARY NOTATION
Kishan G. Mehrotra and H. Liu are from Syracuse University

17. COSATI CODES			18. SUBJECT TERMS (Continue on reverse if necessary and identify by block number)
FIELD	GROUP	SUB-GROUP	
14	01, 06		Radar Antennas Polarization
23	01		

19. ABSTRACT (Continue on reverse if necessary and identify by block number)

Relatively simple expressions for the polarimetric scattering function of randomly oriented dipoles have yielded expressions for SIR in some simple but important cases, and these expressions have been analyzed in order to interpret the computational results. Some important insights have been obtained from the SIR expression for distributed planar targets and randomly oriented dipole clutter, i.e., for the typical "target in chaff" problem. These insights have resulted in the design of a new polarimetric clutter canceller which theoretically allows a polarimetric radar to "see" through chaff.

Signal-to-interference ratio (SIR) maximization has been used to obtain an optimum signal-filter pair for a polarimetric radar when targets and/or clutter exhibit random polarization modulation. The results can easily be extended to include the design of a likelihood ratio receiver for the same problem. Considerable insight into the theoretical solutions has been obtained by implementation and test of a computer program to yield the maximum SIR and Bayesian systems, i.e., the "best" signal and receiver configurations in each case.

20. DISTRIBUTION/AVAILABILITY OF ABSTRACT	21. ABSTRACT SECURITY CLASSIFICATION
☒ UNCLASSIFIED/UNLIMITED ☐ SAME AS RPT ☐ OTIC USERS	UNCLASSIFIED
22a NAME OF RESPONSIBLE INDIVIDUAL Vincent C. Vannicola	22b TELEPHONE (Include Area Code) (315) 330-4437 22c OFFICE SYMBOL RADC (OCTS)

DD Form 1473, JUN 86 — Previous editions are obsolete. — SECURITY CLASSIFICATION OF THIS PAGE

UNCLASSIFIED

TABLE OF CONTENTS

TABLE OF CONTENTS (Cont.)

LIST OF FIGURES

LIST OF TABLES

1.0 INTRODUCTION

1.1 Background

Extended, randomly time varying radar targets, clutter, and communication channels have been considered in the past [1-4]. An important additional variable for such problems is considered here, namely, random polarization modulation [5]. Sea echo, for example, exhibits random, Doppler-dependent polarization effects [6].

The design of radar or communications systems for randomly time varying targets or channels has typically been accomplished by using one of two approaches: (i) a likelihood ratio test [4] or (ii) implementation of a receiver with maximum signal-to-interference ratio (SIR) [7-11]. Both of these approaches often use a scattering function description of the target, clutter, and channel.

SIR maximization is typically more straightforward, does not depend on a Guassianity assumption, and gives usable results. Maximization of SIR, however, does not necessarily result in an optimum receiver, i.e., an implementation of a likelihood ratio test. For the special case of a known signal in colored noise, both SIR maximization and a likelihood ratio test yield the same result (a whiten and match filter), but this correspondence does not always hold.

For Gaussian data, a likelihood ratio test for random, extended targets can be implemented if the scattering functions of target and clutter are known, since the covariance functions of the echoes are then also known [12,13]. There are, however, no straightforward signal design techniques associated with the likelihood ratio test, and it is difficult to define such a test in the polarimetric case [5].

The SIR maximization technique would be especially attractive if: (i) it could be modified in such a way as to implement a Bayes optimum (likelihood ratio) receiver, (ii) the performance of such a receiver could be predicted, and (iii) SIR maximization could be applied to the design of polarization-sensitive radar and communication systems. This report shows that all three goals are attainable, and gives specific examples.

The basic problem is illustrated in Figure 1-1, along with some of the notation used in the sequel. The problem is to obtain a suitable representation of doubly spread target and clutter (a polarimetric scattering function), and to use this representation to obtain optimum vertically and horizontally polarized signal and filter functions $u_1(t)$, $u_2(t)$, $f_1(t)$ and $f_2(t)$. It is also desirable to generalize the receiver in Figure 1-1 to implement a likelihood ratio test and to predict the performance of such a test.

1.2 Overview

Section 2 analyzes the relation between maximization of signal-to-interference ratio and a likelihood ratio test for discrimination of zero mean random signals in two channels. Section 3 establishes the dependence of SIR on polarimetric scattering functions. The connection between scattering functions and a tapped delay line scattering model with randomly time varying tap weights is also given in Section 3. The tap weights describe energy coupling from one polarization channel to another. Section 4 introduces physical insight and specific mathematical models into the polarimetric scattering function formulation by considering planar point targets and randomly tilted dipoles with a restricted maximum tilt relative to vertical. Section 5 gives some mathematical details necessary for implementation of a computer program for polarimetric SIR optimization. Sections 5.3 and 5.4 can be skipped if the reader is not interested in such details. Sections 6 and 7 describe the application of the computer

program to some specific examples. Analysis of the SIR expression for detecting a distribution of planar reflectors in a background of randomly oriented dipoles (distributed planar target in chaff) yields a new polarimetric chaff cancellation method. This method is obtained in Section 7.6. A disparity between the SIR maximization criterion and the power of a likelihood ratio test appears in the context of a receiver with multiple orthogonal filters, which converts the maximum SIR processor to a Bayes optimum processor. This disparity between SIR and power measures is analyzed in Section 7.7. A review of the results is given in Section 8.0.

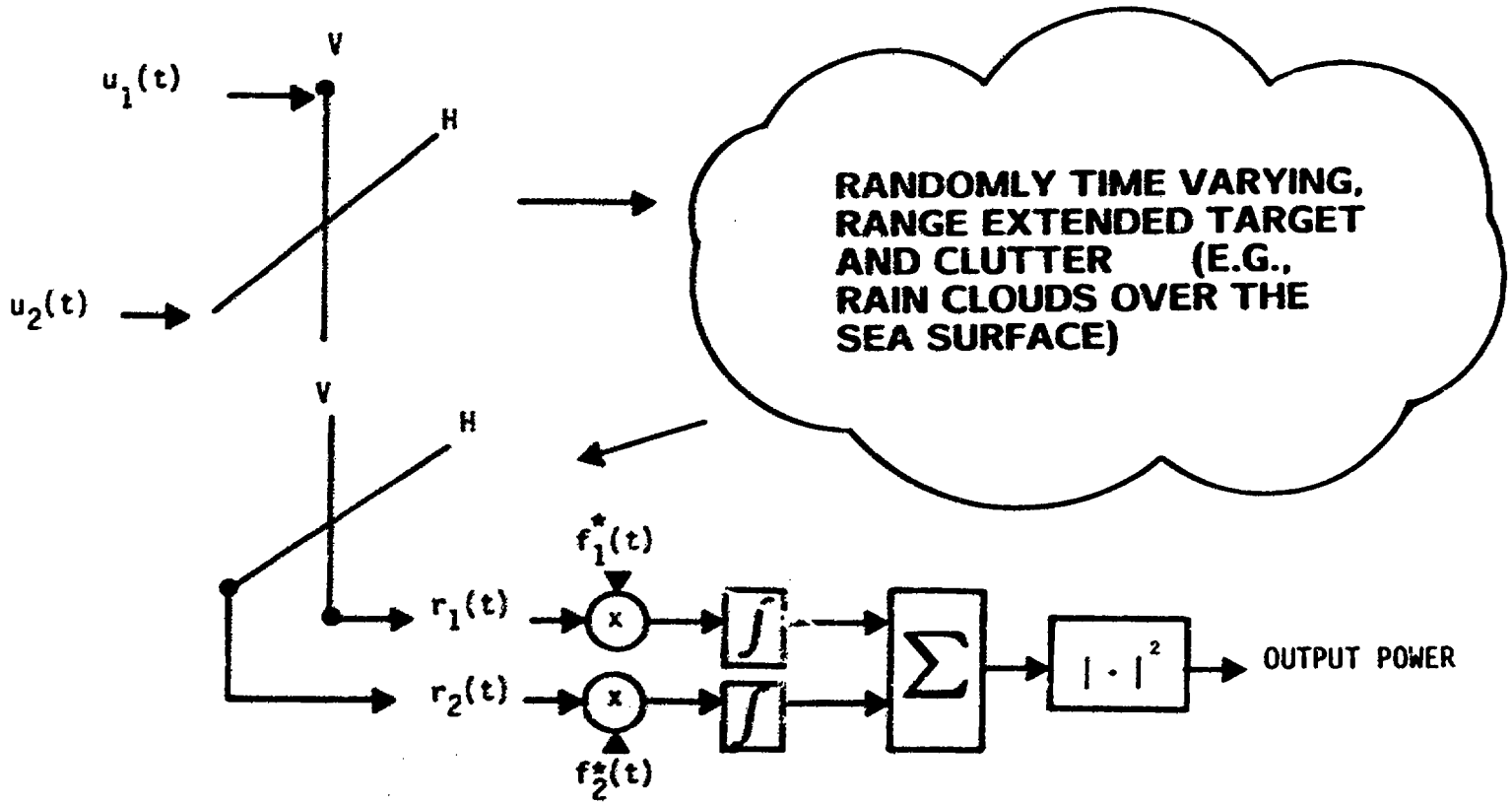

Figure 1-1. Polarimetric Radar Configuration

2.0 SIR MAXIMIZATION AND OPTIMUM HYPOTHESIS TESTS

The following analysis demonstrates that orthogonal filters which maximize SIR can also be used for simultaneous diagonalization of both signal and interference covariance matrices. The filter responses are independent random variables under either hypothesis, and the log likelihood statistic is easily obtained. Receiver performance is also easily obtained in closed form. These results are important because SIR maximization yields a "best" signal as well as an appropriate set of orthogonal filters. A direct likelihood ratio approach is based on echo covariance matrices which can only be evaluated after the signal has been specified.

2.1 Signal-to-Interference Ratio (SIR) Maximization and an Eigenfunction Equation

The signal to interference ratio is

$$SIR = \frac{E\left\{\left|\int_{-\infty}^{\infty} \underline{r}^*(x)\ \underline{f}(x)\ dx\right|^2 \middle| \text{signal}\right\}}{E\left\{\left|\int_{-\infty}^{\infty} \underline{r}^*(x)\ \underline{f}(x)\ dx\right|^2 \middle| \text{interference}\right\}} \tag{2-1}$$

where $\underline{r}^*(x)$ is the conjugate-transpose of the 2 × 1 data column vector. This data vector is composed of a vertically polarized component, $r_1(x)$, and a horizontally polarized component, $r_2(x)$. Thus

$$\underline{r}^*(x) = [r_1^*(x) \quad r_2^*(x)]$$

where $r_1^*(x)$ is the conjugate of the complex scalar time function $r_1(x)$. Similarly, $\underline{f}(x)$ represents a 2 × 1 column vector representing the time function $f_1(x)$ that is to be correlated with the vertically polarized data, and another function $f_2(x)$ that is to be correlated with horizontally polarized data. These functions are illustrated in Figure 1-1.

Using the identity

$$E\left\{ \left| \int_{-\infty}^{\infty} \underline{r}^*(x)\ \underline{f}(x)\ dx \right|^2 \right\}$$

$$= \int_{-\infty}^{\infty}\int_{-\infty}^{\infty} \underline{f}^*(x)\ E\{\underline{r}(x)\ \underline{r}^*(y)\}\ \underline{f}(y)\ dxdy$$

$$= \int_{-\infty}^{\infty}\int_{-\infty}^{\infty} \underline{f}^*(x)\ \underline{\underline{C}}(x,y)\ \underline{f}(y)\ dxdy \qquad (2\text{-}2)$$

we have

$$SIR = \frac{\int_{-\infty}^{\infty}\int_{-\infty}^{\infty} \underline{f}^*(x)\ \underline{\underline{C}}_S(x,y)\ \underline{f}(y)\ dydx}{\int_{-\infty}^{\infty}\int_{-\infty}^{\infty} \underline{f}^*(x)\ \underline{\underline{C}}_I(x,y)\ \underline{f}(y)\ dydx} \qquad (2\text{-}3)$$

where $\underline{\underline{C}}_S(x,y)$ is the signal covariance matrix. The interference covariance matrix is

$$\underline{\underline{C}}_I(x,y) = \underline{\underline{C}}_C(x,y) + (N_0/2)\ \underline{\underline{I}}\ \delta(x-y) \qquad (2\text{-}4)$$

where $\underline{\underline{C}}_C$ is the 2×2 clutter covariance matrix and $N_0/2$ is the noise power spectral density.

To maximize SIR, one can maximize the numerator of (2-3) with a constraint on the denominator. If the denominator is constrained to equal one, an equivalent problem to maximizing (2-3) is to maximize the functional

$$\begin{aligned} Q(\underline{f}) &= \iint \underline{f}^*(x)\ \underline{\underline{C}}_S\ (x,y)\ \underline{f}(y)\ dydx \\ &\quad - \lambda_D \left[\iint \underline{f}^*(x)\ \underline{\underline{C}}_I\ (x,y)\ \underline{f}(y)\ dydx \right] \\ &= \iint \underline{f}^*(x) \left[\underline{\underline{C}}_S(x,y) - \lambda_D\ \underline{\underline{C}}_I\ (x,y) \right] \underline{f}(y)\ dydx \end{aligned} \tag{2-5}$$

where unlabelled integration limits are $(-\infty, \infty)$ and λ_D is any positive constant. Another constraint is to make the filter energy equal to unity, i.e.,

$$\mathrm{Egy}(\underline{f}) = \int \underline{f}^*(x)\ \underline{f}(x)\ dx = 1 \quad . \tag{2-6}$$

The energy constraint is not included explicitly in (2-3) because SIR is invariant when $\underline{f}(x)$ is multiplied by a nonzero scalar constant. Such a constraint, however, can easily be incorporated in a computer optimization algorithm. If $\mathrm{Egy}(\underline{f})$ is specified as in (2-6), then the problem is to maximize

$$\int \underline{f}^*(x)\ \underline{g}(x)\ dx \tag{2-7}$$

when (2-6) holds and when

$$\underline{g}(x) = \int \left[\underline{\underline{C}}_S(x,y) - \lambda_D \underline{\underline{C}}_I(x,y) \right] \underline{f}(y)\, dy \quad . \tag{2-8}$$

By the Schwarz inequality, (2-7) is maximized when $\underline{f}(x)$ is square-integrable as in (2-6) and when

$$\underline{g}(x) = k\, \underline{f}(x) \quad , \tag{2-9}$$

i.e., when $\underline{g}(x)$ is proportional to $\underline{f}(x)$. Substituting (2-8) into (2-9), we have

$$\int \left[\underline{\underline{C}}_S(x,y) - \lambda_D C_I(x,y) \right] f(y)\, dy = k\, \underline{f}(x) \quad . \tag{2-10}$$

Equation (2-10) will be satisfied if $\underline{f}(y)$ is an eigenfunction of both $\underline{\underline{C}}_S(x,y)$ and $\underline{\underline{C}}_I(x,y)$, i.e., if

$$\int \underline{\underline{C}}_S(x,y)\, \underline{f}(y)\, dy = \lambda_S\, \underline{f}(x) \tag{2-11}$$

and

$$\int \underline{\underline{C}}_I(x,y)\, \underline{f}(y)\, dy = \lambda_I\, \underline{f}(x) \quad . \tag{2-12}$$

A more general solution of (2-10) can be obtained if

$$\int \underline{\underline{C}}_S(x,y)\, \underline{f}(y)\, dy = \lambda_S\, \underline{f}(x) + \underline{b}(x) \tag{2-13}$$

and

$$\int \underline{\underline{C}}_I(x,y)\, \underline{f}(y)\, dy = \lambda_I\, \underline{f}(x) + \underline{d}(x) \tag{2-14}$$

where $\underline{b}(x)$ and $\underline{d}(x)$ are such that $\underline{b}(x) - \lambda_D \underline{d}(x)$ is zero for any positive constant, λ_D. But $\underline{b}(x)$ equals $\lambda_D \underline{d}(x)$ for any λ_D only if $\underline{b}(x) = \underline{d}(x) = 0$, and we are back to (2-11) and (2-12).

Combining (2-11) and (2-12) yields

$$\int \underline{\underline{C}}_S(x,y)\ \underline{f}(y)\ dy = (\lambda_S/\lambda_I) \int \underline{\underline{C}}_I(x,y)\ \underline{f}(y)\ dy \quad . \tag{2-15}$$

To obtain further insight into (2-15), we can define an inverse kernel as follows. If $\underline{\underline{C}}_I^{-1}(x,y)$ is the inverse kernel of $\underline{\underline{C}}_I(x,y)$ then

$$\int \underline{\underline{C}}_I^{-1}(x,z)\ \underline{\underline{C}}_I(z,y)\ dz = \underline{\underline{I}}\ \delta(x - y) \quad . \tag{2-16}$$

Applying this definition to (2-15), we have

$$\iint \underline{\underline{C}}_I^{-1}(x,z)\ \underline{\underline{C}}_S(z,y)\ \underline{f}(y)\ dydz = (\lambda_S/\lambda_I)\ \underline{f}(x) \quad . \tag{2-17}$$

The solution $\underline{f}(x)$ to the SIR maximization problem is then an eigenfunction of

$$\underline{\underline{C}}(x,y) = \int \underline{\underline{C}}_I^{-1}(x,z)\ \underline{\underline{C}}_S(z,y)\ dz \tag{2-18}$$

with eigenvalue λ_S/λ_I. The significance of this eigenvalue emerges when (2-11) and (2-12) are substituted into (2-3):

$$SIR = \frac{\lambda_S \int \underline{f}^*(x)\ \underline{f}(x)\ dx}{\lambda_I \int \underline{f}^*(x)\ \underline{f}(x)\ dx} = \frac{\lambda_S}{\lambda_I} \quad . \tag{2-19}$$

The energy-constrained filter that maximizes SIR is thus the eigenfunction of $\underline{\underline{C}}(x,y)$ in (2-18) with largest possible eigenvalue. This relation does not imply that one can easily obtain the best $\underline{f}(x)$ from an eigenfunction equation, however, since $\underline{\underline{C}}(x,y)$ is undefined until the best signal, $\underline{u}(x)$, is specified. The SIR maximization approach allows one

to obtain both $\underline{u}(x)$ and $\underline{f}(x)$. To obtain the best signal with an eigenfunction formulation, different signals must be tried, the corresponding covariance matrices $\underline{\underline{C}}(x,y)$ must be calculated, and the covariance matrix with largest principal eigenvalue must be identified.

If the unit energy filter function $\underline{f}_1(x)$ that maximizes SIR is the principal eigenfunction of $\underline{\underline{C}}(x,y)$ in (2-18), then can the other eigenfunctions of $\underline{\underline{C}}(x,y)$ also be obtained by SIR maximization? Consider another filter function, $\underline{f}_2(x)$, with the following properties:

(i) $\underline{f}_2(x)$ is orthogonal to $\underline{f}_1(x)$, i.e.,

$$\int \underline{f}_1^*(x)\ \underline{f}_2(x)\ dx = 0 \quad , \tag{2-20}$$

(ii) $\underline{f}_2(x)$ has unit energy as in (2-6), and

(iii) $\underline{f}_2(x)$ maximizes SIR.

From the analysis in (2-5)-(2-19), $\underline{f}_2(x)$ is an eigenfunction of $\underline{\underline{C}}(x,y)$ in (2-18), if such an eigenfunction satisfies (2-20). In fact, all the eigenvectors of a covariance matrix with distinct eigenvalues are orthogonal [14], and (2-20) is satisfied.

All the eigenvectors of $\underline{\underline{C}}(x,y)$ can thus be obtained by SIR maximization, provided that each new filter function is constrained to be orthogonal to those found previously. If the maximum possible SIR is obtained for each filter function, then (2-17) implies that the n^{th} computed eigenfunction will have the n^{th} largest eigenvalue, as in principal component analysis [15].

Maximization of SIR under orthogonality constraints as in (2-20) is particularly straightforward if the simplex method [16] is used. If the initial simplex is constrained to a subspace of R^n, then the solution will

be constrained to the same subspace. The starting points for SIR maximization will correspond to functions that are orthogonal to previously determined filters if Gram-Schmidt orthogonalization is used. After constraining the starting points (i.e., the vertices of the initial simplex) to be orthogonal to previously determined filters, the simplex algorithm can be run without further modification.

2.2 Significance of the Relation between SIR Maximization and Eigenfunction Analysis

By maximizing signal-to-interference ratio, one can obtain the eigenfunctions and eigenvalues of $\underline{C}(x,y)$ in (2-18). The eigenfunctions are found in two contexts in the literature. First, they are the best set of linear discriminants for discriminating between two zero-mean Gaussian processes [17,18,19]. Second, they can be used for simultaneous diagonalization of both signal and interference covariance matrices [20]. If the data are projected along the N eigenvectors of $\underline{C}(x,y)$ in (2-18), the resulting projections will be uncorrelated, with variances $\{\lambda_{Sn}\}_{n=1}^{N}$ for the signal process and $\{\lambda_{In}\}_{n=1}^{N}$ for the interference process. This observation follows from the fact that each eigenfunction must satisfy both (2-11) and (2-12). Another proof is given in [20].

Simultaneous diagonalization yields a likelihood ratio formulation involving simple operations on the outputs of the filters that maximize SIR. Under hypothesis H_1 the output of the n^{th} filter is

$$E\{|\hat{r}_n|^2|H_1\} = \lambda_{Sn} + \lambda_{In} \quad , \tag{2-21}$$

the sum of the variances of the uncorrelated echo and interference processes. Under H_0, only the interference is present and

$$E\{|\hat{r}_n|^2|H_0\} = \lambda_{In} \quad . \tag{2-22}$$

Because of simultaneous diagonalization and Gaussianity, the filter outputs are independent under both H_1 (signal + interference) and H_0 (interference alone).

The likelihood ratio is then

$$\Lambda(\underline{\hat{r}}) = \prod_{n=1}^{N} \Lambda(\hat{r}_n) \tag{2-23}$$

where $\underline{\hat{r}}$ is the vector of N filter responses, $\hat{r}_1, \hat{r}_2, \ldots, \hat{r}_N$. Since $\hat{r}_n$ is complex, we have [21,22,23]

$$\Lambda(\hat{r}_n) = \frac{[\pi(\lambda_{Sn} + \lambda_{In})]^{-1} \exp[-|\hat{r}_n|^2/(\lambda_{Sn} + \lambda_{In})]}{(\pi \lambda_{In})^{-1} \exp[-|\hat{r}_n|^2/\lambda_{In}]} \tag{2-24}$$

The log-likelihood ratio for the n^{th} filter output is

$$\ell(r_n) = -\ell n[1 + (\lambda_{Sn}/\lambda_{In})] + \left[\frac{\lambda_{Sn}/\lambda_{In}}{\lambda_{Sn} + \lambda_{In}}\right] |\hat{r}_n|^2 \quad . \tag{2-25}$$

The log-likelihood ratio can be written strictly in terms of SIR if the filter outputs are whitened before being passed through a likelihood ratio test. To whiten the interference, the n^{th} filter output is multiplied by $\lambda_{In}^{-1/2}$:

$$r_n \equiv \lambda_{In}^{-1/2} \hat{r}_n \quad . \tag{2-26}$$

For the whitened filter outputs, we have

$$E\left\{ |r_n|^2 \mid H_0 \right\} = 1 \quad , \quad n = 1, 2, \ldots, N \tag{2-27}$$

and

$$E\left\{ |r_n|^2 \mid H_1 \right\} = (\lambda_{Sn}/\lambda_{In}) + 1$$

$$= 1 + SIR_n \quad , n = 1, \ldots, N \quad . \tag{2-28}$$

As a consequence of whitening, (2-25) can be written

$$\ell(r_n) = -\ell n(1 + SIR_n) + \left[\frac{SIR_n}{1 + SIR_n} \right] |r_n|^2 \quad . \tag{2-29}$$

From (2-23), the log-likelihood ratio of the whitened filter responses, $\underline{r}$, is

$$\ell(\underline{r}) = \sum_{n=1}^{N} \frac{SIR_n}{1 + SIR_n} |r_n|^2 - \sum_{n=1}^{N} \ell n(1 + SIR_n) \quad . \tag{2-30}$$

Equation (2-30) is the usual form for a quadratic discriminant. Given this form, where the expected values of $|r_n|^2$ depend upon n, an exact, closed form expression for system performance can be found, and this expression can be written in terms of $\{SIR_n\}_{n=1}^{N}$, the signal-to-interference ratios at the outputs of the N orthogonal filters obtained from an SIR maximization algorithm.

By finding a set of orthogonal filters for SIR maximization, we have obtained the major part of an optimum detector configuration. The complete optimum detector is constructed by computing a weighted sum

of magnitude-squared (square-envelope detected) filter outputs, as in (2-30). The resulting detector configuration is illustrated in Figure 2-1.

2.3 Detection Performance

In order to conform to the notation in Van Trees [14], let

$$SIR_n \equiv \lambda_n \tag{2-31}$$

and

$$\lambda_{In}^{-1/2}\, \hat{r}_n = r_n \tag{2-32}$$

as in (2-26). In this case

$$E\{|r_n|^2 \mid H_1\} = \lambda_n + 1 \tag{2-33}$$

and

$$E\{|r_n|^2 \mid H_0\} = 1 \quad , \quad n = 1, 2, \ldots, N \quad . \tag{2-34}$$

Each square-envelope detected filter output $|r_n|^2$ is the sum of the squares of two uncorrelated Gaussian random variables, $x_n = \mathrm{Re}\{r_n\}$ and $y_n = \mathrm{Im}\{r_n\}$. The power is assumed to be split equally between these two variables, so that they have equal probability distributions

$$p(x_n) = \left(2\pi\sigma_n^2\right)^{-1/2} \exp\left[-x_n^2/(2\sigma_n^2)\right] \tag{2-35}$$

$$p(y_n) = \left(2\pi\sigma_n^2\right)^{-1/2} \exp\left[-y_n^2/(2\sigma_n^2)\right] \tag{2-36}$$

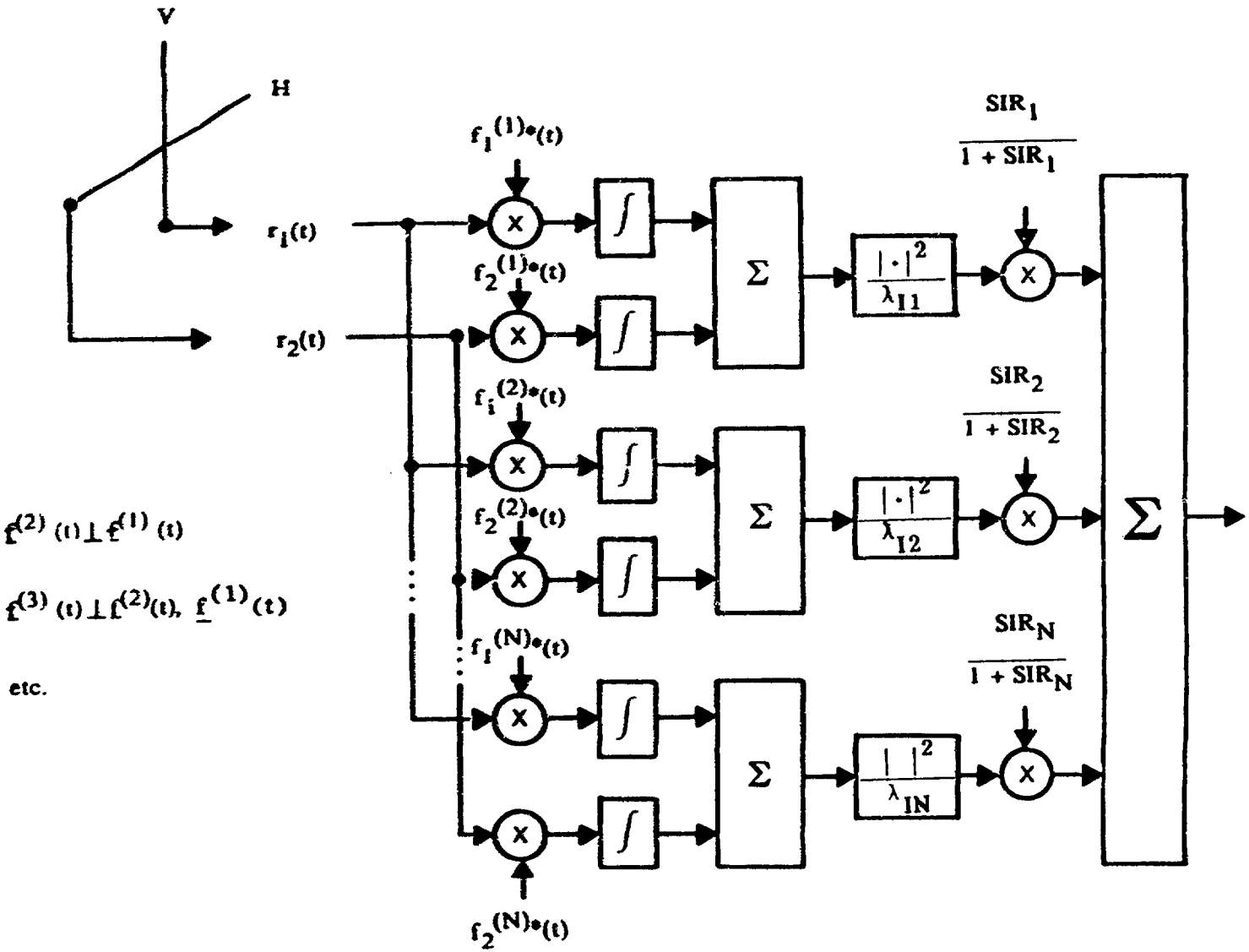

Figure 2-1. Implementation of the Log-Likelihood Function from Orthogonal SIR solutions

where

$$\sigma_n^2 = \begin{cases} (\lambda_n + 1)/2 & \text{when } H_1 \text{ is true} \quad (2\text{-}37) \\ 1/2 & \text{when } H_0 \text{ is true} \quad . \quad (2\text{-}38) \end{cases}$$

It follows that [21]

$$p(|r_n|^2) = p(x_n^2 + y_n^2)$$

$$= (2\sigma_n^2)^{-1} \exp[-|r_n|^2/(2\sigma_n^2)] \quad . \quad (2\text{-}39)$$

The corresponding characteristic function is

$$\text{C.F. of } |r_n|^2 = \begin{cases} [1 - j(\lambda_n + 1)\omega]^{-1} & \text{when } H_1 \text{ is true} \quad (2\text{-}40) \\ [1 - j\omega]^{-1} & \text{when } H_0 \text{ is true} \quad . \quad (2\text{-}41) \end{cases}$$

The data dependent part of the log-likelihood ratio is

$$\ell(\underline{r}) = \sum_{n=1}^{N} \frac{\lambda_n}{\lambda_n + 1} |r_n|^2 \quad . \quad (2\text{-}42)$$

In order to evaluate detection performance, we want to find the probability distribution of $\ell(\underline{r})$.

$$p(\ell) \longleftrightarrow \prod_{n=1}^{N} \left[\text{C.F. of } \frac{\lambda_n}{\lambda_n + 1} |r_n|^2 \right] \tag{2-43}$$

where the double arrow indicates a Fourier transform relation.

If the characteristic function of $|r_n|^2$ is $\Phi_n(\omega)$, then the C.F. of $\alpha|r_n|^2$ is $\Phi_n(\alpha\omega)$. It follows that

$$\text{C.F. of } \frac{\lambda_n}{\lambda_n+1} |r_n|^2 = \begin{cases} [1 - j \lambda_n \omega]^{-1} & \text{when } H_1 \text{ is true} \quad (2\text{-}44) \\ \left[1 - j \frac{\lambda_n}{\lambda_n+1} \omega\right]^{-1} & \text{when } H_0 \text{ is true} \quad (2\text{-}45) \end{cases}$$

and

$$p(\ell) \longleftrightarrow \begin{cases} \prod_{n=1}^{N} [1 - j \lambda_n \omega]^{-1} & \text{given } H_1 \quad (2\text{-}46) \\ \prod_{n=1}^{N} [1 - j \lambda_n' \omega]^{-1} & \text{given } H_0 \quad (2\text{-}47) \end{cases}$$

where

$$\lambda_n' = \lambda_n/(\lambda_n + 1) \quad . \tag{2-48}$$

The products in (2-46) and (2-47) can be represented as sums by using a Heaviside expansion, which is extensively exploited in network theory [25]. For N distinct values of λ_n,

$$\prod_{n=1}^{N} (1 - j \lambda_n \omega)^{-1} = \sum_{i=1}^{N} \frac{a_i}{1 - j \lambda_i \omega} \qquad (2\text{-}49)$$

where

$$a_i = \left. \frac{1 - j \lambda_i \omega}{\prod_{n=1}^{N} (1 - j \lambda_n \omega)} \right|_{\omega = -j/\lambda_i}$$

$$= \prod_{\substack{n=1 \\ n \neq i}}^{N} (1 - \lambda_n/\lambda_i)^{-1} \quad . \qquad (2\text{-}50)$$

Substituting (2-49) into (2-46) yields

$$p(\ell|H_1) = \sum_{i=1}^{N} a_i \int_{-\infty}^{\infty} \frac{1}{1 - j \lambda_i \omega} e^{-j\omega\ell} \, d\omega$$

$$= \sum_{i=1}^{N} (a_i/\lambda_i) \exp(-\ell/\lambda_i) \quad . \qquad (2\text{-}51)$$

Similarly,

$$p(\ell|H_0) = \sum_{i=1}^{N} (a_i'/\lambda_i') \exp(-\ell/\lambda_i') \qquad (2\text{-}52)$$

where

$$a_i' = \prod_{\substack{n=1 \\ n \neq i}}^{N} (1 - \lambda_n'/\lambda_i')^{-1} \quad . \tag{2-53}$$

Probabilities of detection and false alarm can now be computed for any threshold setting, γ. The detection probability is

$$P_D = \int_{\gamma}^{\infty} p(\ell|H_1)\, d\ell$$

$$= \sum_{i=1}^{N} a_i \int_{\gamma}^{\infty} \exp[-(\ell/\lambda_i)]\, d(\ell/\lambda_i)$$

$$= \sum_{i=1}^{N} a_i \exp(-\gamma/\lambda_i) \tag{2-54}$$

and the false alarm probability is

$$P_F = \int_{\gamma}^{\infty} p(\ell|H_0)\, d\ell$$

$$= \sum_{i=1}^{N} a_i' \exp[-\gamma(\lambda_i+1)/\lambda_i] \tag{2-55}$$

where

$$a_i = \prod_{\substack{n=1 \\ n \neq i}}^{N} (1 - \lambda_n/\lambda_i)^{-1} \quad , \tag{2-56}$$

$$a_i' = \prod_{\substack{n=1 \\ n \neq i}}^{N} \left[1 - \frac{\lambda_n/(\lambda_n + 1)}{\lambda_i/(\lambda_i + 1)} \right]^{-1} \quad , \tag{2-57}$$

and

$$\lambda_i = SIR_i \quad , \tag{2-58}$$

the signal-to-interference ratio at the output of the i^{th} filter $\underline{f}_i(x)$. Similar results are found in [24].

Equations (2-54)-(2-58) constitute a closed form expression for the performance of a detector for Gaussian signals in Gaussian noise, for the case in which the signal covariance matrix has unequal diagonal elements. If some of the diagonal elements are equal, a generalized version of the technique in (2-50) can be used [25]. The expression depends upon the eigenvalues of the matrix $\underline{C}(x,y)$ in (2-18). The eigenvalues are the same as the signal-to-interference ratios at the outputs of a set of orthogonal filters, if the filters are designed to maximize these ratios.

2.4 Summary of Section 2

Maximization of signal-to-interference ratio for signal-filter design is generally used as a way to obtain usable, albeit suboptimum, results. A straightforward extension of the SIR algorithm, however, yields not only a "best" signal-filter pair, but a set of additional orthogonal filters. The resulting filter set is apparently the same as one would obtain with

linear discriminant analysis or with a Karhunen-Loève transformation of whitened data. The similarity to linear (Kullback) discriminants is not surprising when one considers that the functional Q(f) in (2-5) is very similar to the Kullback divergence [18,19]

$$J(\underline{f}) = E\left[\ell(\underline{r}^T\underline{f}) \mid H_1\right] - E\left[\ell(\underline{r}^T\underline{f}) \mid H_0\right] \tag{2-59}$$

where $\ell(\underline{r}^T\underline{f})$ is the log-likelihood ratio when the quantity $\underline{r}^T\underline{f}$ is taken as data.

The maximum SIR filter set, which also implements a simultaneous diagonalization of signal and interference covariance matrices, can be used for optimum (quadratic discriminant) detection. It is only necessary to form a weighted sum of the squared envelopes of the filter outputs. The performance of the resulting detector can be written as an exact, closed form expression that depends upon the signal-to-interference ratios at the filter outputs.

3.0 A POLARIMETRIC SCATTERING FUNCTION

3.1 Dependence of SIR on Target and Clutter Scattering Functions

From (2-1), SIR depends upon the expected magnitude-squared filter output

$$E\left\{\left|\int_{-\infty}^{\infty} \underline{f}^*(x)\ \underline{r}(x)\ dx\ \right|^2\right\}$$

$$= E\left\{\left|\sum_{i=1}^{2}\int_{-\infty}^{\infty} f_i^*(x)\ r_i(x)\ dx\ \right|^2\right\} \tag{3-1}$$

where $f_1(x)$ is the filter that processes the output of the vertically polarized antenna $r_1(x)$, and $f_2(x)$ is the filter for the horizontally polarized antenna output, $r_2(x)$.

The received vertically and horizontally polarized echoes, $r_1(x)$ and $r_2(x)$, are related to the transmitted signal components $u_1(x)$ and $u_2(x)$ by [5]

$$r_i(x) = \sum_{j=1}^{2} \int_{-\infty}^{\infty} \tilde{b}_{ij}\,(x - \tau/2,\ \tau)\ u_j(x - \tau)\ d\tau \qquad (3\text{-}2)$$

where $\tilde{b}_{ij}\,(t,\tau)$ is the impulse response of a time varying random filter at time τ when the impulse is applied at time zero. In terms of distributed radar reflectors, $\tilde{b}_{ij}(t - \tau/2,\ \tau)$ is the reflectivity of a scattering element with delay τ, measured at the time of reflection $t - \tau/2$. The subscripts of $\tilde{b}_{ij}\,(t,\tau)$; $i = 1,\ 2$; $j = 1,\ 2$, imply that there are actually four time varying weights in a tapped delay line model of the filter at delay τ, i.e., a 2×2 scattering matrix that depends upon time t and delay τ. These weights describe the backscatter with polarization i for an incident signal component with polarization j.

Substituting (3-2) into (3-1) yields

$$E\left\{\left|\int_{-\infty}^{\infty} \underline{f}^*(x)\ \underline{r}\,(x)\ dx\ \right|^2\right\}$$

$$= E\left\{\left|\sum_{i=1}^{2}\int_{-\infty}^{\infty} f_i^*(x) \sum_{j=1}^{2}\int_{-\infty}^{\infty} \tilde{b}_{ij}(x - \tau/2,\ \tau)\ u_j(x - \tau)\ d\tau\ dx\ \right|^2\right\}$$

$$= \sum_{i=1}^{2}\sum_{j=1}^{2}\sum_{m=1}^{2}\sum_{n=1}^{2} \iiiint_{-\infty}^{\infty} f_i^*(x)\ f_m(y)\ u_j(x - \tau)\ u_n^*(y - \tau')$$

$$E\left\{\tilde{b}_{ij}\,(x - \tau/2,\ \tau)\ \tilde{b}_{mn}^*(y - \tau'/2,\ \tau')\right\} dx\ dy\ d\tau\ d\tau' \quad . \qquad (3\text{-}3)$$

The Fourier transform in time of the time-varying tap weight at delay τ can be used to assess the Doppler spread induced by the time variation. In order to express the receiver output in terms of Doppler spread, one can use the definitions

$$b_{ij}(\phi, \tau) \equiv \int_{-\infty}^{\infty} \tilde{b}_{ij}(t - \tau/2, \tau) \exp(-j2\pi\phi t)\, dt \qquad (3\text{-}4)$$

or

$$\tilde{b}_{ij}(x - \tau/2, \tau) \equiv \int_{-\infty}^{\infty} b_{ij}(\phi, \tau) \exp(j2\pi\phi x)\, d\phi \quad . \qquad (3\text{-}5)$$

The integral in (3-4) is performed on a sample function of the time-varying tap weight $\tilde{b}_{ij}(t - \tau/2, \tau)$. The expected product of two such sample functions is

$$E\left\{\tilde{b}_{ij}(x - \tau/2, \tau)\, \tilde{b}^{*}_{mn}(y - \tau'/2, \tau')\right\}$$

$$= \iint_{-\infty}^{\infty} E\left\{b_{ij}(\phi, \tau)\, b^{*}_{mn}(\phi', \tau')\right\}$$

$$\exp[j2\pi(\phi x - \phi' y)]\, d\phi d\phi' \qquad (3\text{-}6)$$

This equation can be simplified by assuming that tap weights at different delays are statistically uncorrelated and that the temporal variation of the weights is wide-sense stationary, so that the expression in (3-6) is a function only of the difference $(x - \tau/2) - (y - \tau'/2)$. This wide-sense stationary, uncorrelated scatterer (WSSUS) assumption implies that

$$E\left\{b_{ij}(\phi,\tau)\ b^{*}_{mn}(\phi',\tau')\right\}$$

$$= E\left\{b_{ij}(\phi,\tau)\ b^{*}_{mn}(\phi,\tau)\right\}\ \delta(\phi - \phi')\ \delta(\tau - \tau') \qquad (3\text{-}7)$$

and

$$E\left\{\tilde{b}_{ij}(x - \tau/2,\ \tau)\ \tilde{b}^{*}_{mn}(y - \tau'/2,\ \tau')\right\}$$

$$= \int_{-\infty}^{\infty} E\left\{b_{ij}(\phi,\tau)\ b^{*}_{mn}(\phi,\tau)\right\}\ \exp[j2\pi\phi\,(x - y)]$$

$$d\phi\ \delta(\tau - \tau') \quad . \qquad (3\text{-}8)$$

In (3-8) the expectation is a function of specific ϕ and τ values:

$$E\left\{b_{ij}(\phi,\tau)\ b^{*}_{mn}(\phi,\tau)\right\} = E\left\{b_{ij}\ b^{*}_{mn} \mid \phi,\tau\right\} p_b(\phi,\tau) \qquad (3\text{-}9)$$

where $p_b(\phi,\tau)$ is the probability that the specified range and Doppler values will actually occur.

Substituting (3-9) into (3-8) and (3-8) into (3-3) yields

$$E\left\{\left|\int_{-\infty}^{\infty} \underline{f}^*(x)\,\underline{r}(x)\,dx\right|^2\right\} = \sum_{i=1}^{2}\sum_{j=1}^{2}\sum_{m=1}^{2}\sum_{n=1}^{2}\int_{-\infty}^{\infty}\int_{-\infty}^{\infty}$$

$$\left[\int_{-\infty}^{\infty} f_i^*(x)\,u_j(x-\tau)\exp(j2\pi\phi x)\,dx\right]$$

$$\left[\int_{-\infty}^{\infty} f_m(y)\,u_n^*(y-\tau)\exp(-j2\pi\phi y)\,dy\right]$$

$$E\left\{b_{ij}\,b_{mn}^* \mid \phi,\tau\right\}\,p_b(\phi,\tau)\,d\phi d\tau$$

$$= \sum_{i=1}^{2}\sum_{j=1}^{2}\sum_{m=1}^{2}\sum_{n=1}^{2}\int_{-\infty}^{\infty}\int_{-\infty}^{\infty} S_{ijmn}(\phi,\tau)\,\chi^*_{f_i u_j}(\tau,\phi)$$

$$\chi_{f_m u_n}(\tau,\phi)\,d\tau d\phi \qquad (3\text{-}10)$$

where

$$\chi_{f_k u_\ell}(\tau,\phi) \equiv \int_{-\infty}^{\infty} f_k(t)\,u_\ell^*(t-\tau)\exp(-j2\pi\phi t)\,dt \qquad (3\text{-}11)$$

is the narrowband cross-ambiguity function of the reference function $f_k(t)$ and the signal $u_\ell(t)$ and

$$S_{ijmn}(\phi,\tau) \equiv E\left\{b_{ij}\,b_{mn}^* \mid \phi,\tau\right\}\,p_b(\phi,\tau) \qquad (3\text{-}12)$$

is a polarimetric version of the target scattering function.

3.2 Comparison with Less General Problem Formulations

Fundamental results are embodied in (3-10)-(3-12). Eq. (3-10) shows the dependence of SIR on the scattering function of target or clutter and upon signal-filter design as manifested by various cross-ambiguity functions. Eq. (3-12) defines the scattering function in terms of expected values of products of Fourier transformed tap weight variations, as defined in (3-4).

If $i = j = m = n = 1$, then $S_{1111}(\phi,\tau)$ is the power spectrum of the time variation of the tap weight at delay τ, for the vertically polarized channel. If only the term $i = j = m = n = 1$ is considered in (3-10), then we obtain the usual expression for SIR for the non-polarimetric case [11]. Polarimetric processing introduces fifteen additional terms into the SIR expression, and significant improvements in SIR should occur if there are any polarization-sensitive differences between target and clutter.

Another very general aspect of the problem formulation is the inclusion of Doppler spread in cross polarization terms, e.g., $i \neq j$ and/or $m \neq n$ in (3-10). These cases account for twelve of the sixteen terms in (3-10), i.e., all the terms except for i, j, m, n equal to (1111), (2222), (1122), and (2211). Even if the number of cross polarization terms is effectively halved by the realistic assumption that $b_{ij} = b_{ji}^{*}$, there are still six Doppler sensitive cross polarization terms which may be different for target and clutter. If any of these terms <u>is</u> different for target and clutter, the SIR maximization technique will exploit it. The most obvious cross polarization term is $E\{|b_{12}(\phi,\tau)|^2\}$, the power spectrum of the time variation of $\tilde{b}_{12}(t,\tau)$. Cross-spectral terms such as $E\{b_{12}(\phi,\tau)\, b_{22}^{*}(\phi,\tau)\}$ may also be important.

It is difficult to visualize specific advantages of the general formulation, to conceptualize problems, and to obtain physical insight into the solutions. In order to facilitate this process, it is helpful to use a dipole model of the tap weights $\tilde{b}_{ij}(t,\tau)$. This model is discussed in the next section.

4.0 DIPOLE MODELS FOR ELEMENTARY SCATTERERS

4.1 Single Dipoles

Instead of the usual collection of point scatterers, we assume that we have a collection of dipoles or thin wires. Let u_1 and u_2 be the vertical and horizontal components of the transmitted signal, and let i_L and i_C be the along-length and cross-length currents induced on the dipole by the signal. For an ideal dipole, we assume that the cross-length current is negligible. For a dipole that is tilted θ radians from vertical, it follows that

$$\begin{bmatrix} i_L \\ i_C \end{bmatrix} \propto \begin{bmatrix} \cos\theta & \sin\theta \\ 0 & 0 \end{bmatrix} \begin{bmatrix} u_1 \\ u_2 \end{bmatrix}. \tag{4-1}$$

When the dipole re-radiates energy, the vertical and horizontal components of the echo, r_1 and r_2, are given by

$$\begin{bmatrix} r_1 \\ r_2 \end{bmatrix} \propto \begin{bmatrix} \cos\theta & -\sin\theta \\ \sin\theta & \cos\theta \end{bmatrix} \begin{bmatrix} i_L \\ i_C \end{bmatrix}$$

$$= \sigma \begin{bmatrix} \cos^2\theta & \cos\theta\sin\theta \\ \cos\theta\sin\theta & \sin^2\theta \end{bmatrix} \begin{bmatrix} u_1 \\ u_2 \end{bmatrix}, \tag{4-2}$$

where σ is the radar reflectivity of the dipole. The radar cross section is σ^2.

4.2 Collections of Dipoles

Point scatterers can also be replaced by collections of dipoles. Suppose, for example, that each uncorrelated scatterer is a pair of dipoles that are separated slightly in range. The scattering matrix for each uncorrelated scatterer is then

$$S = \sigma_1 \begin{bmatrix} \cos^2 \theta_1 & \cos \theta_1 \sin \theta_1 \\ \cos \theta_1 \sin \theta_1 & \sin^2 \theta_1 \end{bmatrix}$$

$$+ \sigma_2 \begin{bmatrix} \cos^2 \theta_2 & \cos \theta_2 \sin \theta_2 \\ \cos \theta_2 \sin \theta_2 & \sin^2 \theta_2 \end{bmatrix} e^{-j2\pi f(\frac{2\Delta R}{c})} , \qquad (4\text{-}3)$$

where the first dipole is oriented θ_1 degrees from vertical, the second dipole is oriented θ_2 degrees from vertical, and the two dipoles are separated by ΔR meters. In Eq. (4-3), f is the signal frequency and c is speed of light.

In the case of a vertical dipole in front of a horizontal dipole with ΔR equal to a quarter wavelength and $\sigma_1 = \sigma_2$, we have

$$S = \sigma_1 \begin{bmatrix} 1 & 0 \\ 0 & 0 \end{bmatrix} + \sigma_1 \begin{bmatrix} 0 & 0 \\ 0 & 1 \end{bmatrix} e^{j\pi} = \sigma_1 \begin{bmatrix} 1 & 0 \\ 0 & -1 \end{bmatrix} . \qquad (4\text{-}4)$$

The scattering matrix in (4-4) induces a polarization reversal of a circularly polarized wave with vertical component $u_1 = A \cos(2\pi ft)$ and horizontal component $u_2 = A \sin(2\pi ft)$.

If a distributed reflector is modeled as a collection of single dipoles as in (4-2), then no frequency dependent phase shift is introduced into the echo, since the WSSUS assumption eliminates interaction between different scatterers. To obtain frequency dependent phase shifts, a distributed reflector must be constructed from elementary reflectors that are themselves collections of dipoles, as in (4-3). This observation could lead to a useful discriminant if the target size is known, i.e., if ΔR is specified in (4-3), and if clutter scatterers can be modelled as in (4-2).

More specific target models can be obtained by considering specific structures known to exist on particular targets, and modeling these structures in terms of measured scattering matrices or as combinations of dipoles and planar point targets. Planar point targets are discussed in the next subsection.

4.3 Planar Point Target Models

Another type of elementary scatterer is the usual planar point target or perfect mirror. Since the currents induced on such a reflector are parallel to the applied field, there are no polarization shifts. The scattering matrix is $\sigma\underline{I}$, where $\underline{I}$ is the identity matrix; $b_{11} = b_{22} = \sigma$ and $b_{12} = b_{21} = 0$. Thus,

$$E\left\{b_{ij} b^*_{mn} \mid \phi, \tau\right\} = \begin{cases} E(\sigma^2) & \text{if } i = j \text{ and } m = n \\ 0 & \text{otherwise} \end{cases} . \qquad (4\text{-}5)$$

As in Eq. (4-3), one can combine a dipole and a planar point target to model various physical effects. If a planar point target with reflectivity σ is placed a quarter wavelength behind a vertical dipole with reflectivity 2σ, then

$$S = 2\sigma \begin{bmatrix} 1 & 0 \\ 0 & 0 \end{bmatrix} + \sigma \begin{bmatrix} 1 & 0 \\ 0 & 1 \end{bmatrix} e^{j\pi}$$

$$= \sigma \begin{bmatrix} 1 & 0 \\ 0 & -1 \end{bmatrix} \qquad (4\text{-}6)$$

which is the same as the scattering matrix for circular polarization reversal in (4-4).

A horizontal dipole and a ground plane with variable distance $\Delta R(t)$ between dipole and ground yield

$$S = \sigma_1 \begin{bmatrix} 0 & 0 \\ 0 & 1 \end{bmatrix} + \sigma_2 \begin{bmatrix} 1 & 0 \\ 0 & 1 \end{bmatrix} e^{-j2\pi f \left[\frac{2\Delta R(t)}{c}\right]} . \qquad (4\text{-}7)$$

The scattering matrix model in (4-7) could be a useful representation of a low-flying cruise missile against a background of ground clutter, if both missile and clutter are within the same resolution cell [26].

4.4 Polarimetric Scattering Functions for Dipole Scatterers

Equation (4-2) indicates that a dipole scatterer can be represented by its reflectivity σ and its tilt θ relative to vertical. If both of these quantities are dependent upon Doppler and range, then the polarimetric scattering function in (3-12) is

$$S_{ijmn}(\phi,\tau) = E\left\{ b_{ij}\left[\sigma(\phi,\tau),\theta(\phi,\tau)\right] b^{*}_{mn}\left[\sigma(\phi,\tau),\theta(\phi,\tau)\right] \mid \phi,\tau \right\} p_b(\phi,\tau)$$

$$= \left\{ \int_{\theta=-\pi/2}^{\pi/2} \int_{\sigma=0}^{\infty} b_{ij}(\sigma,\theta)\, b^{*}_{mn}(\sigma,\theta)\, p(\sigma,\theta \mid \phi,\tau)\, d\sigma d\theta \right\} p_b(\phi,\tau) \quad . \tag{4-8}$$

From (4-2),

$$b_{11}(\sigma,\theta) = \sigma \cos^2 \theta \tag{4-9}$$

$$b_{12}(\sigma,\theta) = b_{21}(\sigma,\theta) = \sigma \cos \theta \sin \theta \tag{4-10}$$

$$b_{22}(\sigma,\theta) = \sigma \sin^2 \theta \quad . \tag{4-11}$$

Assuming that σ and θ are statistically independent random variables, we have

$$p(\sigma,\theta \mid \phi,\tau) \equiv p(\sigma \mid \phi,\tau)\, p(\theta \mid \phi,\tau) \tag{4-12}$$

and $S_{ijmn}(\phi,\tau)$ is proportional to

$$E(\sigma^2 \mid \phi,\tau) = \int_0^{\infty} \sigma^2\, p(\sigma \mid \phi,\tau)\, d\sigma \quad . \tag{4-13}$$

A second simplifying assumption is that $p(\theta \mid \phi,\tau)$ is uniformly and symmetrically distributed between $\pm\alpha(\phi,\tau)$. In this case,

$$S_{ijmn}(\phi,\tau) = \frac{E(\sigma^2 \mid \phi,\tau)\, p_b(\phi,\tau)}{2\alpha(\phi,\tau)} \int_{-\alpha(\phi,\tau)}^{\alpha(\phi,\tau)} b_{ij}(\theta)\, b^*_{mn}(\theta)\, d\theta$$

$$= E(\sigma^2 \mid \phi,\tau)\, p_b(\phi,\tau) \begin{cases} \frac{1}{4\alpha}\left[\frac{3\alpha}{2} + \sin(2\alpha) + \frac{\sin(4\alpha)}{8}\right], \\ \quad \text{if } i = j = m = n = 1 \\ \frac{1}{4\alpha}\left[\frac{3\alpha}{2} - \sin(2\alpha) + \frac{\sin(4\alpha)}{8}\right], \\ \quad \text{if } i = j = m = n = 2 \\ \frac{1}{8\alpha}\left[\alpha - \frac{\sin(4\alpha)}{4}\right], \text{ if } i \neq j \text{ and } m \neq n \\ \quad \text{or if } i = j \neq m = n \\ 0, \text{ if } i = j \text{ and } m \neq n \text{ or if} \\ \quad i \neq j \text{ and } m = n \end{cases} \tag{4-14}$$

where $\alpha = \alpha(\phi,\tau)$. The expressions on the right hand side of (4-14) are obtained by integrating b_{ij} from (4-9)-(4-11) over θ from $\theta = -\alpha$ to $\theta = \alpha$.

Each tap weight in a tapped delay line model of an extended target is envisioned as a moving dipole. In many physical situations, one would expect the Doppler spread induced by dipole rotation to be correlated with the amount of rotation, in which case $\alpha(\phi,\tau)$ will increase monotonically with ϕ. In any case, the dipole model allows one to conceptualize the difference between polarimetric extended target models and non-polarimetric

models. We have also obtained a specific expression for the polarimetric scattering function $S_{ijmn}(\phi,\tau)$. Such a specific expression is very useful for synthesis and analysis of SIR optimization programs.

5.0 IMPLEMENTATION OF A COMPUTER PROGRAM FOR POLARIMETRIC SIR OPTIMIZATION

In order to set up a computer program for SIR maximization, it is useful to express the signal-to-interference ratio in a form that can be easily evaluated by a computer with user-supplied target and clutter data. To find the best signal and filter functions with a computer, it is necessary to parameterize these functions in terms of (say) time samples or frequency domain samples (Fourier coefficients). The optimization problem is formulated by expressing SIR in terms of these parameters.

5.1 Signal and Filter Parameters

The vertical component of the transmitted signal is $u_1(t)$ and the horizontal component is $u_2(t)$. Each component is represented as a weighted sum of complex orthonormal basis functions $\{\theta_k(t);\ k = 0, 1, \ldots, K\}$. The vertical and horizontal signal components are thus

$$u_i(t) = \sum_{k=0}^{K} u_{ik}\,\theta_k(t) \quad , \quad i = 1,2$$

$$= \sum_{k=0}^{K} |u_{ik}|\exp(ju_{ik})\,\theta_k(t) \quad , \quad i = 1,2 \quad . \tag{5-1}$$

where $|u_{ik}|$ is the magnitude of the kth expansion coefficient u_{ik} and u_{ik} is the corresponding phase parameter.

Similarly, the filter components are written

$$f_i(t) = \sum_{k=0}^{K} f_{ik}\, \theta_k(t) = \sum_{k=0}^{K} |f_{ik}| \exp(j\nu_{ik})\, \theta_k(t) \quad , \qquad (5\text{-}2)$$

$$i = 1,2 \quad .$$

The basis functions of particular interest are either sinusoids

$$\theta_k(t) = T^{-1/2} \exp(j2\pi kt/T), \qquad (5\text{-}3)$$

or sin(t)/t functions from sampling theory

$$\theta_k(t) = B^{1/2}\, \mathrm{sinc}\{\pi B[t - k/B]\} \quad . \qquad (5\text{-}4)$$

In (5-3), T is the signal or filter duration. In (5-4), B is the system bandwidth. Fourier series representations using the components in (5-3) are desirable if the receiver already incorporates DFT operations, as in coherent pulse Doppler or synthetic aperture radars. Sinc functions are desirable if the radar uses a coded waveform and the receiver can implement a matched filter for such a waveform in the time domain.

5.2 General Expressions for Expected Filter Output Power in Response to Target, Clutter, or Noise

The expected filter output power in response to the target echo is given by (3-10) in terms of cross ambiguity functions and a polarimetric scattering function. The ambiguity functions are defined in (3-11), and the scattering function is given in (3-12) and (4-8). Similar expressions apply to the filter output power in response to the clutter echo, except that (3-12) becomes

$$S_{ijmn}^{(c)}(\phi,\tau) = E\left\{c_{ij}\, c_{mn}^{*} \mid \phi,\tau\right\} p_c(\phi,\tau) \qquad (5\text{-}5)$$

where c_{ij} and c_{mn} are elements of the clutter polarization scattering matrix.

The expected filter output power in response to noise $\underline{n}(t)$ is

$$E\{\left|\int \underline{f}^{*}(t)\underline{n}(t)\, dt\right|^2 = (N_0/2)\int \underline{f}^{*}(t)\underline{f}(t)\, dt$$

$$= (N_0/2)\sum_{i=1}^{2} \chi_{f_i f_i}(0,0) \quad . \qquad (5\text{-}6)$$

5.3 Expressions in Terms of Expansion Coefficients and Basis Functions

This section contains mathematical details that can be ignored without the loss of much understanding. If the reader is not interested in such details, he can turn to Section 5.4.

5.3.1 Ambiguity Functions

For orthonormal basis functions as in Eqs. (5-1) and (5-2), we have

$$\chi_{f_i u_j}(\tau,\phi) = \sum_{k=0}^{K}\sum_{\ell=0}^{K} u_{jk}^{*} f_{i\ell} \int_0^T \theta_k^{*}(t-\tau)\theta_\ell(t)\, e^{-j2\pi\phi t}\, dt \quad . \qquad (5\text{-}7)$$

For sinusoidal (Fourier) basis functions as in (5-3), we have

$$\int_0^T \theta_k^{*}(t-\tau)\theta_\ell(t)\, e^{-j2\pi\phi t}\, dt = \chi_{\theta_\ell\theta_k}(\tau,\phi)$$

$$= \frac{e^{j2\pi k\tau/T}}{2\pi j(\ell-k-\phi T)}\left[e^{-j2\pi\phi T} - 1\right]$$

$$= \frac{e^{j[(2\pi k\tau/T) - \pi\phi T]}\,\mathrm{sinc}(\pi\phi T)}{1 + [(k-\ell)/\phi T]} \quad , \qquad (5\text{-}8)$$

41

and for sinc(t) basis functions we have (using Parseval's Theorem)

$$\chi_{\theta_\ell \theta_k}(\tau,\phi) = \int_{-\infty}^{\infty} \theta_k^*(t-\tau)\theta_\ell(t)\, e^{-j2\pi\phi t}\, dt$$

$$= \int_{-B/2}^{B/2} [\tilde{\theta}_k(f)\, e^{-j2\pi f\tau}]^*\, \tilde{\theta}_\ell(f+\phi)\, df$$

$$= \int_{-B/2}^{B/2} \tilde{\theta}_\ell(f+\phi)\, \tilde{\theta}_k^*(f)\, e^{j2\pi f\tau}\, df \quad , \qquad (5\text{-}9)$$

where $\tilde{\theta}_k(f)$ is the Fourier transform of $\theta_k(t)$, i.e.,

$$\tilde{\theta}_k(f) = \begin{cases} B^{-1/2} \exp(-j2\pi fk/B) & , \quad -B/2 \le f \le B/2 \\ 0 & , \quad \text{otherwise} \end{cases} \qquad (5\text{-}10)$$

It follows that, for sinc basis functions,

$$\chi_{\theta_\ell \theta_k}(\tau,\phi) = e^{-j2\pi\ell(\phi/B)}\, \mathrm{sinc}[\pi(k-\ell+B\tau)] \quad . \qquad (5\text{-}11)$$

Expressions for the ambiguity functions in (3-11) are thus as follows. For sinusoids on a time interval [0,T],

$$\chi_{f_i u_j}(\tau,\phi) = e^{-j\pi\phi T}\, \mathrm{sinc}(\pi\phi T) \sum_k \sum_\ell \frac{u_{jk}^* f_{i\ell}\, e^{j2\pi k\tau/T}}{1 + [(k-\ell)/\phi T]} \quad , \qquad (5\text{-}12)$$

and for sinc basis functions with frequency domain support on [-B/2, B/2],

$$\chi_{f_i u_j} = \sum_k \sum_\ell u^*_{jk} f_{i\ell}\, e^{-j2\pi\ell\phi/B}\, \mathrm{sinc}[\pi(k-\ell+B\tau)] \quad . \tag{5-13}$$

5.3.2 Expected Filter Output Power in Response to Time-Varying, Distributed Target or Clutter

Substitution of $\chi_{f_i u_j}(\tau,\phi)$ from (5-12) or (5-13) into (3-10) yields expressions for the expected filter output power. These expressions contain the integral

$$\int_{-\infty}^{\infty}\int \chi^*_{f_i u_j}(\tau,\phi)\ \chi_{f_m u_n}(\tau,\phi)\ E[b_{ij}\, b^*_{mn}\,|\tau,\phi]\ p_b(\tau,\phi)\ d\tau\ d\phi \ . \tag{5-14}$$

Further analysis of this integral is possible if it is assumed that $p(\tau,\phi)$ can be represented by a two dimensional histogram, i.e., $p(\tau,\phi)$ is constant over histogram intervals of size $\Delta\tau$, $\Delta\phi$. The integral in (5-14) is then a sum (over the indices r and s) of simpler integrals of the form

$$p_b(\tau_r,\phi_s)E[b_{ij}b^*_{mn}\,|\,\tau_r,\phi_s] \int_{\phi_s-\Delta\phi/2}^{\phi_s+\Delta\phi/2}\int_{\tau_r-\Delta\tau/2}^{\tau_r+\Delta\tau/2} \chi^*_{f_i u_j}(\tau,\phi)\ \chi_{f_m u_n}(\tau,\phi)\ d\tau\ d\phi \quad . \tag{5-15}$$

The double integral in (5-15) can be evaluated by using (5-12) for sinusoidal basis functions or (5-13) for sinc functions. For sinusoids,

$$\int_{\phi_s-\Delta\phi/2}^{\phi_s+\Delta\phi/2} \int_{\tau_r-\Delta\tau/2}^{\tau_r+\Delta\tau/2} \chi^*_{f_i u_j}(\tau,\phi)\chi_{f_m u_n}(\tau,\phi)\,d\tau\,d\phi$$

$$= \sum_{k,\ell,p,q} u_{jk} f^*_{i\ell}\, u^*_{np} f_{mq}\, I_1(k,\ell,p,q,\tau_r,\phi_s) I_2(k,\ell,p,q,\tau_r,\phi_s) \quad , \qquad (5\text{-}16)$$

where

$$I_1 = \int_{\phi_s-\Delta\phi/2}^{\phi_s+\Delta\phi/2} \frac{(\phi T)^2 \mathrm{sinc}^2(\pi\phi T)}{[\phi T + (k-\ell)][\phi T + (p-q)]}\, d\phi \quad , \qquad (5\text{-}17)$$

and

$$I_2 = \int_{\tau_r-\Delta\tau/2}^{\tau_r+\Delta\tau/2} e^{-j2\pi(k-p)\tau/T}\, d\tau \quad . \qquad (5\text{-}18)$$

The integrals in (5-17) and (5-18) are evaluated in Appendix A.

For sinc functions, we have the same form as in (5-18) except that

$$I_1 = \int_{\tau_r-\Delta\tau/2}^{\tau_r+\Delta\tau/2} \mathrm{sinc}[\pi(k-\ell+B\tau)]\ \mathrm{sinc}[\pi(p-q+B\tau)]\,d\tau \quad , \qquad (5\text{-}19)$$

and

$$I_2 = \int_{\phi_s-\Delta\phi/2}^{\phi_s+\Delta\phi/2} e^{-j2\pi(\ell-q)\phi/B}\, d\phi \quad . \tag{5-20}$$

The integrals in (5-19) and (5-20) are also evaluated in Appendix A.

From (3-10), the expected filter output power in response to the target echo $\underline{r}_T(t)$ is

$$E\{|\int \underline{f}^*(t)\underline{r}_T(t)dt\,|^2\}$$

$$= \sum_{r,s} p_b(\tau_r,\phi_s) \sum_{i,j,m,n} E(b_{ij}b^*_{mn}\,|\tau_r,\phi_s) \sum_{k,\ell,p,q} u_{jk}f^*_{i\ell}\,u^*_{np}f_{mq}$$

$$I_1(k,\ell,p,q,\tau_r,\phi_s)I_2(k,\ell,p,q,\tau_r,\phi_s) \quad . \tag{5-21}$$

A similar expression yields the clutter response, provided that $E[c_{ij}c^*_{mn}\,|\tau_r,\phi_s]$ is used instead of $E[b_{ij}b^*_{mn}\,|\tau_r,\phi_s]$, and $p_b(\tau_r,\phi_s)$ is replaced by $p_c(\tau_r,\phi_s)$.

From (5-6) and (5-7), the expected filter output power in response to noise is

$$E\{|\int \underline{f}^*(t)\underline{n}(t)dt\,|^2\} = (N_0/2)\sum_{i=1}^{2}\sum_{k=0}^{K}|f_{ik}|^2 \quad . \tag{5-22}$$

5.4 Signal-to-Interference Ratio Optimization

Using Eqs. (5-21) and (5-22), the signal-to-interference ratio can be written

$$\text{SIR} = \frac{E\{|\text{target response}|^2\}}{E\{|\text{clutter response}|^2\} + E\{|\text{noise response}|^2\}} \quad , \tag{5-23}$$

where

$$E\{|\text{target response}|^2\} = \sum_{r,s} p_b(\tau_r, \phi_s) \sum_{i,j,m,n} E(b_{ij} b^*_{mn} | \tau_r, \phi_s)$$

$$\sum_{k,\ell,p,q} u_{jk} f^*_{i\ell}\, u^*_{np} f_{mq}\, I_1(k,\ell,p,q,\tau_r,\phi_s) I_2(k,\ell,p,q,\tau_r,\phi_s) \quad , \tag{5-24}$$

$$E\{|\text{clutter response}|^2\} = \sum_{r,s} p_c(\tau_r, \phi_s) \sum_{i,j,m,n} E(c_{ij} c^*_{mn} | \tau_r, \phi_s)$$

$$\sum_{k,\ell,p,q} u_{jk} f^*_{i\ell}\, u^*_{np} f_{mq}\, I_1(k,\ell,p,q,\tau_r,\phi_s) I_2(k,\ell,p,q,\tau_r,\phi_s) \quad , \tag{5-25}$$

$$E\{|\text{noise response}|^2\} = (N_0/2) \sum_{i=1}^{2} \sum_{k=0}^{K} |f_{ik}|^2 \quad . \tag{5-26}$$

The optimization problem is to find the signal and filter parameters $\{|u_{ik}|, \mu_{ik}, |f_{ik}|, \nu_{ik};\ i = 1, 2;\ k = 0, \ldots, K\}$ such that SIR is maximized.

From the above equations, it is straightforward to obtain the derivatives of SIR with respect to each unknown coefficient, and a gradient-search type of optimization program can be used to maximize SIR. In Section 2, however, it was shown that a likelihood ratio test is not

generally implemented with a single linear filter; a sequence of orthogonal filters must be used. Each filter in this sequence should maximize SIR for the signal specified by the first signal-filter pair, and each filter function should be orthogonal to the previously determined filter functions.

Such a sequence of orthogonal filters can generally be obtained by adding constraints to the SIR expression via Lagrange multipliers [19,27]. An easier technique, however, is to exploit a property of the simplex method for maximizing a function [16]. The starting or trial solutions in the simplex algorithm define a subspace containing the "optimum" solution found by the algorithm. To constrain the search to functions that are orthogonal to a set of previous solutions, the initial points (simplex vertices) can deliberately be made orthogonal to the previous solutions, and no further modifications of the algorithm are necessary. A disadvantage of the simplex technique as it presently exists in the literature is that it functions without gradient information. Such information is available for SIR and would presumably speed up the search for a maximum if it were used. A summary of the discussion in [16] about the simplex method is given below.

A simplex is the convex hull of n+1 points in R^n: A triangle in R^2, a tetrahedron in R^3, etc. If we want to maximize a function of n variables, we evaluate the function at each of n+1 vertices which specify an initial simplex. For one of these points, x^h, the function f(x) is largest, and for another point, x^ℓ, it is smallest. The object at each step is to replace x^ℓ, the vertex of the current simplex with the lowest function value, by a new and better point.

A tentative direction for the new point is obtained by drawing a line from x^ℓ through the mean of all the other points, computed by excluding x^ℓ. The resulting point is computed from the "reflection" operation

$$x^r = \bar{x} + \alpha(\bar{x} - x^\ell) \quad , \tag{5-27}$$

where α is a positive constant (a value of 1 is recommended) and

$$\bar{x} = \frac{1}{n} \sum_{i=0}^{n} x_i \quad , \quad x_i \neq x^\ell \quad . \tag{5-28}$$

If $f(x^h) < f(x^r)$, i.e., the reflection step has generated a new maximum, then we take an "expansion" step in the same direction by computing

$$x^e = \bar{x} + \gamma(x^r - \bar{x}) \quad , \tag{5-29}$$

where $\gamma > 1$ is a given constant (a value of 2 is recommended). If $f(x^e) > f(x^r)$, then x^e replaces x^r. If, however, $f(x^e) \leq f(x^r)$, then the expansion step failed and x^ℓ is replaced by x^r to form a new simplex. If the reflection step results in a new point that no longer has the smallest function value but is also not the largest value, then x^ℓ is replaced by x^r without implementing an expansion step.

Another possibility is that the original reflection step fails in the sense that the point x^r still has the lowest function value, i.e.,

$$f(x^r) < \min_i \{f(x_i) \quad , \quad x_i \neq x^\ell\} \quad . \tag{5-30}$$

In this case, x^r would just be a new version of the least desirable point. If (5-30) is true, then a "contraction" step is used:

$$x^c = \bar{x} + \beta(x^{\ell'} - \bar{x}) \quad , \tag{5-31}$$

where $0 < \beta < 1$ is the contraction coefficient (a value of $\beta = 1/2$ is recommended) and $x^{\ell'}$ is identical with either x^r or x^ℓ, depending upon which point yields the largest function value, i.e.,

$$f(x^{\ell'}) = \max \{f(x^\ell), f(x^r)\} \quad . \tag{5-32}$$

If $x^{\ell'} = x^\ell$, then x^c establishes a new vertex in the direction opposite to x^r, as we see by comparing (5-27) and (5-31). If $x^{\ell'} = x^r$, then we proceed in the direction of $x^r - \bar{x}$ from the point $\bar{x}$, but our step size is $0 < \beta < 1$ rather than $\gamma > 1$ as in (5-29).

If $f(x^c) < f(x^{\ell'})$, then we still need to find a new vertex that is not the least desirable point, i.e., we still have not reversed the inequality (5-30). In this case, all the original simplex vertices are moved toward the point with the largest function value, i.e, the whole simplex is concentrated near the best point. The new simplex vertices are:

$$\hat{x}_i = x_i + \frac{1}{2}(x^h - x_i) \quad , \quad i = 0, \ldots, n \quad . \tag{5-33}$$

A suggested termination criterion is based on the observation that as a result of (5-33), all the vertices of the simplex near a maximum will move close together and close to $\bar{x}$. Thus, if

$$\frac{1}{n+1} \sum_{i=0}^{n} [f(x_i) - f(\bar{x})]^2 \tag{5-34}$$

is sufficiently small, then the algorithm should terminate.

An important property of the simplex method is its dependence upon the initial vertices chosen for the first simplex. For example, if these vertices do not completely span R^n, then the solution will be found

in a subspace of R^n. Although this property may be viewed as an annoyance, it is, in fact, very useful for finding solutions that are orthogonal to a given function, e.g., a previously determined filter function. The importance of this observation has been pointed out with respect to filters for maximizing SIR and the optimum (likelihood ratio test) receiver structure.

5.5 Iterative Optimization of Signal and Filter Vectors

In order to find the best signal-filter pair for SIR optimization, it is nearly always necessary to iteratively improve one set of parameters with the others held fixed. We have four functions to optimize: The vertically polarized signal $u_1(t)$, the horizontally polarized signal $u_2(t)$, the vertically polarized filter function $f_1(t)$, and the horizontally polarized filter function $f_2(t)$. Each of these functions has been represented in terms of two parameter sets: the magnitudes of the expansion coefficients $\{|u_{1k}|, |u_{2k}|, |f_{1k}|, |f_{2k}|; k = 0, 1, \ldots, K\}$ and the corresponding phase parameters $\{\mu_{1k}, \mu_{2k}, \nu_{1k}, \nu_{2k}; k = 0, 1, \ldots, K\}$. There are thus eight vectors, each with K + 1 terms, that specify the signal and filter:

$$|\underline{u}_1|, |\underline{u}_2|, |\underline{f}_1|, |\underline{f}_2|, \underline{\mu}_1, \underline{\mu}_2, \underline{\nu}_1, \underline{\nu}_2 \quad .$$

The vertical and horizontal signal component magnitudes, $|\underline{u}_1|$ and $|\underline{u}_2|$, are linked by an energy constraint:

$$\text{Signal Energy} = \sum_{i=1}^{2} \sum_{k=0}^{K} |u_{ik}|^2 = 1 \quad . \tag{5-35}$$

The coefficients $|\underline{u}_1|$ and $|\underline{u}_2|$ are scaled in order to satisfy (5-35) before they are used to evaluate SIR at each stage of the simplex algorithm. The search for an optimum signal is thus constrained to the space of unit energy functions.

The link between $|\underline{u}_1|$ and $|\underline{u}_2|$ in (5-35) implies that a straightforward optimization technique should find all the signal magnitude coefficients (vertical and horizontal) with other coefficients (filter magnitude, signal phase, and filter phase) held fixed. The same is true of the filter magnitude coefficients if one uses the constraint

$$\text{Filter Energy} = \sum_{i=1}^{2} \sum_{k=0}^{K} |f_{ik}|^2 = 1 \quad . \tag{5-36}$$

It can be argued that a constraint on filter energy is unnecessary because SIR is insensitive to multiplication of $\underline{f}(t)$ by a nonzero scalar constant. For ease in interpreting the results as well as for faster convergence, however, (5-36) has been implemented as well as (5-35). The resulting simplex algorithm automatically energy normalizes all signal or filter magnitude coefficients before evaluating SIR, and the method iteratively optimizes signal magnitude, filter magnitude, signal phase, and filter phase with all other components held fixed.

6.0 TESTING THE SIR MAXIMIZATION ALGORITHM: A SIMPLE EXAMPLE

This section describes a simple test of a computer optimization program for maximization of signal-to-interference ratio (SIR). The test demonstrates the basic input/output parameters of the program. The results are reasonable from an analytical viewpoint, indicating that the algorithm is working properly.

The test is incomplete in two important respects which will be addressed further on in the report. First, there is no polarization-dependent random Doppler or frequency spread difference between target and clutter (or, alternatively, no Doppler-dependent polarization effects). Second, only the first SIR filter is found, whereas we have shown that additional filters can be used to implement a Bayes optimum detector (likelihood ratio test) for discriminating signal from interference.

6.1 Description of the Simple Test Problem

The polarimetric scattering function for dipoles that are uniformly distributed in vertical tilt between $\pm\alpha(\phi,\tau)$ is given by (4-14).

As a simple test case, let the target dipoles be nearly vertical ($-1° \leq \alpha \leq 1°$) and let the clutter dipoles be oriented randomly ($-90° \leq \alpha \leq 90°$). In this case, if $E(\sigma^2|\phi,\tau) = 1$, the target scattering function is

$$S^b_{ijmn}(\phi,\tau) \cong \begin{cases} p_b(\phi,\tau) & \text{if} \quad i = j = m = n = 1 \\ 0 & \text{otherwise} \end{cases}, \tag{6-1}$$

and the polarimetric scattering function of the clutter is

$$S^c_{ijmn}(\phi,\tau) = \begin{cases} (3/8)\ p_c(\phi,\tau) & \text{if} \quad i = j = m = n = 1 \text{ or } 2 \\ (1/8)\ p_c(\phi,\tau) & \text{if} \quad i \neq j \quad \text{and} \quad m \neq n \\ \qquad \text{or} & \text{if} \quad i = j \neq m = n \\ 0 & \text{otherwise} \end{cases}, \tag{6-2}$$

where $p_b(\phi,\tau)$ is the distribution of the target in Doppler and range, and $p_c(\phi,\tau)$ is the corresponding clutter distribution. In order to accentuate discrimination on the basis of polarization, it will be assumed that $p_b(\phi,\tau)$ equals $p_c(\phi,\tau)$. This assumption eliminates features that are generally used for non-polarimetric SIR maximization.

6.2 Analytical Investigation of the Simple Test Case

The signal-to-interference ratio is

$$SIR = \frac{E[\,|\text{filter response}|^2 | \text{target echo alone}]}{E[\,|\text{fltr. resp.}|^2 | \text{clutter}] + E[\,|\text{fltr. resp.}|^2 | \text{noise}]} \quad . \tag{6-3}$$

Substituting (6-1) into (3-10)

$$E\{|\text{fltr. resp.}|^2 | \text{target}\} \cong \int_{-\infty}^{\infty}\int p_b(\phi,\tau)\,|\chi_{f_1u_1}(\tau,\phi)|^2 d\tau\, d\phi \quad . \tag{6-4}$$

Substituting (6-2) into (3-10)

$$E\{|\text{fltr. resp.}|^2 | \text{clutter}\} = \frac{1}{8} \int_{-\infty}^{\infty}\int p_c(\phi,\tau)\ \Sigma(\tau,\phi)\ d\tau\, d\phi \tag{6-5}$$

where

$$\Sigma(\tau,\phi) = \frac{3}{8}\,|\chi_{f_1u_1}(\tau,\phi)|^2 + \frac{3}{8}\,|\chi_{f_2u_2}(\tau,\phi)|^2$$

$$+ \frac{1}{8}\,|\chi_{f_1u_2}(\tau,\phi)|^2 + \frac{1}{8}\,|\chi_{f_2u_1}(\tau,\phi)|^2$$

$$+ \frac{1}{8}\,\{2\,\mathrm{Re}[\chi^*_{f_1u_1}(\tau,\phi)\ \chi_{f_2u_2}(\tau,\phi)]\}$$

$$+ \frac{1}{8} \{2\,\mathrm{Re}[\chi^{*}_{f_1u_2}(\tau,\phi)\ \chi_{f_2u_1}(\tau,\phi)]\}$$

$$= \frac{1}{4} [\,|\chi_{f_1u_1}|^2 + |\chi_{f_2u_2}|^2]$$

$$+ \frac{1}{8} [\,|\chi_{f_1u_1} + \chi_{f_2u_2}|^2 + |\chi_{f_1u_2} + \chi_{f_2u_1}|^2] \quad . \tag{6-6}$$

Finally, the noise response is

$$E[\,|\text{fltr. resp.}|^2|\text{noise}] = \frac{N_o}{2} [\chi_{f_1f_1}(0,0) + \chi_{f_2f_2}(0,0)]$$

$$\equiv N_o/2 \quad . \tag{6-7}$$

In the computer algorithm, N_o is set equal to 0.02 in order to allow the SIR to be dominated by clutter. The filter energy in (6-7) is constrained to be unity, as is the signal energy (the sum of the squares of the vertical and horizontal signal components).

Even with all our simplifications, it is still difficult to analytically obtain a signal-filter pair to maximize SIR. It is possible, however, to suggest two different solutions on the basis of physical and mathematical insight.

From a physical viewpoint, we observe that the target dipoles are nearly vertical, while the clutter dipoles are uniformly distributed in orientation. From this viewpoint, we would expect all signal and filter energy to be concentrated in the vertical direction, while the horizontal components should have zero energy. Our physical-insight solution is then

$$\hat{u}_2(t) = \hat{f}_2(t) = 0 \quad , \tag{6-8}$$

which implies that

$$\hat{SIR} = \frac{\iint_{-\infty}^{\infty} p_b(\phi,\tau) |\chi_{\hat{f}_1\hat{u}_1}(\tau,\phi)|^2 d\tau\, d\phi}{3/8 \iint_{-\infty}^{\infty} p_c(\phi,\tau) |\chi_{\hat{f}_1\hat{u}_1}(\tau,\phi)|^2 d\tau\, d\phi + .01}$$

$$\approx \frac{8}{3} = 2.67 \tag{6-9}$$

if

$$p_b(\phi,\tau) = p_c(\phi,\tau) \quad . \tag{6-10}$$

From a mathematical viewpoint, a possible solution is obtained by noting that the clutter response in (6-5) is minimized if $f_1(t)$, $f_2(t)$, $u_1(t)$ and $u_2(t)$ are chosen so as to minimize the right hand side of (6-6). To make the expected clutter response small, let

$$\chi_{f_1u_1} = - \chi_{f_2u_2} \quad , \tag{6-11}$$

and

$$\chi_{f_1u_2} = - \chi_{f_2u_1} \quad , \tag{6-12}$$

such that the two last terms in (6-6) are both minimized. In order for (6-11) and (6-12) to hold simultaneously, we can let

$$\tilde{u}_1(t) = - \tilde{u}_2(t) \quad , \tag{6-13}$$

$$\tilde{f}_1(t) = \tilde{f}_2(t) \quad . \tag{6-14}$$

A simple sign reversal or 180° phase shift is thus a tentative solution. In this case,

$$\widetilde{SIR} = \frac{\iint_{-\infty}^{\infty} p_b(\phi,\tau)\,|\chi_{\tilde{f}_1\tilde{u}_1}(\tau,\phi)|^2\,d\tau\,d\phi}{\frac{1}{4}\iint_{-\infty}^{\infty} p_c(\phi,\tau)[\,|\chi_{\tilde{f}_1\tilde{u}_1}|^2 + |\chi_{\tilde{f}_2\tilde{u}_2}|^2]\,d\phi\,d\tau + .01} \qquad (6\text{-}15)$$

where (6-13) and (6-14) imply that

$$|\chi_{\tilde{f}_1\tilde{u}_1}(\tau,\phi)|^2 = |\chi_{\tilde{f}_2\tilde{u}_2}(\tau,\phi)|^2 \quad . \qquad (6\text{-}16)$$

Substituting (6-16) into (6-15), we have

$$\widetilde{SIR} \cong 2 \quad , \qquad (6\text{-}17)$$

where $p_b(\phi,\tau) = p_c(\phi,\tau)$ as in (6-10).

Physical insight and the form of the clutter response in (6-5) and (6-6) have suggested two possible solutions to the SIR maximization problem. The first solution yields the larger SIR, but this solution is only expected to be optimum when the target dipoles are vertical and all the clutter dipoles are horizontal. In the given problem, clutter dipole orientations are not all horizontal, but are uniformly distributed with respect to tilt angle.

6.3 Computer Solution for the Test Case

A computer solution for the test case has been generated with the algorithm described in Section 5. From Eq. (3-12) the target scattering function is

$$S^{b}_{ijmn}(\phi,\tau) = E\{b_{ij}\ b^{*}_{mn}|\phi,\tau\}\ p_b(\phi,\tau) \quad , \tag{6-18}$$

where

$$E\{b_{ij}\ b^{*}_{mn}|\phi,\tau\} = \int_{\theta=-\pi/2}^{\pi/2} \int_{\sigma=0}^{\infty} b_{ij}(\sigma,\theta)\ b^{*}_{mn}(\sigma,\theta)$$

$$p_b(\sigma,\theta|\phi,\tau)\ d\sigma\ d\theta \quad . \tag{6-19}$$

Expression (6-19) is the description of the target that is employed in the SIR maximization algorithm. In addition to (6-19), one must also specify the distribution $p_b(\phi,\tau)$ as in (6-18). Similar expressions are used for the clutter.

The input to the computer program was thus $E\{b_{ij}\ b^{*}_{mn}|\phi,\tau\}$ as given by (4-14) for the target, with $\alpha = \pi/180°$ radians. For the clutter, $E\{c_{ij}\ c^{*}_{mn}|\phi,\tau\}$ was also given by (4-14), but with $\alpha = \pi/2$. The distributions $p_b(\phi,\tau)$ and $p_c(\phi,\tau)$ were both uniform on the τ,ϕ plane, extending from -T to T in range and from $-4\pi/T$ to $4\pi/T$ in Doppler, where T is the duration of the signal.

The iterations that were performed by the computer are described and documented in Appendix B. Two runs were made. In the first run, the magnitudes of signal and filter Fourier coefficients were adjusted first, with the phases held fixed. The phases were then adjusted with magnitudes held fixed, etc. In the second run, the phases were adjusted

first. The results are in terms of the Fourier coefficients of the signal and filter functions, i.e., the parameters $\{|u_{ik}|, |f_{ik}|, \mu_{ik}, \nu_{ik}; i = 1,2; k = 0, \ldots, 4\}$ in the expansions (5-1) and (5-2). For the first run, the vertically polarized signal and filter components of the solution are

$$
\begin{aligned}
u_{10} &= 0.317\, e^{j\pi} & f_{10} &= 0.307\, e^{j0} \\
u_{11} &= 0.411\, e^{j\pi} & f_{11} &= 0.516\, e^{j0} \\
u_{12} &= 0.599\, e^{j\pi} & f_{12} &= 0.555\, e^{j0} \\
u_{13} &= 0.359\, e^{j\pi} & f_{13} &= 0.353\, e^{j0} \\
u_{14} &= 0.281\, e^{j\pi} & f_{14} &= 0.141\, e^{j0} \quad ,
\end{aligned}
\tag{6-20}
$$

and the horizontally polarized components are

$$
\begin{aligned}
u_{20} &= 0.143\, e^{j0} & f_{20} &= 0.119\, e^{j0} \\
u_{21} &= 0.139\, e^{j0} & f_{21} &= 0.333\, e^{j0} \\
u_{22} &= 0.293\, e^{j0} & f_{22} &= 0.191\, e^{j0} \\
u_{23} &= 0.138\, e^{j0} & f_{23} &= 0.128\, e^{j0} \\
u_{24} &= 0.141\, e^{j0} & f_{24} &= 0.097\, e^{j0} \quad .
\end{aligned}
\tag{6-21}
$$

The resulting SIR is 2.697, which is better than either $\hat{SIR}$ in (6-9) or $\tilde{SIR}$ in (6-17). The solution, however, seems to be a compromise between Eq. (6-8) and Eqs. (6-13) and (6-14). The horizontally polarized signal and filter functions in (6-21) have less energy than the vertically polarized functions in (6-20), but the horizontal energy has not been driven to zero as in (6-8). The vertical signal has been multiplied by $\exp(j\pi) = -1$ as in (6-13), but (6-11) is obviously violated.

The second run, which starts by optimzing coefficient phases rather than magnitudes, yields somewhat different coefficient values (see Appendix B). Nevertheless, the same multiplication of $u_1(t)$ by -1 and a similar imbalance of energy in favor of the vertical components is again observed, and the SIR is 2.680.

7.0 DETECTION OF AN EXTENDED TARGET IN SEA CLUTTER

In this section, the SIR maximization algorithm is applied to a more challenging problem with some practical significance. The goal is to apply the method to a problem that involves Doppler dependent polarization modulation. Such a problem arises naturally in the context of radar sea echo. The dipole modelling concept in Section 4 is especially useful in this context.

Sea clutter can be said to possess Doppler dependent radar reflectivity and polarization properties. Doppler spread, however, is not really the independent variable; radar reflectivity and polarization both depend upon wind speed, and so does Doppler spread.

According to M. Skolnik's Radar Handbook, p. 26-14: "In calm seas with little wind, the echo obtained with horizontal polarization is considerably less than that with vertical polarization. The echo with horizontal polarization increases with increasing wind speed faster than the increase with vertical polarization, so that with rough-sea conditions

there is less difference in the magnitude of the echo from horizontal or vertical polarization." [6]

According to p. 26-30 of [6], some measurements indicate that the spectral width of sea echo is approximately proportional to wind speed. Quantities that vary with wind speed might then be said to vary with Doppler-induced frequency spread. If the sea is modelled by a collection of dipoles, then the orientations and cross sections of these dipoles are correlated with wind speed, but we can say that "polarization and cross section is Doppler dependent" if Doppler spread (ϕ), rather than wind speed, is viewed as the independent variable.

A calm sea can be represented with dipoles that are randomly distributed over a small interval in vertical angle (θ);

$$-\alpha(\phi) \leq \theta \leq \alpha(\phi) \qquad (7\text{-}1)$$

where θ is the dipole tilt measured from vertical and $\alpha(\phi)$ is the maximum excursion from vertical. As wind speed increases, θ increases to as much as

$$-\pi/2 \leq \theta \leq \pi/2 \quad , \qquad (7\text{-}2)$$

yielding random polarization for high wind speed. The dipole cross section (or the density of dipole reflectors) also increases with wind speed and thus with Doppler spread (ϕ).

A boat or ship can be modelled as a collection of randomly oriented dipoles or as planar reflectors (specular point targets). These dipoles or specular glints can be assumed to be uniformly distributed over a range interval that is small relative to the clutter extent.

Translational motion of the target causes its mean Doppler frequency to be displaced from the clutter mean, while pitching and rolling cause the

target echo to exhibit some Doppler spread about the mean. The radar cross sections of the dipoles or specular glints comprising the target are independent of wind speed and thus of ϕ.

It will be of interest to determine the effect of the dipole model vs. the planar reflector target model upon receiver design and performance. If a significant difference exists, then it should be possible to discriminate a target composed of planar reflectors from a chaff cloud composed of randomly oriented dipoles. For planar point scatterers, the scattering matrix is $\sigma\underline{I}$ where $\underline{I}$ is the identity matrix; $b_{11} = b_{22} = \sigma$ while $b_{12} = b_{21} = 0$. It follows that, for planar point targets,

$$E\{b_{ij}\, b^{*}_{mn} | \tau, \phi\} = \begin{cases} E(\sigma^2) & \text{if} \quad i = j \quad \text{and} \quad m = n \\ \\ 0 & \text{otherwise} \quad . \end{cases} \tag{7-3}$$

7.1 Target and Clutter Descriptions

The models used here portray the qualitative description of sea clutter in [6] with the simplest possible functions: Uniform probability distributions and linear dependence on Doppler spread.

7.1.1 Random Dipole Target

For the random dipole target, we use (4-14) with

$$\alpha(\phi, \tau) \equiv \alpha_b = \pi/2 \quad , \tag{7-4}$$

which means that target dipoles are uniformly distributed at all possible angles, and

$$E\{\sigma_b^2 | \phi, \tau\} = 10/3 \quad , \tag{7-5}$$

which corresponds to a uniform distribution of dipole reflectivity σ between zero and 10 dB.

The distribution of the target on the range-Doppler plane completes the target scattering function description in (4-14). Let

$$p_b(\phi,\tau) = \left[\frac{T}{4\pi}\ \text{rect}\ \left(\frac{\phi - 2\pi/T}{2\pi/T}\right)\right]\left[\frac{5}{2T}\ \text{rect}\left(\frac{\tau}{T/5}\right)\right] , \qquad (7\text{-}6)$$

where

$$\text{rect}(x) = \begin{cases} 1 , & -1 \leq x \leq 1 \\ 0 , & \text{otherwise} . \end{cases} \qquad (7\text{-}7)$$

The target scatterer distribution has a Doppler spread of $2\pi/T$ on either side of a mean Doppler frequency. The mean Doppler shift is equal to $2\pi/T$, corresponding to translational motion. The signal duration is T, so that $2\pi/T$ denotes a Doppler resolution cell or bin width. The delay spread of the target is $2T/5$ seconds, or two range resolution cells. A range resolution cell for a single frequency component T seconds long is $\sim T$ seconds. Five frequency components yield five times the bandwidth, and the range resolution cell is thus approximately $T/5$ seconds. A top view of $p_b(\phi,T)$, looking down on the range-Doppler plane, is shown in Figure 7-1.

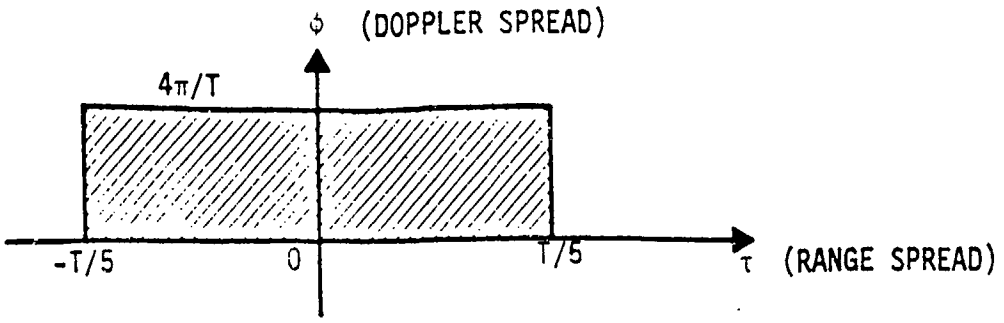

Figure 7-1. Range-Doppler distribution of target scatterers

7.1.2 Specular Glint Target

A collection of specular (planar target) glints is specified by $E\{b_{ij}\, b^{*}_{mn} \,|\tau, \phi\}$ in (7-3) and by $p_b(\tau, \phi)$. It can be assumed that $E(\sigma_b^2)$ equals 10/3 as in (7-5) and that $p_b(\tau, \phi)$ is the same as in (7-6) and Figure 1.

7.1.3 Sea Clutter at Low Wind Speed (Calm Sea)

Let the maximum tilt of the clutter dipoles be given by a linear function of Doppler magnitude:

$$\alpha_c(\phi) = \frac{10\pi}{180} + \frac{80\pi}{180}\ \frac{|\phi|}{(8\pi/T)} \quad . \tag{7-8}$$

The average clutter dipole cross section is defined as

$$E\{\sigma_c{}^2 |\phi\} = \frac{1}{3}\left[1 + \frac{9|\phi|}{8\pi/T}\right] \quad , \tag{7-9}$$

which is another linear function of Doppler magnitude. The sea's polarization spread and reflectivity are thus assumed to be linearly dependent upon Doppler spread, which is itself monotone increasing with wind speed. If the true variation of maximum dipole tilt α_c with wind speed W is $\alpha_c = g(W)$, and if Doppler spread is related to wind speed by $|\phi| = h(W)$, then our simple model assumes that $g[h^{-1}(|\phi|)]$ is linear.

Plots of $\alpha_c(\phi)$ and $E\{\sigma_c^2|\phi\}$ are shown in Figures 7-2 and 7-3. For a calm sea, these plots are only relevant for $|\phi| \leq 2\pi/T$, since it is assumed that

$$p_c(\phi,\tau) = \frac{T}{4\pi} \text{ rect}\left(\frac{\phi}{2\pi/T}\right) \frac{1}{2T} \text{ rect}\left(\frac{\tau}{T}\right) \quad , \tag{7-10}$$

i.e., a calm sea has no Doppler spread beyond $|\phi| = 2\pi/T$. The area of the τ,ϕ plane covered by $p_c(\phi,\tau)$ is shown in Figure 7-4.

The assumption that $p_c(\phi,\tau)$ is uniformly distributed on (-T,T) in the delay (τ) direction is equivalent to an assumption of uniformly distributed clutter for all ranges. This equivalence follows from the fact that the ambiguity function is nonzero only over a delay interval between -T and T when the target is hypothesized to be at delay zero.

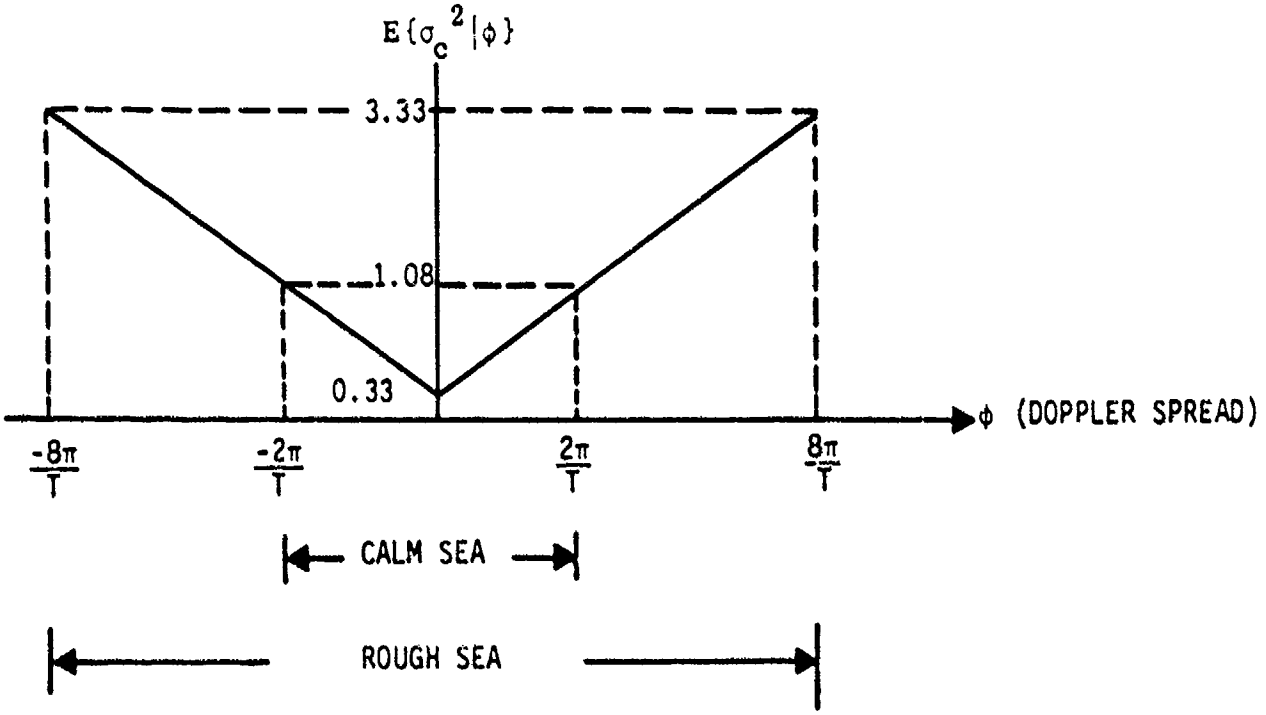

Figure 7-2. Assumed variation of clutter dipole cross section with maximum clutter Doppler spread

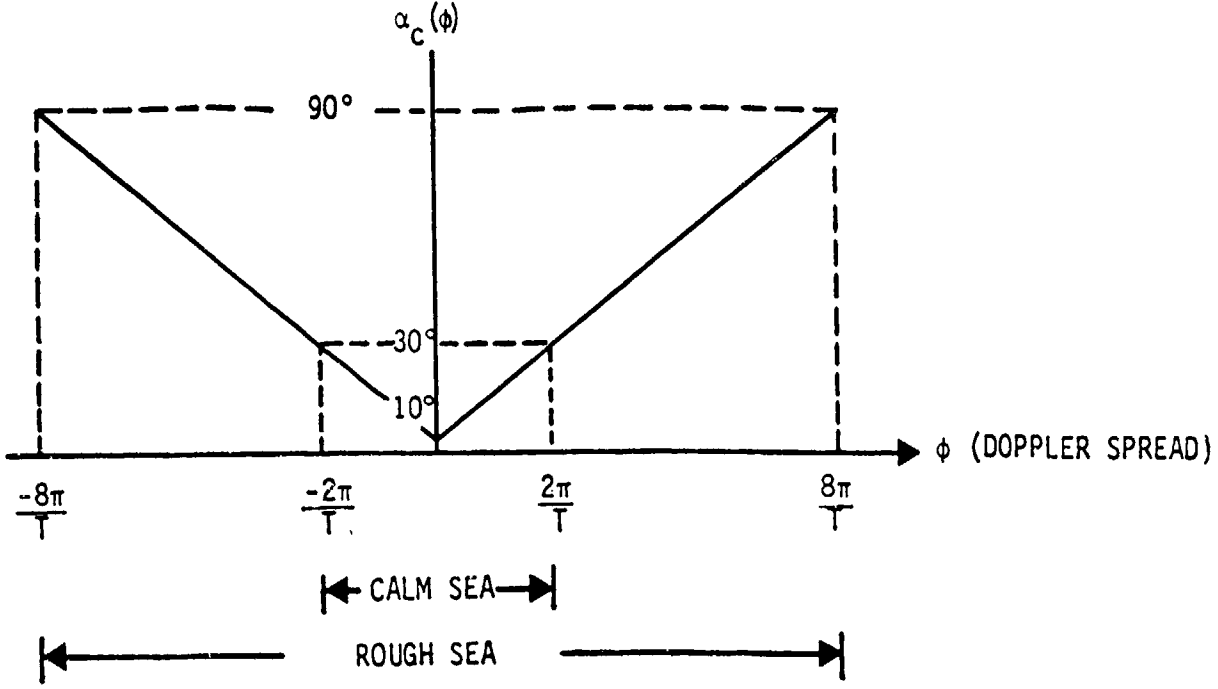

Figure 7-3. Assumed maximum effective dipole tilt relative to vertical (for a distributed dipole model of sea clutter) as a function of maximum clutter Doppler spread.

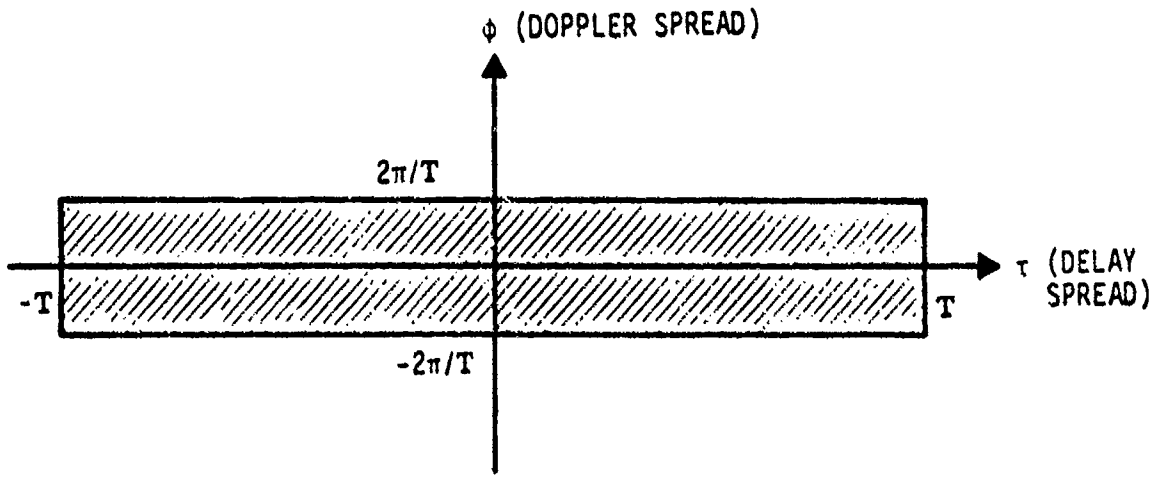

Figure 7-4. Assumed delay-Doppler distribution of sea clutter for low wind speed (calm sea)

7.1.4 Sea Clutter at High Wind Speed (Rough Sea)

For a distributed dipole model of sea clutter, it has been assumed that the maximum tilt of any dipole is $\alpha_c(\phi)$, and that the tilt is uniformly distributed between $-\alpha_c(\phi)$ and $\alpha_c(\phi)$. To be consistent with the observations in [6], the maximum tilt should increase monotonically with ϕ until, at maximum wind speed and Doppler spread, $\alpha_c(\phi_{max})$ equals $\pi/2$. At maximum wind speed, vertically and horizontally polarized dipoles are equally likely, and there is no preferred polarization for minimizing sea echo.

A simple linear dependence of $\alpha_c(\phi)$ on $|\phi|$ can accomplish the above objectives. This dependence is the same as in (7-8), provided that

$$|\phi_{max}| \equiv 8\pi/T \quad . \tag{7-11}$$

The resulting maximum tilt as a function of ϕ is shown in Figure 7-3.

The experimentally observed increase in sea clutter cross section with increasing wind speed or Doppler is modelled as in (7-9). For Doppler shifts limited as in (7-11), the expected clutter cross section varies between 0.33 and 3.33, as shown in Figure 7-2.

The assumed distribution of sea clutter in delay and Doppler for a rough sea is:

$$p_c(\phi,\tau) = \left[\frac{T}{16\pi}\ \text{rect}\left(\frac{\phi}{8\pi/T}\right)\right]\left[\frac{1}{2T}\ \text{rect}\left(\frac{\tau}{T}\right)\right] \quad , \tag{7-12}$$

so that the maximum Doppler spread is given by (7-11). The area covered by this distribution is shown in Figure 7-5.

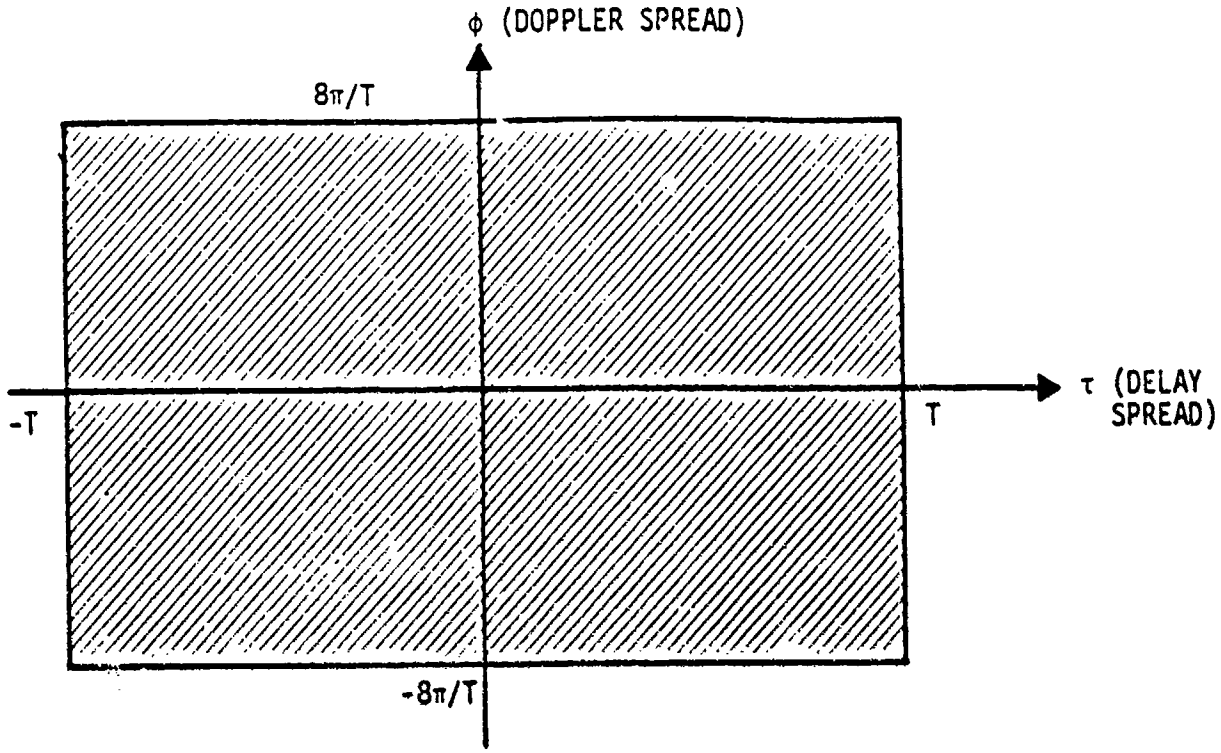

Figure 7-5. Assumed delay-Doppler distribution of sea clutter for high wind speed (rough sea)

7.2 Computer Experiments

The SIR maximization program has been applied to signal-filter design for the situations given in Table 1. In most cases, only one filter has been associated with the optimum signal. It was shown in Section 2, however, that multiple orthogonal filters should be obtained in order to implement a Bayes optimum detector as well as one with maximum signal to interference ratio. The additional filters are easy to find by always using the signal that yields largest SIR with the first filter, i.e., the signal associated with the "best" signal-filter pair. Additional filter functions, orthogonal to the ones found previously, are then determined such that SIR is maximized with the given signal. Since a simplex algorithm is used, orthogonalization is accomplished by using initial "guesses" or simplex vertices that are all orthogonal to previous solutions. The solution from such an initial simplex is in the subspace defined by the "guesses," and is thus orthogonal to previously derived filter functions for SIR maximization. Multiple orthogonal filters were found for two cases: the specular glint (planar) distributed target in rough sea clutter and the same target type in uniformly distributed dipoles (chaff). The latter problem is described in Section 7.5. The last line of Table 1 refers to a polarimetric interference canceller to be discussed in Section 7.6. This device computes the weighted difference between the outputs of a signal detector with maximum SIR and a clutter detector with minimum SIR.

TABLE 1

COMPUTER EXPERIMENTS

Target Model	Clutter Model	Receiver Configuration
Random dipole	Calm sea	One filter (H and V components)
Random dipole	Rough sea	One filter (H and V components)
Specular glint	Calm sea	One filter (H and V components)
Specular glint	Rough sea	One filter (H and V components)
Specular glint	Rough sea	Many orthogonal filters
Specular glint	Random dipole (chaff)	One Filter (H and V components)
Specular glint	Random dipole (chaff)	Many orthogonal filters
Specular glint	Random dipole (chaff)	Polarimetric interference canceller

7.3 Results for the Random Dipole Target Model in Calm and Rough Seas

If the target is a collection of randomly oriented dipoles and the clutter is composed of nearly vertical dipoles, the problem is very similar to the simple one that was analyzed in Section 6. The solution for sea clutter would then be a system with energy concentrated in the horizontal signal and filter channels, with one signal component phase shifted by 180°.

In the sea clutter problem, a difference in range-Doppler clutter distributions has been introduced. The target has a measurable average Doppler displacement relative to the clutter, and the range extent of the target is restricted. These two changes should ideally result in signals with large time-bandwidth product. If the best strategy is to exploit only Doppler resolution, however, then the signal energy will become concentrated at a single Doppler component, and the filter energy will do the same.

In summary, a reasonable solution would involve horizontally polarized signal and filter functions, with signal or filter phase shifted by 180° and with energy concentrated at one frequency to exploit Doppler displacement between target and clutter.

A similar solution has been obtained by the SIR maximization algorithm. For a calm sea, the vertically polarized signal Fourier components $\{u_{10}, u_{11}, \ldots, u_{14}\}$ and vertically polarized filter components $\{f_{10}, f_{11}, \ldots, f_{14}\}$ are relatively small:

$$\begin{aligned} u_{10} &= 0.003 \exp(j\pi) & f_{10} &= 0.009 \exp(j0) \\ u_{11} &= 0.037 \exp(j\pi) & f_{11} &= 0.002 \exp(j0) \\ u_{12} &= 0.007 \exp(j\pi) & f_{12} &= 0.003 \exp(j0) \\ u_{13} &= 0.015 \exp(j\pi) & f_{13} &= 0.005 \exp(j0) \\ u_{14} &= 0.005 \exp(j\pi) & f_{14} &= 0.003 \exp(j0) \end{aligned} \qquad (7\text{-}14)$$

The horizontally polarized signal and filter components for a calm sea are

$$\begin{aligned} u_{20} &= 0.222 \exp(j0) & f_{20} &= 0.454 \exp(j0) \\ u_{21} &= 0.602 \exp(j0) & f_{21} &= 0.755 \exp(j0) \\ u_{22} &= 0.630 \exp(j0) & f_{22} &= 0.469 \exp(j0) \\ u_{23} &= 0.407 \exp(j0) & f_{23} &= 0.056 \exp(j0) \\ u_{24} &= 0.152 \exp(j0) & f_{24} &= 0.003 \exp(j0) \end{aligned} \qquad (7\text{-}15)$$

and the resulting signal-to-interference ratio for a calm sea is

$$SIR = 51.54 \quad . \qquad (7\text{-}16)$$

In Eq. (7-15), there appears to be a mismatch between signal and filter, such that the filter pass band is approximately a frequency shifted version of the transmitted signal spectrum. The shift is approximately one frequency component downward. From Fig. 7-1, the average target Doppler shift is exactly one frequency resolution cell, $2\pi/T$. A positive ϕ-value in Fig. 7-1 corresponds to a target with range increasing with time, which means that the echo is shifted downward in frequency by an average Doppler displacement corresponding to one frequency component. A filter matched to the expected echo will then have a transfer function that is a downward-shifted version of the signal spectrum, as observed in (7-15). The simplex SIR maximization algorithm used three iterations for adjustment of each set of coefficients (signal phase, filter phase, signal magnitude, filter magnitude). The total run time for computer design of the polarimetric radar was about six hours, but the program used disk storage for many computed variables. Subsequent examples were computed using large RAM arrays, and run time was reduced to approximately two hours.

For a rough sea, slightly more energy is relegated to the vertically polarized signal and filter components, as one would expect from Figure 7-3. For the calm sea case, part of the target Doppler spread is outside the

Doppler band of the clutter, as shown by Figures 7-1 and 7-4. For the rough sea, the target Doppler spread is wholly immersed in the clutter, as shown by Figures 7-1 and 7-5. This difference, along with larger average clutter reflectivity, leads to a smaller maximum SIR for rough seas.

The vertically polarized signal and filter components for the rough sea model, as obtained by the SIR optimization algorithm, are:

$$\begin{aligned} u_{10} &= 0.019 \exp(j\pi) & f_{10} &= 0.011 \exp(j0) \\ u_{11} &= 0.122 \exp(j\pi) & f_{11} &= 0.010 \exp(j0) \\ u_{12} &= 0.061 \exp(j\pi) & f_{12} &= 0.044 \exp(j0) \\ u_{13} &= 0.017 \exp(j\pi) & f_{13} &= 0.002 \exp(j0) \\ u_{14} &= 0.021 \exp(j\pi) & f_{14} &= 0.005 \exp(j0) \end{aligned} \qquad (7\text{-}17)$$

The horizontally polarized signal and filter components for a rough sea are:

$$\begin{aligned} u_{20} &= 0.203 \exp(j0) & f_{20} &= 0.422 \exp(j0) \\ u_{21} &= 0.758 \exp(j0) & f_{21} &= 0.809 \exp(j0) \\ u_{22} &= 0.598 \exp(j0) & f_{22} &= 0.406 \exp(j0) \\ u_{23} &= 0.076 \exp(j0) & f_{23} &= 0.002 \exp(j0) \\ u_{24} &= 0.030 \exp(j0) & f_{24} &= 0.003 \exp(j0) \end{aligned} \qquad (7\text{-}18)$$

The above signal and filter functions yield a signal-to-interference ratio for the rough sea clutter model of

$$SIR = 26.83 \quad . \qquad (7\text{-}19)$$

As one would expect, this SIR is considerably less than for a calm sea.

The signal and filter functions for SIR maximization for a random dipole target in sea clutter combine Doppler resolution with accentuation of horizontally polarized energy. As in the simple test case in Section 6, the vertical signal components are all multiplied by minus one or $\exp(j\pi)$.

This result is not generally exploited by sea surface search radars, and the design may yield improved performance in rough seas.

7.4 Results for the Range-Distributed Planar Target (Specular Glint) Model in Calm and Rough Seas

The specular glint target model is similar to the classical non-polarimetric concept of a distributed target composed of randomly spaced "highlights" or points of high reflectivity that behave as perfect mirrors (planar reflectors). These highlights are assumed to have the same cross section as the corresponding dipoles in the distributed dipole target model, i.e., $E[\sigma^2]$ is the same in (7-3) and (4-14).

The same values of $E[\sigma^2]$ in (7-3) and (4-14), however, seem to make the planar target more detectable. For example, if the target dipoles are randomly tilted such that α equals $\pi/2$ in (4-14), we have

$$S_{ijmn}(\phi,\tau)\Big|_{\substack{\text{randomly}\\ \text{tilted}\\ \text{dipoles}}} = E(\sigma^2)\, p(\phi,\tau) \begin{cases} 3/8 & \text{if } i=j=m=n=1 \text{ or } 2 \\ 1/8 & \text{if } i\neq j \text{ and } m\neq n \\ & \text{or if } i=j\neq m=n \\ 0 & \text{otherwise} \end{cases} \tag{7-20}$$

as in (6-2), while from (7-3),

$$S_{ijmn}(\phi,\tau)\Big|_{\substack{\text{planar}\\ \text{points}}} = E(\sigma^2)\, p(\phi,\tau) \begin{cases} 1 & \text{if } i=j=m=n=1 \text{ or } 2 \\ 1 & \text{if } i=j\neq m=n \\ 0 & \text{otherwise} \end{cases} . \tag{7-21}$$

If most signal and filter energy is horizontally polarized, then the dominant term in the polarimetric scattering function is $S_{2222}(\phi,\tau)$, which is 8/3 times larger for the planar target model than for uniformly

distributed dipoles.

Despite the difference between planar targets and randomly tilted dipoles in (7-20), a non-random dipole orientation is consistent with (7-21). For a vertically oriented dipole with $\alpha << 1$, (4-14) yields

$$S_{ijmn}(\phi,\tau)\Big|_{\substack{\text{vert}\\ \text{dipole}}} = E(\sigma^2)\; p(\phi,\tau) \begin{cases} 1 & \text{if } i=j=m=n=1 \\ 0 & \text{otherwise} \end{cases} \qquad (7\text{-}22)$$

which is commensurate with the planar point target in (7-21). A randomly oriented dipole has smaller effective cross section than the same dipole with known orientation. The planar point target cross section has been chosen to be equal to that of a dipole with known orientation, while SIR depends upon the effective cross section of a randomly oriented dipole.

The above observations imply that the effective radar cross section of a target can be reduced by more than 3 dB if different reflecting surfaces have different polarizations or effective dipole tilts. If all reflecting surfaces have the same, known polarization, then the equivalent specular glint model must use a higher glint cross section in order to represent the target.

For a calm sea, the SIR maximization algorithm with a distributed planar target model yields vertical signal and filter coefficients

$u_{10} = 0.010 \exp(j0)$ $\qquad$ $f_{10} = 0.007 \exp(j0)$
$u_{11} = 0.019 \exp(j0)$ $\qquad$ $f_{11} = 0.001 \exp(j0)$
$u_{12} = 0.002 \exp(j0)$ $\qquad$ $f_{12} = 0.005 \exp(j0)$
$u_{13} = 0.001 \exp(j0)$ $\qquad$ $f_{13} = 0.004 \exp(j0)$
$u_{14} = 0.014 \exp(j0)$ $\qquad$ $f_{14} = 0.003 \exp(j0)$

and horizontal coefficients

$$
\begin{aligned}
u_{20} &= 0.229 \exp(j0) & f_{20} &= 0.400 \exp(j0) \\
u_{21} &= 0.590 \exp(j0) & f_{21} &= 0.779 \exp(j0) \\
u_{22} &= 0.606 \exp(j0) & f_{22} &= 0.481 \exp(j0) \\
u_{23} &= 0.426 \exp(j0) & f_{23} &= 0.041 \exp(j0) \\
u_{24} &= 0.223 \exp(j0) & f_{24} &= 0.001 \exp(j0)
\end{aligned}
\qquad (7\text{-}24)
$$

The best SIR for the planar glint distributed target model in calm seas is found to be

$$\text{SIR} = 137.87 \qquad (7\text{-}25)$$

When the planar glint target model is used with our model for a rough sea, we obtain vertical coefficients

$$
\begin{aligned}
u_{10} &= 0.028 \exp(j\pi) & f_{10} &= 0.006 \exp(j0) \\
u_{11} &= 0.004 \exp(j\pi) & f_{11} &= 0.008 \exp(j0) \\
u_{12} &= 0.002 \exp(j\pi) & f_{12} &= 0.004 \exp(j0) \\
u_{13} &= 0.004 \exp(j\pi) & f_{13} &= 0.003 \exp(j0) \\
u_{14} &= 0.009 \exp(j\pi) & f_{14} &= 0.025 \exp(j0)
\end{aligned}
\qquad (7\text{-}26)
$$

and horizontal coefficients

$$
\begin{aligned}
u_{20} &= 0.212 \exp(j0) & f_{20} &= 0.340 \exp(j0) \\
u_{21} &= 0.780 \exp(j0) & f_{21} &= 0.856 \exp(j0) \\
u_{22} &= 0.578 \exp(j0) & f_{22} &= 0.388 \exp(j0) \\
u_{23} &= 0.105 \exp(j0) & f_{23} &= 0.001 \exp(j0) \\
u_{24} &= 0.017 \exp(j0) & f_{24} &= 0.000 \exp(j0)
\end{aligned}
\qquad (7\text{-}27)
$$

The corresponding SIR for a target with distributed planar (point target) reflectors in a rough sea is

$$\text{SIR} = 75.43 \quad . \qquad (7\text{-}28)$$

From our interpretation of (7-20) - (7-22), we expect that the SIR for the planar glint target model will be 8/3 or 2.67 larger than the corresponding SIR for the distributed, randomly oriented dipole target model. Indeed, for calm seas, the signal-to-interference ratio in (7-25) is 2.68 times larger than the one in (7-16), and SIR in (7-28) is 2.81 times larger than SIR in (7-19).

7.5 Results for Distributed Planar Reflectors in a Background of Randomly Oriented Dipoles

An interesting problem is to discriminate between the two target types: planar reflectors and randomly oriented dipoles. In this case, $E(\sigma^2)$ for the planar targets is set equal to 3/8 in order to compensate for the disparity between (7-20) and (7-21). The range-Doppler distribution of both targets is the same, and is shown in Figure 7-1. The only difference between the two models is that

$$S_{ijmn}(\phi,\tau)\Big|_{\substack{\text{randomly}\\ \text{tilted}\\ \text{dipoles}}} = p(\phi,\tau) \left\{ \begin{array}{l} 1/8 \quad \text{if } i \neq j \text{ and } m \neq n \\ \\ \quad \text{or if } i = j \neq m = n \end{array} \right\} \tag{7-29}$$

while

$$S_{ijmn}(\phi,\tau)\Big|_{\substack{\text{planar}\\ \text{points}}} = p(\phi,\tau) \left\{ \begin{array}{l} 3/8 \quad \text{if } i = j \neq m = n \\ \\ 0 \quad \text{if } i \neq j \text{ and } m \neq n \end{array} \right\}. \tag{7-30}$$

The SIR maximization algorithm must thus rely upon differences in S_{1122}, S_{2211}, S_{1212}, S_{1221}, S_{2112}, and S_{2121}. The first two terms are larger for the planar point target model, and the last four terms are larger for the randomly tilted dipoles.

The SIR maximization algorithm for the target discrimination problem yields vertical signal and filter coefficients

$$\begin{aligned} u_{10} &= 0.316 \exp(j0) & f_{10} &= 0.316 \exp(j0) \\ u_{11} &= 0.316 \exp(j0) & f_{11} &= 0.316 \exp(j0) \\ u_{12} &= 0.316 \exp(j0) & f_{12} &= 0.316 \exp(j0) \\ u_{13} &= 0.316 \exp(j0) & f_{13} &= 0.316 \exp(j0) \\ u_{14} &= 0.316 \exp(j0) & f_{14} &= 0.316 \exp(j0) \end{aligned} \qquad (7\text{-}31)$$

and horizontal coefficients

$$\begin{aligned} u_{20} &= 0.316 \exp(j0) & f_{20} &= 0.316 \exp(j0) \\ u_{21} &= 0.316 \exp(j0) & f_{21} &= 0.316 \exp(j0) \\ u_{22} &= 0.316 \exp(j0) & f_{22} &= 0.316 \exp(j0) \\ u_{23} &= 0.316 \exp(j0) & f_{23} &= 0.316 \exp(j0) \\ u_{24} &= 0.316 \exp(j0) & f_{24} &= 0.316 \exp(j0) \end{aligned} \qquad (7\text{-}32)$$

The corresponding signal-to-interference ratio is

$$SIR = 0.973 \quad . \qquad (7\text{-}33)$$

The above results can be explained by substituting the polarimetric scattering functions $S_{ijmn}(\alpha,\tau)$ for target or clutter into (3-10). For distributed planar reflectors, substitution of (7-21) into (3-10) yields

$$E\{|\text{target response}|^2\} = \frac{3}{8}\iint |\chi_{f_1 u_1} + \chi_{f_2 u_2}|^2 \, p(\tau,\phi) \, d\tau \, d\phi \qquad (7\text{-}34)$$

and for distributed randomly oriented dipoles

$$E\{|\text{clutter response}|^2\} = \frac{1}{8}\iint\{2[\,|\chi_{f_1u_1}|^2 + |\chi_{f_2u_2}|^2] + |\chi_{f_1u_1} + \chi_{f_2u_2}|^2 + |\chi_{f_1u_2} + \chi_{f_2u_1}|^2\}\, p(\tau,\phi)\, d\tau\, d\phi \qquad (7\text{-}35)$$

as in (6-5).

From (7-31) and (7-32), the SIR maximization algorithm has found a solution of the form

$$u_1(t) = u_2(t) = f_1(t) = f_2(t) \equiv u(t) \quad . \qquad (7\text{-}36)$$

Substitution of (7-36) into both (7-34) and (7-35) yields

$$SIR = \frac{3/2 \iint |\chi_{uu}(\tau,\phi)|^2\, p(\tau,\phi)\, d\tau\, d\phi}{3/2 \iint |\chi_{uu}(\tau,\phi)|^2\, p(\tau,\phi)\, d\tau\, d\tau + N_0/2} \qquad (7\text{-}37)$$

$$\approx 1,$$

as in (7-33).

It can be shown from (7-34) and (7-35) that the same SIR value is obtained if all signal and filter energy is concentrated in one polarization channel (either horizontal or vertical). This result seems to imply that polarimetric radar is not superior to non-polarimetric radar with respect to detection of planar target distributions in chaff composed of randomly oriented dipoles, despite the differences between (7-29) and (7-30). It will be demonstrated, however, that polarimetric radar is

superior if a clutter cancellation method is used. The use of many orthogonal filters, as in Section 2, has also been investigated.

The interference cancellation concept is discussed in the next section, and the use of multiple orthogonal filters is discussed in Section 7.7.

7.6 A Polarimetric Interference Canceller

The poor detection performance implied by (7-33) and (7-37) can be greatly improved by augmenting the receiver with a second one, in parallel with the first, which estimates the interference response of the first receiver. The estimated interference is then subtracted out or cancelled.

In order to estimate interference in the possible presence of a target echo, the interference estimator should have relatively small response to the target. Such a processor will have small SIR. Alternatively, it should have large SIR for the inverse problem where target and clutter are interchanged and the target echo is viewed as interference.

For planar reflector vs. random dipole discrimination, the inverse problem, i.e., detecting an array of randomly tilted dipoles while minimizing receiver response to specular glints, yields much larger SIR than the original problem. This large SIR difference for the original and inverse problems is the key to successful clutter cancellation.

The interference cancellation concept is illustrated in Figure 7-6. Filter #2 for interference estimation should ideally be able to observe the interference in the absence of signal. In other words, the interference-to-signal ratio should be maximized by filter #2, or the output signal-to-interference ratio.

$$SIR_2 = S_2/I_2 \qquad (7\text{-}38)$$

should be minimized. Alternatively, the SIR for the inverse problem, with clutter and target interchanged, should be maximized by filter #2.

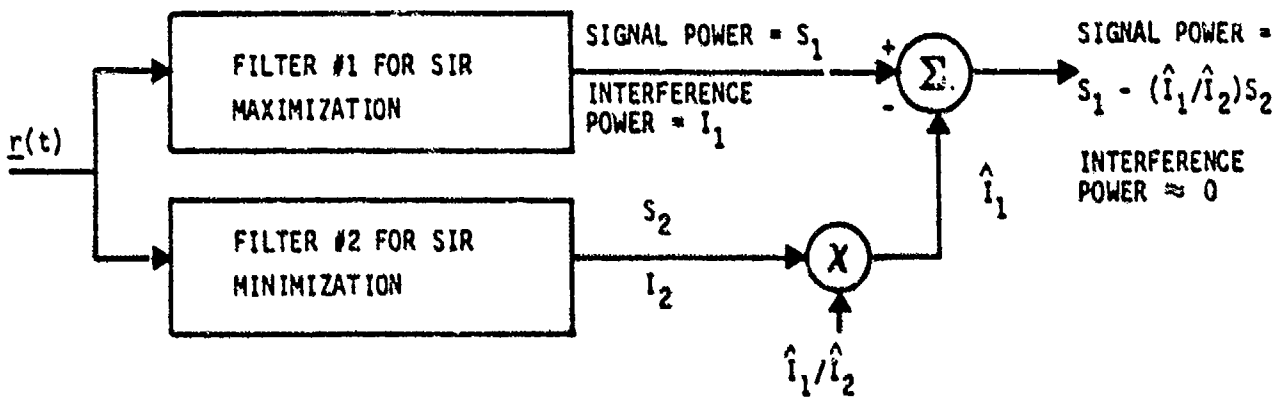

Figure 7-6. An interference canceller using filters for SIR maximization and minimization.

Figure 7-7 shows the polarimetric version of Figure 7-6. In the figures, $\hat{I}_1$ and $\hat{I}_2$ are estimated or predicted interference levels at the outputs of filter #1 and filter #2, respectively.

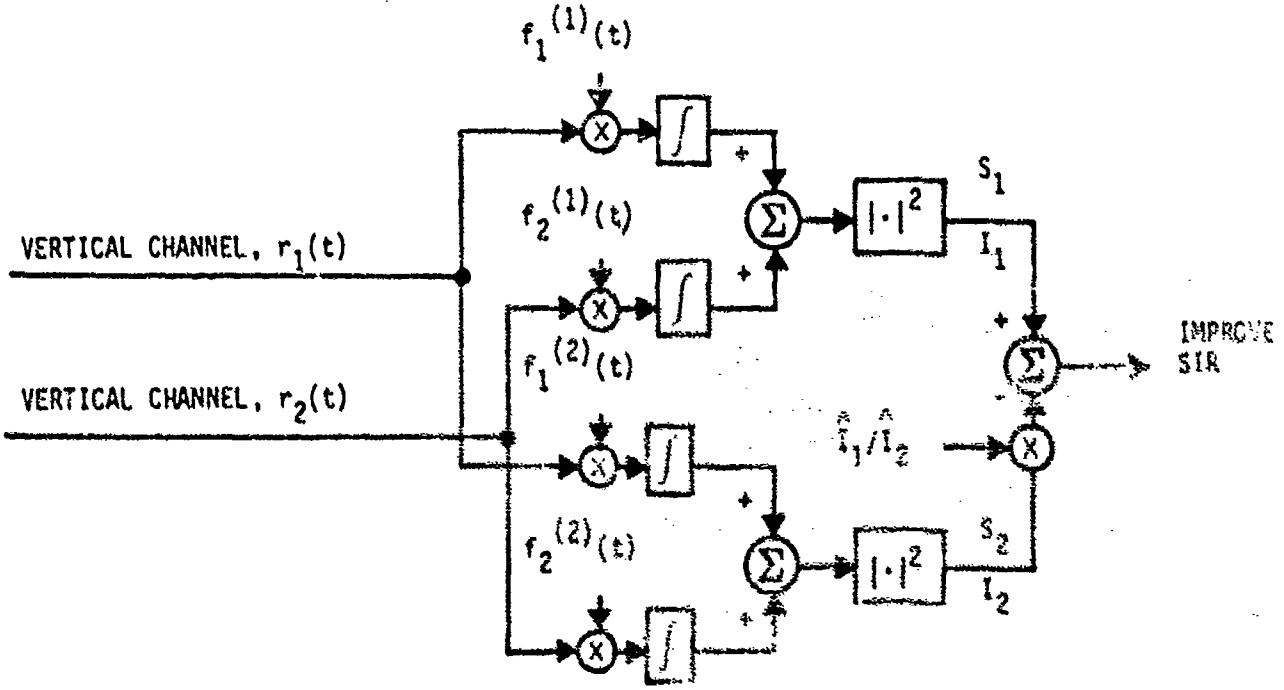

Figure 7-7. Polarimetric version of the interference canceller in Figure 7-6.

In order to accentuate the response of the interference canceller to the desired signal, the system should maximize

$$S_1 - (I_1/I_2)S_2 = S_1\left[1 - \frac{S_o/I_2}{S_1/I_1}\right] \quad , \tag{7-39}$$

which implies that filter #1 should be designed to maximize SIR, while filter #2 should be designed to minimize it, as already stated.

The expected magnitude-squared target response in (7-34) is zero for the second filter in Figure 7-7 if

$$\chi_{f_1^{(2)}u_1}(\tau,\phi) = -\chi_{f_2^{(2)}u_2}(\tau,\phi) \tag{7-40}$$

where

$$u_1(t) = u_2(t) = u(t) \tag{7-41}$$

from (7-36). Eq. (7-40) is satisfied if

$$f_2^{(2)}(t) = -f_1^{(2)}(t) = u(t) \quad . \tag{7-42}$$

In this case, the SIR for the inverse problem (target and clutter interchanged) is

$$(SIR)_{inverse} = \frac{1/2 \iint |\chi_{uu}(\tau,\phi)|^2 \, p(\tau,\phi) \, d\tau \, d\phi}{N_0/2} \quad . \tag{7-43}$$

For the receiver defined by (7-42),

$$S_2 = 0 \tag{7-44}$$

and from (7-43) and (7-37)

$$I_2 \approx \frac{1}{3} I_1 \quad . \tag{7-45}$$

The output of filter #2 should be multiplied by approximately three in order to cancel the interference in Figures 7-6 and 7-7.

The resulting inteference canceller theoretically allows the polarimetric radar to "look" through chaff. From (7-39) and (7-44), the response to the target echo or signal is unaffected, while the response to interference is greatly reduced.

Although the example given above does not exploit Doppler dependent cross-polarization effects, the general concept can be applied to a variety of problems.

7.7 Computer Results for Multiple Orthogonal Filters

The analysis in Section 2 has demonstrated that an SIR maximization result can be extended to yield a Bayes optimum detector or likelihood ratio test implementation by adding orthogonal filters, as in Figure 2-1. It would appear that the $n^{\underline{th}}$ orthogonal filter should increase SIR as well as yielding a better approximation to a likelihood ratio test. It will be shown, however, that an SIR increase does <u>not</u> occur, even though

the $n^{\underline{th}}$ filter causes P_D to increase more than P_F for sufficiently high detection threshold, γ. Although SIR is a useful measure of performance for system design, it can be misleading as a detectability measure.

7.7.1 SIR Computation when Multiple Filters are Used

Equations (2-54) and (2-55) yield the improvement in performance (P_D vs P_F) that is expected to occur from the use of multiple orthogonal filters. Another measure of performance is the signal-to-interference ratio itself, as measured at the output of the system in Figure 2-1. To compute this SIR value, one can exploit the observation that the output of each orthogonal filter is statistically independent of the output of any other filter. If the filter outputs are denoted r_1, r_2, ..., r_n, and if the $n^{\underline{th}}$ filter output is transformed with a function $f_n(r_n)$, then statistical independence implies that

$$E\left\{ \sum_{n=1}^{N} f_n(r_n) \right\} = \sum_{n=1}^{N} E\left\{ f_n(r_n) \right\} \quad . \tag{7-46}$$

For the receiver in Figure 2-1,

$$f_n(r_n) = \frac{|r_n|^2}{\lambda_{In}} \quad \frac{SIR_n}{1 + SIR_n} \tag{7-47}$$

where

$$SIR_n = \lambda_{Sn} / \lambda_{In} \quad . \tag{7-48}$$

The SIR of the whole filter bank in Figure 2-1 is the output when only signal is present, divided by the output when only interference is present. When only signal is present,

$$E\left\{|r_n|^2 \mid \text{signal}\right\} \equiv \lambda_{Sn} \tag{7-49}$$

and for interference,

$$E\left\{|r_n|^2 \mid \text{interference}\right\} = \lambda_{In} \quad . \tag{7-50}$$

It follows that

$$E\left\{\text{output} \mid \text{signal}\right\} = E\left\{\sum_{n=1}^{N} f_n(r_n) \mid \text{signal}\right\}$$

$$= \sum_{n=1}^{N} \frac{SIR_n^2}{1 + SIR_n} \tag{7-51}$$

and

$$E\left\{\text{output} \mid \text{interference}\right\} = \sum_{n=1}^{N} \frac{SIR_n}{1 + SIR_n} \quad . \tag{7-52}$$

Finally, the signal-to-interference ratio at the output of the system in Figure 2-1 is

$$SIR = \left[\sum_{n=1}^{N} \frac{SIR_n^2}{1 + SIR_n} \right] \left[\sum_{n=1}^{N} \frac{SIR_n}{1 + SIR_n} \right]^{-1} . \tag{7-53}$$

The computer optimization program yields the optimum signal, a set of optimum orthogonal filters, and the SIR value at the output of each filter, $\{SIR_n\}_{n=1}^{N}$. The SIR values can be used to compute ROC curves from (2-54) - (2-55), and to compute the overall SIR from (7-53).

Although additional filters as in Figure 2-1 are needed to implement a likelihood ratio test, (7-53) implies that additional filters do not increase SIR. It has been shown that

$$SIR_1 > SIR_2 > .... > SIR_N \tag{7-54}$$

since the SIR_n values correspond to solutions of a maximization problem with n-1 orthogonality constraints, and because SIR_n is the $n^{\underline{th}}$ largest eigenvalue of $\underline{\underline{C}}(x,y)$ in (2-18). If $SIR_n < SIR_1$ for all $n > 1$, then (7-53) becomes

$$SIR = \frac{\frac{SIR_1^2}{1 + SIR_1} \left[1 + \sum_{n=2}^{N} \left(\frac{SIR_n}{SIR_1} \right)^2 \left(\frac{1 + SIR_1}{1 + SIR_n} \right) \right]}{\frac{SIR_1}{1 + SIR_1} \left[1 + \sum_{n=2}^{N} \left(\frac{SIR_n}{SIR_1} \right) \left(\frac{1 + SIR_1}{1 + SIR_n} \right) \right]}$$

$$< SIR_1 \tag{7-55}$$

since each term in the numerator sum is equal to each term in the denominator sum, multiplied by (SIR_n/SIR_1), which is less than unity. Eq. (7-55) states that SIR for more than one filter is always less than SIR for a single "best" filter. The use of multiple orthogonal filters as in Figure 2-1 cannot be justified in terms of SIR improvement. In fact, SIR decreases, indicating a decrease in the ratio of the mean receiver output given signal to the mean receiver output given interference.

SIR, however, may not be a good measure of performance. The usual detectability index, for example, is

$$d^2 = \frac{[E\{\ell(\underline{r}) \mid H_1\} - E\{\ell(\underline{r}) \mid H_0\}]^2}{\text{Var}\{\ell(\underline{r}) \mid H_0\}}$$

$$= \frac{\left\{\sum_{n=1}^{N} \frac{SIR_n}{1+SIR_n}(SIR_n - 1)\right\}^2}{2\left[\sum_{n=1}^{N} \frac{SIR_n}{1+SIR_n}\right]^2} \qquad (7\text{-}56)$$

For N=1, i.e., for a single filter pair $\underline{f}^{(1)}(t)$, d^2 equals $\frac{1}{2}(SIR_1 - 1)^2$, which is monotone increasing with SIR_1 if $SIR_1 > 1$. The d^2 measure decreases, however, when additional filters have $SIR_n < 1$. Theoretically, such additional filters may still improve detectability. The problem is that ROC performance depends strongly on the tails of the distributions $p(\ell|H_1)$ and $p(\ell|H_0)$ in (2-54) and (2-55), while SIR and d^2 are not very sensitive to tail behavior.

The above results imply that although SIR is a useful measure for system <u>design</u>, it should be used with caution for system <u>evaluation</u>. For system evaluation, the expressions for P_D and P_F in (2-54) and (2-55) should be used. When the $n^{\underline{th}}$ filter is added in Fig. 2-1, P_D increases by

$$\Delta P_D = a_n \exp\ (-\gamma/SIR_n) \tag{7-57}$$

and P_F increases by

$$\Delta P_F = a_n' \exp\ [-\gamma(SIR_n + 1)/SIR_n] \tag{7-58}$$

$$= a_n' \exp\ (-\gamma/SIR_n) \exp\ (-\gamma)$$

where γ is the threshold level of the detector. It follows that $\Delta P_D > \Delta P_F$ if

$$a_n > a_n' \exp\ (-\gamma) \tag{7-59}$$

or if

$$\exp\ (\gamma) > a_n'/a_n = \frac{\prod_{i=1}^{n-1} \left[1 - \dfrac{SIR_i/(SIR_i + 1)}{SIR_n/SIR_n + 1)} \right]^{-1}}{\prod_{i=1}^{n-1} \left[1 - (SIR_i/SIR_n) \right]^{-1}}$$

$$= SIR_n \prod_{i=1}^{n-1} (SIR_i + 1)/SIR_i \quad . \tag{7-60}$$

The addition of the $n^{\underline{th}}$ filter will improve receiver performance if the threshold γ is such that (7-60) is satisfied. From Fig. 2-1, $\ell(\underline{r})$ is always ≥ 0, and a negative threshold value makes no sense. Therefore, it always pays to add an extra filter if the filter output has a signal-to-

interference ratio such that the right hand side of (7-60) is greater than unity. This result follows from expressions for P_D and P_F, and is not in agreement with SIR results.

7.7.2 Further Results for a Target Consisting of Distributed Planar Reflectors in Randomly Oriented Dipole Clutter

After finding the signal and filter functions $u_1(t)$, $u_2(t)$ and $f_1^{(1)}(t)$, $f_2^{(1)}(t)$ in Figure 2-1, the initial simplex is modified to include only filters that are orthogonal to $\underline{f}^{(1)}(t)$. The resulting filter function for maximum SIR is $\underline{f}^{(2)}(t)$, where the same signal components $u_1(t)$, $u_2(t)$ are assumed. After finding $u_1(t)$, $u_2(t)$, $f_1^{(1)}(t)$, $f_2^{(1)}(t)$, $f_1^{(2)}(t)$, and $f_2^{(2)}(t)$, another filter $f^{(3)}(t)$ is found, such that $\underline{f}^{(3)}(t)$ is orthogonal to both $\underline{f}^{(1)}(t)$ and $\underline{f}^{(2)}(t)$. The $n^{\underline{th}}$ filter $\underline{f}^{(n)}(t)$, has signal-to-noise ratio SIR_n, and SIR_n should decrease monotonically with n because of the extra orthogonality constraints that are included as n increases. Computer results for a target consisting of a random distribution of planar reflectors and for clutter consisting of randomly oriented dipoles or chaff (as in Section 7.5) are given in Table 2.

Substituting the values of $\{SIR_n\}_{n=1}^{6}$ into (7-53) yields an output SIR of 0.820, which is less than the SIR for one filter alone (SIR = 0.973). As predicted by (7-55), SIR is not improved by using additional orthogonal filters.

TABLE 2

COMPUTER RESULTS FOR DISTRIBUTED PLANAR REFLECTOR TARGET MODEL IN RANDOMLY ORIENTED DIPOLE CLUTTER,USING SIX ORTHOGONAL FILTERS

SIR_n and signal/filter coefficients	n=1	n=2	n=3	n=4	n=5	n=6
SIR_n	0.973	0.952	0.951	0.807	0.605	0.428
Vert. Signal	Magnitude, Phase	Magnitude, Phase	Magnitude, Phase	Magnitude, Phase	Magnitude, Phase	Magnitude, Phase
u_{10}	.316, 0	same	same	same	same	same
u_{11}	.316, 0	as	as	as	as	as
u_{12}	.316, 0	n=1	n=1	n=1	n=1	n=1
u_{13}	.316, 0					
u_{14}	.316, 0					
Horiz. Signal	Magnitude, Phase	Magnitude, Phase	Magnitude, Phase	Magnitude, Phase	Magnitude, Phase	Magnitude, Phase
u_{20}	.316, 0	same	same	same	same	same
u_{21}	.316, 0	as	as	as	as	as
u_{22}	.316, 0	n=1	n=1	n=1	n=1	n=1
u_{23}	.316, 0					
u_{24}	.316, 0					
Vert. Filter	Magnitude, Phase	Magnitude, Phase	Magnitude, Phase	Magnitude, Phase	Magnitude, Phase	Magnitude, Phase
f_{10}	.316, 0	.553,0.205	.058,.907	.186,-2.960	.075,-3.066	.302,-0.182
f_{11}	.316, 0	.071,-2.331	.376,-3.131	.058,2.496	.356,-0.055	.418,-3.016
f_{12}	.316, 0	.283,-2.940	.119,-3.073	.251,-2.873	.243,2.702	.652,0.005
f_{13}	.316, 0	.217,-2.787	.492,-.008	.264,-3.084	.205,2.768	.397,3.082
f_{14}	.316, 0	.020,-1.026	.167,.020	.841,-0.029	.248,0.410	.180,-0.145
Horiz. Filter	Magnitude, Phase	Magnitude, Phase	Magnitude, Phase	Magnitude, Phase	Magnitude, Phase	Magnitude, Phase
f_{20}	.316, 0	.535,0.013	.068,0.133	.233,2.854	.392,-0.254	.131,1.696
f_{21}	.316, 0	.050,-0.595	.546,-3.125	.086,-0.222	.355,2.995	.138,2.819
f_{22}	.316, 0	.491,2.868	.165,-3.074	.166,2.361	.454,-0.783	.117,-0.691
f_{23}	.316, 0	.159,2.834	.486,0.020	.045,1.354	.116,-2.017	.040,-1.751
f_{24}	.316, 0	.076,-1.229	.066,3.016	.175,-0.625	.454,2.635	.259,2.980

7.7.3 Further Results for a Target Consisting of Distributed Planar Reflectors in Sea Clutter

The use of multiple orthogonal filters has also been investigated for detection of a distributed target consisting of planar reflectors in rough sea clutter. The results are given in Table 3. The signal and the first filter in Table 3 are the same as those given by (7-26) and (7-27), and SIR_1 is the same as in (7-28).

Substituting the values of $\{SIR_n\}_{n=1}^{N}$ into (7-53) yields the following overall SIR values as a function of N, the number of filters used. For a single filter, N=1,

$$N=1;\ SIR = SIR_1 = 75.43 \quad . \tag{7-61}$$

For two filters,

$$N=2;\ SIR = 72.95 \quad . \tag{7-62}$$

For three filters,

$$N=3;\ SIR = 60.08 \quad . \tag{7-63}$$

For four filters,

$$N=4;\ SIR = 48.46 \quad . \tag{7-64}$$

For five filters,

$$N=5;\ SIR = 44.11 \quad . \tag{7-65}$$

Again, SIR decreases even though better detectability is theoretically obtained from (7-57) - (7-60) as more filters are added.

TABLE 3

COMPUTER RESULTS FOR DISTRIBUTED PLANAR REFLECTOR TARGET MODEL IN ROUGH SEA CLUTTER, USING FIVE ORTHOGONAL FILTERS

SIR_n and signal/filter coefficients	n=1	n=2	n=3	n=4	n=5
SIR_n	75.43	70.48	13.38	1.85	0.48
Vert. Signal	Magnitude, Phase	Magnitude, Phase	Magnitude, Phase	Magnitude, Phase	Magnitude, Phase
u_{10}	.028,3.142	same	same	same	same
u_{11}	.004,3.142	as	as	as	as
u_{12}	.002,3.142	n=1	n=1	n=1	n=1
u_{13}	.004,3.142				
u_{14}	.009,3.142				
Horiz. Signal	Magnitude, Phase	Magnitude, Phase	Magnitude, Phase	Magnitude, Phase	Magnitude, Phase
u_{20}	.212, 0	same	same	same	same
u_{21}	.780, 0	as	as	as	as
u_{22}	.578, 0	n=1	n=1	n=1	n=1
u_{23}	.105, 0				
u_{24}	.017,0				
Vert. Filter	Magnitude, Phase	Magnitude, Phase	Magnitude, Phase	Magnitude, Phase	Magnitude, Phase
f_{10}	.006, 0	.026,2.839	.011,3.076	.234,1.461	.078,-2.452
f_{11}	.008, 0	.035,0.097	.010,3.134	.150,0.491	.049,2.863
f_{12}	.004, 0	.026,3.084	.009,3.112	.313,0.762	.949,0.000
f_{13}	.003, 0	.028,0.126	.002,3.076	.147,2.984	.049,-0.906
f_{14}	.025, 0	.007,1.226	.041,3.129	.401,2.907	.132,-0.999
Horiz. Filter	Magnitude, Phase	Magnitude, Phase	Magnitude, Phase	Magnitude, Phase	Magnitude, Phase
f_{20}	.340, 0	.791,0.010	.503,-3.135	.044,.025	.012,1.123
f_{21}	.856, 0	.040,-3.074	.515,0.000	.000,0.000	.000,0.000
f_{22}	.388, 0	.604,-3.139	.693,3.137	.025,-2.555	.017,-2.989
f_{23}	.001, 0	.063,2.987	.007,2.990	.714,-0.086	.237,2.298
f_{24}	.000, 0	.009,1.341	.001,0.009	.361,-0.372	.120,2.006

8.0 CONCLUSION

Signal-to-interference ratio (SIR) maximization has been used to obtain an optimum signal-filter pair for a polarimetric radar when targets and/or clutter exhibit random polarization modulation. The results can easily be extended to include the design of a likelihood ratio receiver for the same problem. Considerable insight into the theoretical solutions has been obtained by implementation and test of a computer program to yield the maximum SIR and Bayesian systems, i.e., the "best" signal and receiver configurations in each case.

Relatively simple expressions for the polarimetric scattering function of randomly oriented dipoles have yielded expressions for SIR in some simple but important cases, and these expressions have been analyzed in order to interpret the computational results. Some important insights have been obtained from the SIR expression for distributed planar targets and randomly oriented dipole clutter, i.e., for the typical "target in chaff" problem. These insights have resulted in the design of a new polarimetric clutter canceller [Figure 7-7 and Eqs. (7-36) and (7-42)] which theoretically allows a polarimetric radar to "see" through chaff.

The likelihood ratio receiver is obtained by adding a set of mutually orthogonal filters to the maximum SIR receiver. The filter output powers are weighted and summed to implement a Bayes optimum detector for a Gaussian signal in Gaussian interference. A surprising result is that each additional filter reduces overall SIR, even though detection probability P_D is increased more than false alarm probability P_F for a high threshold setting. This result follows from the fact that P_D and P_F for a high detection threshold are dependent upon the tails of the distributions describing the receiver output for signal plus interference and for interference alone. SIR, on the other hand, is the mean value of the output distribution for signal alone divided by the mean value of the output distribution for interference alone. SIR is thus not very dependent upon tail behavior.

Despite the shortcomings of SIR as a measure of receiver performance, SIR has proven extremely useful as a criterion for receiver design. In fact, it is difficult if not impossible to specify an optimum receiver and an associated optimum radar signal for the polarimetric case by direct solution of a likelihood ratio formulation. A solution of the problem using SIR maximization techniques, however, has been demonstrated. A computer program specifies the signal and receiver for maximum SIR and the Bayes optimum signal and receiver, when the polarimetric scattering functions of target and interference have been specified. The relation of the polarimetric scattering function to tapped delay line filter and dipole scattering models has been discussed in Sections 3.1 and 4.4.

9.0 REFERENCES

[1] P. E. Green, "Radar measurement of target characteristics," in Radar Astronomy, (J. V. Harrington and J. V. Evans, eds.) McGraw-Hill, New York, 1962.

[2] T. Kailath, "Measurements on time-variant communication channels," IRE Trans. on Inform. Theory IT-8, 1962, pp. 229-236.

[3] P. Bello, "Characterization of randomly time-variant linear channels," IEEE Trans. Comm. Sys., CS-11, pp. 360-393, 1963.

[4] H. L. Van Trees, Detection, Estimation, and Modulation Theory, Part III, Wiley, New York, 1971, pp. 444-553.

[5] V. C. Vannicola, "On the theory of radar polarization processing for clutter suppression," GACIAC PR-81-02, 1980, pp. 259-279.

[6] M. I. Skolnik, "Sea Echo," in Radar Handbook, M. I. Skolnik, ed., McGraw-Hill, New York, 1970.

[7] C. A. Stutt and L. J. Spafford, "A 'best' mismatched filter response for radar clutter discrimination," IEEE Trans. Inform. Theory, IT-14, 1968, pp. 280-287.

[8] W. D. Rummlar, "Clutter suppression by complex weighting of coherent pulse trains," IEEE Trans. Aerosp. and Electron. Syst., AES-2, 1966, pp. 689-699.

[9] D. F. DeLong, Jr., and E. M. Hofstetter, "On the design of optimum radar waveforms for clutter rejection," IEEE Trans. Inform. Theory, IT-13, 1967, pp. 454-463.

[10] R. A. Altes, "Suppression of radar clutter and multipath effects for wide-band signals," IEEE Trans. Inform. Theory, IT-17, 1971, pp. 344-346.

[11] R. A. Altes, "Radar/sonar signal design for bounded Doppler shifts," IEEE Trans. on Aerosp. and Electron. Sys., AES-18, 1982, pp. 369-380.

[12] R. A. Altes, "Detection, estimation, and classification with spectrograms," J. Acous. Soc. Am. 67, 1980, pp. 1232-1246.

[13] R. A. Altes and W. J. Faust, "A unified method of broad-band echo characterization for diagnostic ultrasound," IEEE Trans. on Biomed. Engr., BME-27, 1980, pp. 500-508.

[14] H. L. Van Trees, Detection, Estimation, and Modulation Theory, Part 1. Wiley, New York, 1968.

[15] W. S. Meisel, Computer-Oriented Approaches to Pattern Recognition. Academic, New York, 1972.

[16] M. Avriel, Nonlinear Programming, Analysis and Methods. Prentice-Hall, Englewood Cliffs, New Jersey, 1976, pp. 244-247.

[17] T. T. Kadota and L. A. Shepp, "On the best finite set of linear observables for discriminating two Gaussian signals," IEEE Trans. on Inform. Theory, Vol. IT-13, 1967, pp. 278-284.

[18] S. Kullback, Information Theory and Statistics, Peter Smith, Goucester, Mass., 1959.

[19] R. A. Altes and S. F. Connelly, "New filters for sonar data analysis," IEEE EASCON '81 Proceedings, 81CH1724-4 (ISSN: 0531-6863), Nov. 1981, pp. 6-12.

[20] K. Fukunaga, Introduction to Statistical Pattern Recognition. Academic, New York, 1972.

[21] A. D. Whalen, Detection of Signals in Noise. Academic, New York, 1971.

[22] N. R. Goodman, "Statistical analysis based on a certain multivariate complex Gaussian distribution," Ann. Math. Stat., Vol. 34, 1963, pp. 152-177.

[23] R. A. Altes, "Angle estimation and binaural processing in animal echolocation," J. Acous. Soc. Am., Vol. 63, 1978, pp. 155-173.

[24] I. Kantor, "A generalization of the detection theory of Swerling," EASCON '74 Proceedings, pp. 198-205.

[25] R. J. Schwarz and B. Friedland, Linear Systems, McGraw-Hill, New York, 1965.

[26] D. A. Hill, "Electromagnetic scattering concepts applied to the detection of targets near the ground," Report 2971-1, Ohio State Univ. ElectroScience Lab, 4 Sept. 1970, AD 875869.

[27] D. H. Foley and J. W. Sammon, "An optimal set of discriminant vectors," IEEE Trans. on Comput., Vol. C-24, 1975, pp. 281-289.

APPENDIX A

EVALUATION OF INTEGRALS FOR COMPUTING SIR WITH SIGNAL AND FILTER DESCRIBED BY COMPLEX FOURIER SERIES AND SINC FUNCTIONS

A.1 Fourier Series Description

We would like to obtain easily computed expressions for the integrals I_1 in Eq. (5-17) and I_2 in Eq. (5-18).

The first integral is

$$I_1 = \int_{\phi_s-\Delta\phi/2}^{\phi_s+\Delta\phi/2} \frac{\sin^2(\pi\phi T)}{\pi^2[\phi T + k-\ell][\phi T + p-q]}\, d\phi \tag{A1}$$

$$= 2 \int_{\phi_s-\Delta\phi/2}^{\phi_s+\Delta\phi/2} \frac{1 - \cos x}{[2\pi\phi T + 2\pi(k-\ell)][2\pi\phi T + 2\pi(p-q)]}\, d\phi \tag{A2}$$

$$= \frac{1}{\pi T} \int_{x_1 = 2\pi T[\phi_s-\Delta\phi/2]}^{x_2 = 2\pi T[\phi_s+\Delta\phi/2]} \frac{1 - \cos x}{[2\pi(k-\ell) + x][2\pi(p-q) + x]}\, dx \,. \tag{A3}$$

Consider two cases. For Case 1, $k-\ell = p-q$. For Case 2, $k-\ell \neq p-q$. For Case 1, we have

$$I_1 = \frac{1}{\pi T} \int_{x_1}^{x_2} \frac{1 - \cos x}{(H_{k\ell} + x)^2}\, dx \,, \tag{A4}$$

where $H_{k\ell} = 2\pi(k-\ell) = 2\pi(p-q)$. Letting $y = x + H_{k\ell}$ and using the fact that $H_{k\ell}$ is an integer multiple of 2π, we have

$$I_1 = \frac{1}{\pi I} \int_{x_1+H_{k\ell}}^{x_2+H_{k\ell}} \frac{1 - \cos y}{y^2}\, dy \quad . \tag{A5}$$

Integration by parts then yields

$$I_1 = \frac{1}{\pi I}\left[- \frac{(1 - \cos x_2)}{x_2 + H_{k\ell}} + \frac{(1 - \cos x_1)}{x_1 + H_{k\ell}} + Si(x_2 + H_{k\ell}) - Si(x_1 + H_{k\ell})\right] \tag{A6}$$

where

$$Si(x) \equiv \int_0^x \operatorname{sinc}(y)dy = -Si(-x) \quad . \tag{A7}$$

For Case 2 ($k-\ell \neq p-q$), we can use a Heaviside expansion to show that

$$\frac{1}{(x + H_{k\ell})(x + H_{pq})} = \frac{(H_{pq} - H_{k\ell})^{-1}}{x + H_{k\ell}} + \frac{(H_{k\ell} - H_{pq})^{-1}}{x + H_{pq}}$$

$$= \frac{1}{H_{pq} - H_{k\ell}}\left[\frac{1}{x + H_{k\ell}} - \frac{1}{x + H_{pq}}\right] \quad . \tag{A8}$$

Substituting Eq. (A8) into Eq. (A3), we have

$$I_1 = \frac{1}{\pi T(H_{pq} - H_{k\ell})} \left[\int_{x_1}^{x_2} \frac{1 - \cos x}{x + H_{k\ell}} \, dx - \int_{x_1}^{x_2} \frac{1 - \cos x}{x + H_{pq}} \, dx \right]$$

$$= |\pi T(H_{pq} - H_{k\ell})|^{-1} \left[\int_{x_1+H_{k\ell}}^{x_2+H_{k\ell}} \frac{1 - \cos y}{y} \, dy - \int_{x_1+H_{pq}}^{x_2+H_{pq}} \frac{1 - \cos y}{y} \, dy \right]$$

$$= |\pi T(H_{pq} - H_{k\ell})|^{-1} \, |Cin(x_2 + H_{k\ell}) - Cin(x_1 + H_{k\ell}) - Cin(x_2 + H_{pq})$$

$$+ Cin(x_1 + H_{pq})| \quad , \tag{A9}$$

where

$$Cin(x) \equiv \int_0^x \frac{1 - \cos x}{x} \, dx$$

$$\equiv -Ci(x) + \ln(x) + \gamma \quad . \tag{A10}$$

and γ is Euler's constant. The functions Ci(x) and Si(x) can be computed from properties given on pp. 231-233 of Abramowitz and Stegun's Handbook of Mathematical Functions. In Eqs. (A6) and (A9),

$$H_{k\ell} = 2\pi(k - \ell) \quad , \tag{A11}$$

$$H_{pq} = 2\pi(p - q) \quad , \tag{A12}$$

$$x_1 = 2\pi T[\phi_s - \Delta\phi/2] \quad , \tag{A13}$$

$$x_2 = 2\pi T[\phi_s + \Delta\phi/2] \quad . \tag{A14}$$

The integral in Eq. (5-18) is

$$I_2 = \int_{\tau_r-\Delta\tau/2}^{\tau_r+\Delta\tau/2} e^{-j2\pi(k-p)\tau/T}\, d\tau$$

$$= \frac{e^{-j2\pi(k-p)\tau/T}}{-j2\pi(k-p)/T}\Bigg|_{\tau_r-\Delta\tau/2}^{\tau_r+\Delta\tau/2}$$

$$= \Delta\tau\, e^{-jH_{kp}\tau_r/T}\, \mathrm{sinc}[H_{kp}\Delta\tau/(2T)] \quad . \tag{A15}$$

where $H_{kp} = 2\pi(k-p)$.

A.2 Sinc Function Description

We would like to obtain easily computed expressions for the integrals I_1 in Eq. (5-19) and I_2 in Eq. (5-20)

The first integral is

$$I_1 = \int_{\tau_r-\Delta\tau/2}^{\tau_r+\Delta\tau/2} \operatorname{sinc}[\pi(k-\ell + B\tau)]\ \operatorname{sinc}[\pi(p-q + B\tau)]d\tau$$

$$= 4 \int_{\tau_r-\Delta\tau/2}^{\tau_r+\Delta\tau/2} \frac{\sin(\frac{1}{2} H_{k\ell} + \pi B\tau)}{H_{k\ell} + 2\pi B\tau} \frac{\sin[\frac{1}{2} H_{pq} + \pi B\tau]}{H_{pq} + 2\pi B\tau} d\tau \quad , \tag{A16}$$

where $H_{k\ell}$ and H_{pq} are defined as in Eqs. (A11) and (A12).

Using the identity

$$\sin(\tfrac{1}{2} H_{k\ell} + \pi B\tau)\ \sin[\tfrac{1}{2} H_{pq} + \pi B\tau]$$

$$= \tfrac{1}{2} \cos[\tfrac{1}{2} (H_{k\ell} - H_{pq})] - \tfrac{1}{2} \cos[2\pi B\tau + \tfrac{1}{2} (H_{k\ell} + H_{pq})] \tag{A17}$$

and letting $x = 2\pi B\tau$, we have

$$I_1 = I_{11} - I_{12} \quad , \tag{A18}$$

where

$$I_{11} = \cos[\tfrac{1}{2}(H_{kp} - H_{pq})]\ (1/\pi B) \int_{x_1}^{x_2} \frac{dx}{(H_{k\ell} + x)(H_{pq} + x)} \tag{A19}$$

and

$$I_{12} = (1/\pi B) \int_{x_1}^{x_2} \frac{\cos[x + \frac{1}{2}(H_{k\ell} + H_{pq})]}{(H_{k\ell} + x)(H_{pq} + x)}\, dx \quad . \tag{A20}$$

In Eqs. (A19) and (A20),

$$x_2 = 2\pi B(\tau_r + \Delta\tau/2) \quad , \tag{A21}$$

$$x_1 = 2\pi B(\tau_r - \Delta\tau/2) \quad . \tag{A22}$$

Consider two cases. For Case 1, $H_{k\ell} = H_{pq}$, i.e., $k-\ell = p-q$. For Case 2, $H_{k\ell} \neq H_{pq}$. For Case 1, Eq. (A16) becomes

$$I_1 = \frac{2}{\pi B} \int_{x_1}^{x_2} \frac{\sin^2[\frac{1}{2}(H_{k\ell} + x)]}{(H_{k\ell} + x)^2}\, dx$$

$$= \frac{1}{\pi B} \int_{x_1}^{x_2} \frac{1 - \cos (H_{k\ell} + x)}{(H_{k\ell} + x)^2} \, dx$$

$$= \frac{1}{\pi B} \int_{x_1+H_{k\ell}}^{x_2+H_{k\ell}} \frac{1 - \cos y}{y^2} \, dy \quad . \tag{A23}$$

From Eqs. (A5) and (A6),

$$I_1 = \frac{1}{\pi B} \left[- \frac{(1 - \cos x_2)}{x_2 + H_{k\ell}} + \frac{(1 - \cos x_1)}{x_1 + H_{k\ell}} + Si(x_2 + H_{k\ell}) - Si(x_1 + H_{k\ell}) \right] . \tag{A24}$$

For Case 2, we can use the identity in Eq. (A8) to obtain

$$I_{11} = \frac{\cos[\frac{1}{2} (H_{k\ell} - H_{pq})]}{\pi B(H_{pq} - H_{k\ell})} \left[\int_{x_1}^{x_2} \frac{dx}{H_{k\ell} + x} - \int_{x_1}^{x_2} \frac{dx}{H_{pq} + x} \right]$$

$$= \frac{\cos[\frac{1}{2} (H_{k\ell} - H_{pq})]}{\pi B(H_{pq} - H_{k\ell})} \left\{ \ln \left[\frac{H_{pq} + x_1}{H_{k\ell} + x_1} \right] + \ln \left[\frac{H_{k\ell} + x_2}{H_{pq} + x_2} \right] \right\} . \tag{A25}$$

To evaluate I_{12}, we can use the additional identity

$$\cos[x + \tfrac{1}{2} (H_{k\ell} + H_{pq})]$$

$$= \cos(x)\cos[\tfrac{1}{2} (H_{k\ell} + H_{pq})] - \sin(x)\sin[\tfrac{1}{2} (H_{k\ell} + H_{pq})] \quad .$$

Substituting Eqs. (A8) and (A26) into Eq. (A20), we have

$$I_{12} = \frac{\cos[\frac{1}{2}(H_{k\ell} + H_{pq})]}{\pi B(H_{pq} - H_{k\ell})} \left[\int_{x_1}^{x_2} \frac{\cos x}{H_{k\ell} + x}\, dx - \int_{x_1}^{x_2} \frac{\cos x}{H_{pq} + x}\, dx \right]$$

$$- \frac{\sin[\frac{1}{2}(H_{k\ell} + H_{pq})]}{\pi B(H_{pq} - H_{k\ell})} \left[\int_{x_1}^{x_2} \frac{\sin x}{H_{k\ell} + x}\, dx - \int_{x_1}^{x_2} \frac{\sin x}{H_{pq} + x}\, dx \right] \tag{A27}$$

Letting $y = H_{k\ell} + x$ and using the fact that $H_{k\ell}$ equals an integer multiple of 2π, the integrals in Eq. (A27) can be written

$$\int_{x_1}^{x_2} \frac{\cos x}{H + x}\, dx = \int_{x_1+H}^{x_2+H} \frac{\cos y}{y}\, dy = Cin(x_2 + H) - Cin(x_1 + H) \tag{A28}$$

$$\int_{x_1}^{x_2} \frac{\sin x}{H + x}\, dx = \int_{x_1+H}^{x_2+H} \frac{\sin y}{y}\, dy = Si(x_2 + H) - Si(x_1 + H) \,. \tag{A29}$$

It follows that

$$I_{12} = \frac{\cos[\frac{1}{2}(H_{k\ell} + H_{pq})]}{\pi B(H_{pq} - H_{k\ell})} [\mathrm{Cin}(x_2 + H_{k\ell}) - \mathrm{Cin}(x_1 + H_{k\ell})$$

$$- \mathrm{Cin}(x_2 + H_{pq}) + \mathrm{Cin}(x_1 + H_{pq})]$$

$$- \frac{\sin[\frac{1}{2}(H_{k\ell} + H_{pq})]}{\pi B(H_{pq} - H_{k\ell})} [\mathrm{Si}(x_2 + H_{k\ell}) - \mathrm{Si}(x_1 + H_{k\ell})$$

$$- \mathrm{Si}(x_2 + H_{pq}) + \mathrm{Si}(x_1 + H_{pq})] \quad . \qquad \text{(A30)}$$

Equation (A24) for Case 1, together with Eqs. (A25) and (A30) for Case 2, yield the desired expressions for the integral I_1 in Eq. (5-19).

The integral I_2 in Eq. (5-20) is

$$I_2 = \int_{\phi_s - \Delta\phi/2}^{\phi_s + \Delta\phi/2} e^{-j2\pi(\ell - q)\phi/B} \, d\phi$$

$$= \frac{e^{-jH_{\ell q}\phi/B}}{-jH_{\ell q}/B} \Bigg|_{\phi_s - \Delta\phi/2}^{\phi_s + \Delta\phi/2}$$

$$= e^{-jH_{\ell q}\phi_s/B} \Delta\phi \, \mathrm{sinc}[H_{\ell q}\Delta\phi/(2B)] \quad . \qquad \text{(A31)}$$

APPENDIX B

DESCRIPTION OF COMPUTER INPUT/OUTPUT FOR THE SIMPLEX SIR MAXIMIZATION PROGRAM

The input to the computer program is given by $E[b_{ij}\, b^*_{mn}|\tau,\phi]$, $E[c_{ij}\, c^*_{mn}|\tau,\phi)]$, $p_b(\phi,\tau)$, and $p_c(\phi,\tau)$. These quantities determine the target and clutter polarimetric scattering functions as in Eq. (3-12), where the indices i, j, m, n are each equal to one (vertical) or two (horizontal).

The output of the program is divided into a separate section for each type of parameter to be optimized. In Table B1, the variable parameters are the magnitudes of the signal frequency components. The table shows the eleven vertices of the initial simplex. At each vertex, a different set of signal magnitudes is used. In the example, all or nearly all the frequency components (#0, #1, #2, #3, and #4) have the same magnitudes, but this need not be true in general. It is only necessary that the initial simplex vertices span the space of all desired solutions. Since only signal magnitude is varied, all other parameters in the table are fixed.

The best magnitudes for the five signal frequency components are found with all other parameters held fixed. These magnitude values are entered at the bottom of Table B1, under the heading "Final Component Coefficients for Iteration #1."

The next output section (Table B2) has the heading: "Maximizing SIR by Varying Filter Magnitude." The variable parameters are now the magnitudes of the filter components. Since only filter magnitude is varied, all other parameters in Table B2 are fixed. The best solution from Table B1 is carried down into Table B2 as the initial vertex (Point #1). This carry-down procedure is used throughout the program, allowing the algorithm to "build" on optimized parameters and ensuring that SIR is nondecreasing.

The best filter magnitude parameters are given under the heading, "Final Component Coefficients for Iteration #1.

The iteration number has not changed because an "iteration" is defined as one cycle through all the different parameter types: signal magnitude, filter magnitude, signal phase, and filter phase. The last parameter variation for Iteration #1, "Maximizing SIR by Varying Filter Phase," is shown in Table B3.

The final coefficients at the bottom of Table B3 comprise the starting set for Iteration #2, which again adjusts all parameter types in turn. Table B4 shows the final parameter variation (filter phase) for Iteration #2. Table B5 shows the same part of Iteration #3. When the SIR improvement between succeeding iterations is less than a small number (0.1 in this case), the optimization program is terminated. The coefficients and associated SIR at the bottom of Table B5 then represent the final result.

The algorithm may be sensitive to initial conditions. One way to test for such sensitivity is to optimize coefficients in a different order, e.g., by starting with signal phase rather than signal magnitude. The first and last parameter variations obtained by optimizing the phase first are shown in Tables B6 and B7. The results in this case are slightly different, but the SIR values are nearly identical (compare Tables B5 and B7).

TABLE B1

MAXIMIZING SIR BY VARYING SIGNAL MAGNITUDE

Starting Component Coefficients for Iteration # 1 :

Point #	Comp. Freq#	Signal Vert.	Signal Pol.	Signal Horiz	Signal Pol.	Filter Vert.	Filter Pol.	Filter Horiz.	Filter Pol.	SIR
1	0	0.316EXP	0.000	0.316EXP	0.000	0.316EXP	0.000	0.316EXP	0.000	
1	1	0.316EXP	0.000	0.316EXP	0.000	0.316EXP	0.000	0.316EXP	0.000	
1	2	0.316EXP	0.000	0.316EXP	0.000	0.316EXP	0.000	0.316EXP	0.000	
1	3	0.316EXP	0.000	0.316EXP	0.000	0.316EXP	0.000	0.316EXP	0.000	
1	4	0.316EXP	0.000	0.316EXP	0.000	0.316EXP	0.000	0.316EXP	0.000	0.648
2	0	0.000EXP	0.000	0.333EXP	0.000	0.316EXP	0.000	0.316EXP	0.000	
2	1	0.333EXP	0.000	0.333EXP	0.000	0.316EXP	0.000	0.316EXP	0.000	
2	2	0.333EXP	0.000	0.333EXP	0.000	0.316EXP	0.000	0.316EXP	0.000	
2	3	0.333EXP	0.000	0.333EXP	0.000	0.316EXP	0.000	0.316EXP	0.000	
2	4	0.333EXP	0.000	0.333EXP	0.000	0.316EXP	0.000	0.316EXP	0.000	0.603
3	0	0.333EXP	0.000	0.333EXP	0.000	0.316EXP	0.000	0.316EXP	0.000	
3	1	0.000EXP	0.000	0.333EXP	0.000	0.316EXP	0.000	0.316EXP	0.000	
3	2	0.333EXP	0.000	0.333EXP	0.000	0.316EXP	0.000	0.316EXP	0.000	
3	3	0.333EXP	0.000	0.333EXP	0.000	0.316EXP	0.000	0.316EXP	0.000	
3	4	0.333EXP	0.000	0.333EXP	0.000	0.316EXP	0.000	0.316EXP	0.000	0.393
4	0	0.333EXP	0.000	0.333EXP	0.000	0.316EXP	0.000	0.316EXP	0.000	
4	1	0.333EXP	0.000	0.333EXP	0.000	0.316EXP	0.000	0.316EXP	0.000	
4	2	0.000EXP	0.000	0.333EXP	0.000	0.316EXP	0.000	0.316EXP	0.000	
4	3	0.333EXP	0.000	0.333EXP	0.000	0.316EXP	0.000	0.316EXP	0.000	
4	4	0.333EXP	0.000	0.333EXP	0.000	0.316EXP	0.000	0.316EXP	0.000	0.379
5	0	0.333EXP	0.000	0.333EXP	0.000	0.316EXP	0.000	0.316EXP	0.000	
5	1	0.333EXP	0.000	0.333EXP	0.000	0.316EXP	0.000	0.316EXP	0.000	
5	2	0.333EXP	0.000	0.333EXP	0.000	0.316EXP	0.000	0.316EXP	0.000	
5	3	0.000EXP	0.000	0.333EXP	0.000	0.316EXP	0.000	0.316EXP	0.000	
5	4	0.333EXP	0.000	0.333EXP	0.000	0.316EXP	0.000	0.316EXP	0.000	0.393
6	0	0.333EXP	0.000	0.333EXP	0.000	0.316EXP	0.000	0.316EXP	0.000	
6	1	0.333EXP	0.000	0.333EXP	0.000	0.316EXP	0.000	0.316EXP	0.000	
6	2	0.333EXP	0.000	0.333EXP	0.000	0.316EXP	0.000	0.316EXP	0.000	
6	3	0.333EXP	0.000	0.333EXP	0.000	0.316EXP	0.000	0.316EXP	0.000	
6	4	0.000EXP	0.000	0.333EXP	0.000	0.316EXP	0.000	0.316EXP	0.000	0.603
7	0	0.333EXP	0.000	0.000EXP	0.000	0.316EXP	0.000	0.316EXP	0.000	
7	1	0.333EXP	0.000	0.333EXP	0.000	0.316EXP	0.000	0.316EXP	0.000	
7	2	0.333EXP	0.000	0.333EXP	0.000	0.316EXP	0.000	0.316EXP	0.000	
7	3	0.333EXP	0.000	0.333EXP	0.000	0.316EXP	0.000	0.316EXP	0.000	
7	4	0.333EXP	0.000	0.333EXP	0.000	0.316EXP	0.000	0.316EXP	0.000	0.731
8	0	0.333EXP	0.000	0.333EXP	0.000	0.316EXP	0.000	0.316EXP	0.000	
8	1	0.333EXP	0.000	0.000EXP	0.000	0.316EXP	0.000	0.316EXP	0.000	
8	2	0.333EXP	0.000	0.333EXP	0.000	0.316EXP	0.000	0.316EXP	0.000	
8	3	0.333EXP	0.000	0.333EXP	0.000	0.316EXP	0.000	0.316EXP	0.000	
8	4	0.333EXP	0.000	0.333EXP	0.000	0.316EXP	0.000	0.316EXP	0.000	0.744
9	0	0.333EXP	0.000	0.333EXP	0.000	0.316EXP	0.000	0.316EXP	0.000	
9	1	0.333EXP	0.000	0.333EXP	0.000	0.316EXP	0.000	0.316EXP	0.000	
9	2	0.333EXP	0.000	0.000EXP	0.000	0.316EXP	0.000	0.316EXP	0.000	
9	3	0.333EXP	0.000	0.333EXP	0.000	0.316EXP	0.000	0.316EXP	0.000	
9	4	0.333EXP	0.000	0.333EXP	0.000	0.316EXP	0.000	0.316EXP	0.000	0.744
10	0	0.333EXP	0.000	0.333EXP	0.000	0.316EXP	0.000	0.316EXP	0.000	
10	1	0.333EXP	0.000	0.333EXP	0.000	0.316EXP	0.000	0.316EXP	0.000	
10	2	0.333EXP	0.000	0.333EXP	0.000	0.316EXP	0.000	0.316EXP	0.000	
10	3	0.333EXP	0.000	0.000EXP	0.000	0.316EXP	0.000	0.316EXP	0.000	
10	4	0.333EXP	0.000	0.333EXP	0.000	0.316EXP	0.000	0.316EXP	0.000	0.744
11	0	0.333EXP	0.000	0.333EXP	0.000	0.316EXP	0.000	0.316EXP	0.000	
11	1	0.333EXP	0.000	0.333EXP	0.000	0.316EXP	0.000	0.316EXP	0.000	
11	2	0.333EXP	0.000	0.333EXP	0.000	0.316EXP	0.000	0.316EXP	0.000	
11	3	0.333EXP	0.000	0.333EXP	0.000	0.316EXP	0.000	0.316EXP	0.000	
11	4	0.333EXP	0.000	0.000EXP	0.000	0.316EXP	0.000	0.316EXP	0.000	0.731

Final Component Coefficients for Iteration # 1

Point #	Comp Freq#	Signal Vert	Signal Pol	Signal Horiz	Signal Pol	Filter Vert	Filter Pol	Filter Horiz	Filter Pol	SIR
Opt	0	0.333EXP	0.000	0.333EXP	0.000	0.316EXP	0.000	0.316EXP	0.000	
Opt	1	0.333EXP	0.000	0.333EXP	0.000	0.316EXP	0.000	0.316EXP	0.000	
Opt	2	0.333EXP	0.000	0.000EXP	0.000	0.316EXP	0.000	0.316EXP	0.000	
Opt	3	0.333EXP	0.000	0.333EXP	0.000	0.316EXP	0.000	0.316EXP	0.000	
Opt	4	0.333EXP	0.000	0.333EXP	0.000	0.316EXP	0.000	0.316EXP	0.000	0.744

TABLE B2

MAXIMIZING SIR BY VARYING FILTER MAGNITUDE

Starting Component Coefficients for Iteration # 1 :

Point #	Comp. Freq#	Signal Vert.	Signal Pol.	Signal Horiz.	Signal Pol.	Filter Vert.	Filter Pol.	Filter Horiz.	Filter Pol.	SIR
1	0	0.333EXP1	0.000	0.333EXP1	0.000	0.316EXP1	0.000	0.316EXP1	0.000	
1	1	0.333EXP1	0.000	0.333EXP1	0.000	0.316EXP1	0.000	0.316EXP1	0.000	
1	2	0.333EXP1	0.000	0.000EXP1	0.000	0.316EXP1	0.000	0.316EXP1	0.000	
1	3	0.333EXP1	0.000	0.333EXP1	0.000	0.316EXP1	0.000	0.316EXP1	0.000	
1	4	0.333EXP1	0.000	0.333EXP1	0.000	0.316EXP1	0.000	0.316EXP1	0.000	0.766
2	0	0.333EXP1	0.000	0.333EXP1	0.000	0.000EXP1	0.000	0.333EXP1	0.000	
2	1	0.333EXP1	0.000	0.333EXP1	0.000	0.333EXP1	0.000	0.333EXP1	0.000	
2	2	0.333EXP1	0.000	0.000EXP1	0.000	0.333EXP1	0.000	0.333EXP1	0.000	
2	3	0.333EXP1	0.000	0.333EXP1	0.000	0.333EXP1	0.000	0.333EXP1	0.000	
2	4	0.333EXP1	0.000	0.333EXP1	0.000	0.333EXP1	0.000	0.333EXP1	0.000	0.748
3	0	0.333EXP1	0.000	0.333EXP1	0.000	0.333EXP1	0.000	0.333EXP1	0.000	
3	1	0.333EXP1	0.000	0.333EXP1	0.000	0.000EXP1	0.000	0.333EXP1	0.000	
3	2	0.333EXP1	0.000	0.000EXP1	0.000	0.333EXP1	0.000	0.333EXP1	0.000	
3	3	0.333EXP1	0.000	0.333EXP1	0.000	0.333EXP1	0.000	0.333EXP1	0.000	
3	4	0.333EXP1	0.000	0.333EXP1	0.000	0.333EXP1	0.000	0.333EXP1	0.000	0.734
4	0	0.333EXP1	0.000	0.333EXP1	0.000	0.333EXP1	0.000	0.333EXP1	0.000	
4	1	0.333EXP1	0.000	0.333EXP1	0.000	0.333EXP1	0.000	0.333EXP1	0.000	
4	2	0.333EXP1	0.000	0.000EXP1	0.000	0.000EXP1	0.000	0.333EXP1	0.000	
4	3	0.333EXP1	0.000	0.333EXP1	0.000	0.333EXP1	0.000	0.333EXP1	0.000	
4	4	0.333EXP1	0.000	0.333EXP1	0.000	0.333EXP1	0.000	0.333EXP1	0.000	0.719
5	0	0.333EXP1	0.000	0.333EXP1	0.000	0.333EXP1	0.000	0.333EXP1	0.000	
5	1	0.333EXP1	0.000	0.333EXP1	0.000	0.333EXP1	0.000	0.333EXP1	0.000	
5	2	0.333EXP1	0.000	0.000EXP1	0.000	0.333EXP1	0.000	0.333EXP1	0.000	
5	3	0.333EXP1	0.000	0.333EXP1	0.000	0.000EXP1	0.000	0.333EXP1	0.000	
5	4	0.333EXP1	0.000	0.333EXP1	0.000	0.333EXP1	0.000	0.333EXP1	0.000	0.734
6	0	0.333EXP1	0.000	0.333EXP1	0.000	0.333EXP1	0.000	0.333EXP1	0.000	
6	1	0.333EXP1	0.000	0.333EXP1	0.000	0.333EXP1	0.000	0.333EXP1	0.000	
6	2	0.333EXP1	0.000	0.000EXP1	0.000	0.333EXP1	0.000	0.333EXP1	0.000	
6	3	0.333EXP1	0.000	0.333EXP1	0.000	0.333EXP1	0.000	0.333EXP1	0.000	
6	4	0.333EXP1	0.000	0.333EXP1	0.000	0.333EXP1	0.000	0.333EXP1	0.000	0.748
7	0	0.333EXP1	0.000	0.333EXP1	0.000	0.333EXP1	0.000	0.333EXP1	0.000	
7	1	0.333EXP1	0.000	0.333EXP1	0.000	0.333EXP1	0.000	0.333EXP1	0.000	
7	2	0.333EXP1	0.000	0.000EXP1	0.000	0.333EXP1	0.000	0.333EXP1	0.000	
7	3	0.333EXP1	0.000	0.333EXP1	0.000	0.333EXP1	0.000	0.333EXP1	0.000	
7	4	0.333EXP1	0.000	0.333EXP1	0.000	0.333EXP1	0.000	0.333EXP1	0.000	0.839
8	0	0.333EXP1	0.000	0.333EXP1	0.000	0.333EXP1	0.000	0.333EXP1	0.000	
8	1	0.333EXP1	0.000	0.333EXP1	0.000	0.333EXP1	0.000	0.000EXP1	0.000	
8	2	0.333EXP1	0.000	0.000EXP1	0.000	0.333EXP1	0.000	0.333EXP1	0.000	
8	3	0.333EXP1	0.000	0.333EXP1	0.000	0.333EXP1	0.000	0.333EXP1	0.000	
8	4	0.333EXP1	0.000	0.333EXP1	0.000	0.333EXP1	0.000	0.333EXP1	0.000	0.864
9	0	0.333EXP1	0.000	0.333EXP1	0.000	0.333EXP1	0.000	0.333EXP1	0.000	
9	1	0.333EXP1	0.000	0.333EXP1	0.000	0.333EXP1	0.000	0.333EXP1	0.000	
9	2	0.333EXP1	0.000	0.000EXP1	0.000	0.333EXP1	0.000	0.000EXP1	0.000	
9	3	0.333EXP1	0.000	0.333EXP1	0.000	0.333EXP1	0.000	0.333EXP1	0.000	
9	4	0.333EXP1	0.000	0.333EXP1	0.000	0.333EXP1	0.000	0.333EXP1	0.000	0.897
10	0	0.333EXP1	0.000	0.333EXP1	0.000	0.333EXP1	0.000	0.333EXP1	0.000	
10	1	0.333EXP1	0.000	0.333EXP1	0.000	0.333EXP1	0.000	0.333EXP1	0.000	
10	2	0.333EXP1	0.000	0.000EXP1	0.000	0.333EXP1	0.000	0.333EXP1	0.000	
10	3	0.333EXP1	0.000	0.333EXP1	0.000	0.333EXP1	0.000	0.000EXP1	0.000	
10	4	0.333EXP1	0.000	0.333EXP1	0.000	0.333EXP1	0.000	0.333EXP1	0.000	0.864
11	0	0.333EXP1	0.000	0.333EXP1	0.000	0.333EXP1	0.000	0.333EXP1	0.000	
11	1	0.333EXP1	0.000	0.333EXP1	0.000	0.333EXP1	0.000	0.333EXP1	0.000	
11	2	0.333EXP1	0.000	0.000EXP1	0.000	0.333EXP1	0.000	0.333EXP1	0.000	
11	3	0.333EXP1	0.000	0.333EXP1	0.000	0.333EXP1	0.000	0.333EXP1	0.000	
11	4	0.333EXP1	0.000	0.333EXP1	0.000	0.333EXP1	0.000	0.000EXP1	0.000	0.839

Final Component Coefficients for Iteration # 1 :

Point #	Comp. Freq#	Signal Vert.	Signal Pol.	Signal Horiz.	Signal Pol.	Filter Vert.	Filter Pol.	Filter Horiz.	Filter Pol.	SIR
Opt.	0	0.333EXP1	0.000	0.333EXP1	0.000	0.333EXP1	0.000	0.333EXP1	0.000	
Opt.	1	0.333EXP1	0.000	0.333EXP1	0.000	0.333EXP1	0.000	0.333EXP1	0.000	
Opt.	2	0.333EXP1	0.000	0.000EXP1	0.000	0.333EXP1	0.000	0.000EXP1	0.000	
Opt.	3	0.333EXP1	0.000	0.333EXP1	0.000	0.333EXP1	0.000	0.333EXP1	0.000	
Opt	4	0.333EXP1	0.000	0.333EXP1	0.000	0.333EXP1	0.000	0.333EXP1	0.000	0.897

TABLE B3

MAXIMIZING SIR BY VARYING ONLY FILTER PHASE

Starting Component Coefficients for Iteration # 1 :

Point #	Comp. Freq#	Signal Vert.	Signal Pol.	Signal Horiz.	Signal Pol.	Filter Vert.	Filter Pol.	Filter Horiz.	Filter Pol.	SIR
1	0	0.333EXP(	3.142	0.333EXP(	0.000	0.333EXP(	0.000	0.333EXP(	0.000	
1	1	0.333EXP(	3.142	0.333EXP(	0.000	0.333EXP(	0.000	0.333EXP(	0.000	
1	2	0.333EXP(	3.142	0.000EXP(	0.000	0.333EXP(	0.000	0.000EXP(	0.000	
1	3	0.333EXP(	3.142	0.333EXP(	0.000	0.333EXP(	0.000	0.333EXP(	0.000	
1	4	0.333EXP(	3.142	0.333EXP(	0.000	0.333EXP(	0.000	0.333EXP(	0.000	1.372
2	0	0.333EXP(	3.142	0.333EXP(	0.000	0.333EXP(	1.047	0.333EXP(	0.000	
2	1	0.333EXP(	3.142	0.333EXP(	0.000	0.333EXP(	1.047	0.333EXP(	0.000	
2	2	0.333EXP(	3.142	0.000EXP(	0.000	0.333EXP(	1.047	0.000EXP(	0.000	
2	3	0.333EXP(	3.142	0.333EXP(	0.000	0.333EXP(	1.047	0.333EXP(	0.000	
2	4	0.333EXP(	3.142	0.333EXP(	0.000	0.333EXP(	1.047	0.333EXP(	0.000	1.323
3	0	0.333EXP(	3.142	0.333EXP(	0.000	0.333EXP(	2.094	0.333EXP(	0.000	
3	1	0.333EXP(	3.142	0.333EXP(	0.000	0.333EXP(	2.094	0.333EXP(	0.000	
3	2	0.333EXP(	3.142	0.000EXP(	0.000	0.333EXP(	2.094	0.000EXP(	0.000	
3	3	0.333EXP(	3.142	0.333EXP(	0.000	0.333EXP(	2.094	0.333EXP(	0.000	
3	4	0.333EXP(	3.142	0.333EXP(	0.000	0.333EXP(	2.094	0.333EXP(	0.000	1.004
4	0	0.333EXP(	3.142	0.333EXP(	0.000	0.333EXP(	3.142	0.333EXP(	0.000	
4	1	0.333EXP(	3.142	0.333EXP(	0.000	0.333EXP(	3.142	0.333EXP(	0.000	
4	2	0.333EXP(	3.142	0.000EXP(	0.000	0.333EXP(	3.142	0.000EXP(	0.000	
4	3	0.333EXP(	3.142	0.333EXP(	0.000	0.333EXP(	3.142	0.333EXP(	0.000	
4	4	0.333EXP(	3.142	0.333EXP(	0.000	0.333EXP(	3.142	0.333EXP(	0.000	0.897
5	0	0.333EXP(	3.142	0.333EXP(	0.000	0.333EXP(	4.189	0.333EXP(	0.000	
5	1	0.333EXP(	3.142	0.333EXP(	0.000	0.333EXP(	4.189	0.333EXP(	0.000	
5	2	0.333EXP(	3.142	0.000EXP(	0.000	0.333EXP(	4.189	0.000EXP(	0.000	
5	3	0.333EXP(	3.142	0.333EXP(	0.000	0.333EXP(	4.189	0.333EXP(	0.000	
5	4	0.333EXP(	3.142	0.333EXP(	0.000	0.333EXP(	4.189	0.333EXP(	0.000	1.004
6	0	0.333EXP(	3.142	0.333EXP(	0.000	0.333EXP(	5.236	0.333EXP(	0.000	
6	1	0.333EXP(	3.142	0.333EXP(	0.000	0.333EXP(	5.236	0.333EXP(	0.000	
6	2	0.333EXP(	3.142	0.000EXP(	0.000	0.333EXP(	5.236	0.000EXP(	0.000	
6	3	0.333EXP(	3.142	0.333EXP(	0.000	0.333EXP(	5.236	0.333EXP(	0.000	
6	4	0.333EXP(	3.142	0.333EXP(	0.000	0.333EXP(	5.236	0.333EXP(	0.000	1.323
7	0	0.333EXP(	3.142	0.333EXP(	0.000	0.333EXP(	0.000	0.333EXP(	1.079	
7	1	0.333EXP(	3.142	0.333EXP(	0.000	0.333EXP(	0.000	0.333EXP(	1.079	
7	2	0.333EXP(	3.142	0.000EXP(	0.000	0.333EXP(	0.000	0.000EXP(	1.079	
7	3	0.333EXP(	3.142	0.333EXP(	0.000	0.333EXP(	0.000	0.333EXP(	1.079	
7	4	0.333EXP(	3.142	0.333EXP(	0.000	0.333EXP(	0.000	0.333EXP(	1.079	1.311
8	0	0.333EXP(	3.142	0.333EXP(	0.000	0.333EXP(	0.000	0.333EXP(	2.157	
8	1	0.333EXP(	3.142	0.333EXP(	0.000	0.333EXP(	0.000	0.333EXP(	2.157	
8	2	0.333EXP(	3.142	0.000EXP(	0.000	0.333EXP(	0.000	0.000EXP(	2.157	
8	3	0.333EXP(	3.142	0.333EXP(	0.000	0.333EXP(	0.000	0.333EXP(	2.157	
8	4	0.333EXP(	3.142	0.333EXP(	0.000	0.333EXP(	0.000	0.333EXP(	2.157	0.492
9	0	0.333EXP(	3.142	0.333EXP(	0.000	0.333EXP(	0.000	0.333EXP(	3.236	
9	1	0.333EXP(	3.142	0.333EXP(	0.000	0.333EXP(	0.000	0.333EXP(	3.236	
9	2	0.333EXP(	3.142	0.000EXP(	0.000	0.333EXP(	0.000	0.000EXP(	3.236	
9	3	0.333EXP(	3.142	0.333EXP(	0.000	0.333EXP(	0.000	0.333EXP(	3.236	
9	4	0.333EXP(	3.142	0.333EXP(	0.000	0.333EXP(	0.000	0.333EXP(	3.236	0.897
10	0	0.333EXP(	3.142	0.333EXP(	0.000	0.333EXP(	0.000	0.333EXP(	4.314	
10	1	0.333EXP(	3.142	0.333EXP(	0.000	0.333EXP(	0.000	0.333EXP(	4.314	
10	2	0.333EXP(	3.142	0.000EXP(	0.000	0.333EXP(	0.000	0.000EXP(	4.314	
10	3	0.333EXP(	3.142	0.333EXP(	0.000	0.333EXP(	0.000	0.333EXP(	4.314	
10	4	0.333EXP(	3.142	0.333EXP(	0.000	0.333EXP(	0.000	0.333EXP(	4.314	1.032
11	0	0.333EXP(	3.142	0.333EXP(	0.000	0.333EXP(	0.000	0.333EXP(	5.393	
11	1	0.333EXP(	3.142	0.333EXP(	0.000	0.333EXP(	0.000	0.333EXP(	5.393	
11	2	0.333EXP(	3.142	0.000EXP(	0.000	0.333EXP(	0.000	0.000EXP(	5.393	
11	3	0.333EXP(	3.142	0.333EXP(	0.000	0.333EXP(	0.000	0.333EXP(	5.393	
11	4	0.333EXP(	3.142	0.333EXP(	0.000	0.333EXP(	0.000	0.333EXP(	5.393	1.379

Final Component Coefficients for Iteration # 1 :

Point #	Comp Freq#	Signal Vert	Signal Pol	Signal Horiz	Signal Pol	Filter Vert	Filter Pol	Filter Horiz	Filter Pol	SIR
Opt.	0	0.333EXP(	3.142	0.333EXP(	0.000	0.333EXP(	0.000	0.333EXP(	0.000	
Opt.	1	0.333EXP(	3.142	0.333EXP(	0.000	0.333EXP(	0.000	0.333EXP(	0.000	
Opt	2	0.333EXP(	3.142	0.000EXP(	0.000	0.333EXP(	0.000	0.000EXP(	0.000	
Opt	3	0.333EXP(	3.142	0.333EXP(	0.000	0.333EXP(	0.000	0.333EXP(	0.000	
Opt	4	0.333EXP(	3.142	0.333EXP(	0.000	0.333EXP(	0.000	0.333EXP(	0.000	1.372

TABLE B4

MAXIMIZING SIR BY VARYING ONLY FILTER PHASE

Starting Component Coefficients for Iteration # 2

Point #	Comp Freq#	Signal Vert	Signal Pol	Signal Horiz	Signal Pol	Filter Vert	Filter Pol	Filter Horiz	Filter Pol	SIR
1	0	0 317EXP	3 142	0 143EXP	0 000	0 307EXP	0 000	0 119EXP	0 000	
1	1	0 411EXP	3 142	0 139EXP	0 000	0 316EXP	0 000	0 333EXP	0 000	
1	2	0 599EXP	3 142	0 293EXP	0 000	0 555EXP	0 000	0 191EXP	0 000	
1	3	0 359EXP	3 142	0 138EXP	0 000	0 353EXP	0 000	0 128EXP	0 000	
1	4	0 281EXP	3 142	0 141EXP	0 000	0 141EXP	0 000	0 097EXP	0 000	2 697
2	0	0 317EXP	3 142	0 143EXP	0 000	0 307EXP	1 047	0 119EXP	0 000	
2	1	0 411EXP	3 142	0 139EXP	0 000	0 316EXP	1 047	0 333EXP	0 000	
2	2	0 599EXP	3 142	0 293EXP	0 000	0 555EXP	1 047	0 191EXP	0 000	
2	3	0 359EXP	3 142	0 138EXP	0 000	0 353EXP	1 047	0 128EXP	0 000	
2	4	0 281EXP	3 142	0 141EXP	0 000	0 141EXP	1 047	0 097EXP	0 000	2 413
3	0	0 317EXP	3 142	0 143EXP	0 000	0 307EXP	2 094	0 119EXP	0 000	
3	1	0 411EXP	3 142	0 139EXP	0 000	0 316EXP	2 094	0 333EXP	0 000	
3	2	0 599EXP	3 142	0 293EXP	0 000	0 555EXP	2 094	0 191EXP	0 000	
3	3	0 359EXP	3 142	0 138EXP	0 000	0 353EXP	2 094	0 128EXP	0 000	
3	4	0 281EXP	3 142	0 141EXP	0 000	0 141EXP	2 094	0 097EXP	0 000	1 993
4	0	0 317EXP	3 142	0 143EXP	0 000	0 307EXP	3 142	0 119EXP	0 000	
4	1	0 411EXP	3 142	0 139EXP	0 000	0 316EXP	3 142	0 333EXP	0 000	
4	2	0 599EXP	3 142	0 293EXP	0 000	0 555EXP	3 142	0 191EXP	0 000	
4	3	0 359EXP	3 142	0 138EXP	0 000	0 353EXP	3 142	0 128EXP	0 000	
4	4	0 281EXP	3 142	0 141EXP	0 000	0 141EXP	3 142	0 097EXP	0 000	1 834
5	0	0 317EXP	3 142	0 143EXP	0 000	0 307EXP	4 189	0 119EXP	0 000	
5	1	0 411EXP	3 142	0 139EXP	0 000	0 316EXP	4 189	0 333EXP	0 000	
5	2	0 599EXP	3 142	0 293EXP	0 000	0 555EXP	4 189	0 191EXP	0 000	
5	3	0 359EXP	3 142	0 138EXP	0 000	0 353EXP	4 189	0 128EXP	0 000	
5	4	0 281EXP	3 142	0 141EXP	0 000	0 141EXP	4 189	0 097EXP	0 000	1 993
6	0	0 317EXP	3 142	0 143EXP	0 000	0 307EXP	5 236	0 119EXP	0 000	
6	1	0 411EXP	3 142	0 139EXP	0 000	0 316EXP	5 236	0 333EXP	0 000	
6	2	0 599EXP	3 142	0 293EXP	0 000	0 555EXP	5 236	0 191EXP	0 000	
6	3	0 359EXP	3 142	0 138EXP	0 000	0 353EXP	5 236	0 128EXP	0 000	
6	4	0 281EXP	3 142	0 141EXP	0 000	0 141EXP	5 236	0 097EXP	0 000	2 413
7	0	0 317EXP	3 142	0 143EXP	0 000	0 307EXP	0 000	0 119EXP	1 079	
7	1	0 411EXP	3 142	0 139EXP	0 000	0 316EXP	0 000	0 333EXP	1 079	
7	2	0 599EXP	3 142	0 293EXP	0 000	0 555EXP	0 000	0 191EXP	1 079	
7	3	0 359EXP	3 142	0 138EXP	0 000	0 353EXP	0 000	0 128EXP	1 079	
7	4	0 281EXP	3 142	0 141EXP	0 000	0 141EXP	0 000	0 097EXP	1 079	2 399
8	0	0 317EXP	3 142	0 143EXP	0 000	0 307EXP	0 000	0 119EXP	2 197	
8	1	0 411EXP	3 142	0 139EXP	0 000	0 316EXP	0 000	0 333EXP	2 197	
8	2	0 599EXP	3 142	0 293EXP	0 000	0 555EXP	0 000	0 191EXP	2 197	
8	3	0 359EXP	3 142	0 138EXP	0 000	0 353EXP	0 000	0 128EXP	2 197	
8	4	0 281EXP	3 142	0 141EXP	0 000	0 141EXP	0 000	0 097EXP	2 197	1 979
9	0	0 317EXP	3 142	0 143EXP	0 000	0 307EXP	0 000	0 119EXP	3 236	
9	1	0 411EXP	3 142	0 139EXP	0 000	0 316EXP	0 000	0 333EXP	3 236	
9	2	0 599EXP	3 142	0 293EXP	0 000	0 555EXP	0 000	0 191EXP	3 236	
9	3	0 359EXP	3 142	0 138EXP	0 000	0 353EXP	0 000	0 128EXP	3 236	
9	4	0 281EXP	3 142	0 141EXP	0 000	0 141EXP	0 000	0 097EXP	3 236	1 839
10	0	0 317EXP	3 142	0 143EXP	0 000	0 307EXP	0 000	0 119EXP	4 314	
10	1	0 411EXP	3 142	0 139EXP	0 000	0 316EXP	0 000	0 333EXP	4 314	
10	2	0 599EXP	3 142	0 293EXP	0 000	0 555EXP	0 000	0 191EXP	4 314	
10	3	0 359EXP	3 142	0 138EXP	0 000	0 353EXP	0 000	0 128EXP	4 314	
10	4	0 281EXP	3 142	0 141EXP	0 000	0 141EXP	0 000	0 097EXP	4 314	2 033
11	0	0 317EXP	3 142	0 143EXP	0 000	0 307EXP	0 000	0 119EXP	5 393	
11	1	0 411EXP	3 142	0 139EXP	0 000	0 316EXP	0 000	0 333EXP	5 393	
11	2	0 599EXP	3 142	0 293EXP	0 000	0 555EXP	0 000	0 191EXP	5 393	
11	3	0 359EXP	3 142	0 138EXP	0 000	0 353EXP	0 000	0 128EXP	5 393	
11	4	0 281EXP	3 142	0 141EXP	0 000	0 141EXP	0 000	0 097EXP	5 393	2 481

Final Component Coefficients for Iteration # 2

Point #	Comp Freq#	Signal Vert	Signal Pol	Signal Horiz	Signal Pol	Filter Vert	Filter Pol	Filter Horiz	Filter Pol	SIR
Opt	0	0 317EXP	3 142	0 143EXP	0 000	0 307EXP	0 000	0 119EXP	0 000	
Opt	1	0 411EXP	3 142	0 139EXP	0 000	0 316EXP	0 000	0 333EXP	0 000	
Opt	2	0 599EXP	3 142	0 293EXP	0 000	0 555EXP	0 000	0 191EXP	0 000	
Opt	3	0 359EXP	3 142	0 138EXP	0 000	0 353EXP	0 000	0 128EXP	0 000	
Opt	4	0 281EXP	3 142	0 141EXP	0 000	0 141EXP	0 000	0 097EXP	0 000	2 697

TABLE B5

MAXIMIZING SIR BY VARYING ONLY FILTER PHASE

Starting Component Coefficients for Iteration # 3 :

Point #	Comp. Freq#	Signal Vert.	Signal Pol.	Signal Horiz.	Signal Pol.	Filter Vert.	Filter Pol.	Filter Horiz	Filter Pol.	SIR
1	0	0.317EXP(	3.142	0.143EXP(	0.000	0.307EXP(	0.000	0.119EXP(	0.000	
1	1	0.411EXP(	3.142	0.139EXP(	0.000	0.916EXP(	0.000	0.333EXP(	0.000	
1	2	0.599EXP(	3.142	0.293EXP(	0.000	0.955EXP(	0.000	0.191EXP(	0.000	
1	3	0.359EXP(	3.142	0.138EXP(	0.000	0.353EXP(	0.000	0.128EXP(	0.000	
1	4	0.281EXP(	3.142	0.141EXP(	0.000	0.141EXP(	0.000	0.097EXP(	0.000	2.697
2	0	0.317EXP(	3.142	0.143EXP(	0.000	0.307EXP(	1.047	0.119EXP(	0.000	
2	1	0.411EXP(	3.142	0.139EXP(	0.000	0.916EXP(	1.047	0.333EXP(	0.000	
2	2	0.599EXP(	3.142	0.293EXP(	0.000	0.955EXP(	1.047	0.191EXP(	0.000	
2	3	0.359EXP(	3.142	0.138EXP(	0.000	0.353EXP(	1.047	0.128EXP(	0.000	
2	4	0.281EXP(	3.142	0.141EXP(	0.000	0.141EXP(	1.047	0.097EXP(	0.000	2.413
3	0	0.317EXP(	3.142	0.143EXP(	0.000	0.307EXP(	2.094	0.119EXP(	0.000	
3	1	0.411EXP(	3.142	0.139EXP(	0.000	0.916EXP(	2.094	0.333EXP(	0.000	
3	2	0.599EXP(	3.142	0.293EXP(	0.000	0.955EXP(	2.094	0.191EXP(	0.000	
3	3	0.359EXP(	3.142	0.138EXP(	0.000	0.353EXP(	2.094	0.128EXP(	0.000	
3	4	0.281EXP(	3.142	0.141EXP(	0.000	0.141EXP(	2.094	0.097EXP(	0.000	1.993
4	0	0.317EXP(	3.142	0.143EXP(	0.000	0.307EXP(	3.142	0.119EXP(	0.000	
4	1	0.411EXP(	3.142	0.139EXP(	0.000	0.916EXP(	3.142	0.333EXP(	0.000	
4	2	0.599EXP(	3.142	0.293EXP(	0.000	0.955EXP(	3.142	0.191EXP(	0.000	
4	3	0.359EXP(	3.142	0.138EXP(	0.000	0.353EXP(	3.142	0.128EXP(	0.000	
4	4	0.281EXP(	3.142	0.141EXP(	0.000	0.141EXP(	3.142	0.097EXP(	0.000	1.834
5	0	0.317EXP(	3.142	0.143EXP(	0.000	0.307EXP(	4.189	0.119EXP(	0.000	
5	1	0.411EXP(	3.142	0.139EXP(	0.000	0.916EXP(	4.189	0.333EXP(	0.000	
5	2	0.599EXP(	3.142	0.293EXP(	0.000	0.955EXP(	4.189	0.191EXP(	0.000	
5	3	0.359EXP(	3.142	0.138EXP(	0.000	0.353EXP(	4.189	0.128EXP(	0.000	
5	4	0.281EXP(	3.142	0.141EXP(	0.000	0.141EXP(	4.189	0.097EXP(	0.000	1.993
6	0	0.317EXP(	3.142	0.143EXP(	0.000	0.307EXP(	5.236	0.119EXP(	0.000	
6	1	0.411EXP(	3.142	0.139EXP(	0.000	0.916EXP(	5.236	0.333EXP(	0.000	
6	2	0.599EXP(	3.142	0.293EXP(	0.000	0.955EXP(	5.236	0.191EXP(	0.000	
6	3	0.359EXP(	3.142	0.138EXP(	0.000	0.353EXP(	5.236	0.128EXP(	0.000	
6	4	0.281EXP(	3.142	0.141EXP(	0.000	0.141EXP(	5.236	0.097EXP(	0.000	2.413
7	0	0.317EXP(	3.142	0.143EXP(	0.000	0.307EXP(	0.000	0.119EXP(	1.079	
7	1	0.411EXP(	3.142	0.139EXP(	0.000	0.916EXP(	0.000	0.333EXP(	1.079	
7	2	0.599EXP(	3.142	0.293EXP(	0.000	0.955EXP(	0.000	0.191EXP(	1.079	
7	3	0.359EXP(	3.142	0.138EXP(	0.000	0.353EXP(	0.000	0.128EXP(	1.079	
7	4	0.281EXP(	3.142	0.141EXP(	0.000	0.141EXP(	0.000	0.097EXP(	1.079	2.399
8	0	0.317EXP(	3.142	0.143EXP(	0.000	0.307EXP(	0.000	0.119EXP(	2.157	
8	1	0.411EXP(	3.142	0.139EXP(	0.000	0.916EXP(	0.000	0.333EXP(	2.157	
8	2	0.599EXP(	3.142	0.293EXP(	0.000	0.955EXP(	0.000	0.191EXP(	2.157	
8	3	0.359EXP(	3.142	0.138EXP(	0.000	0.353EXP(	0.000	0.128EXP(	2.157	
8	4	0.281EXP(	3.142	0.141EXP(	0.000	0.141EXP(	0.000	0.097EXP(	2.157	1.979
9	0	0.317EXP(	3.142	0.143EXP(	0.000	0.307EXP(	0.000	0.119EXP(	3.236	
9	1	0.411EXP(	3.142	0.139EXP(	0.000	0.916EXP(	0.000	0.333EXP(	3.236	
9	2	0.599EXP(	3.142	0.293EXP(	0.000	0.955EXP(	0.000	0.191EXP(	3.236	
9	3	0.359EXP(	3.142	0.138EXP(	0.000	0.353EXP(	0.000	0.128EXP(	3.236	
9	4	0.281EXP(	3.142	0.141EXP(	0.000	0.141EXP(	0.000	0.097EXP(	3.236	1.833
10	0	0.317EXP(	3.142	0.143EXP(	0.000	0.307EXP(	0.000	0.119EXP(	4.314	
10	1	0.411EXP(	3.142	0.139EXP(	0.000	0.916EXP(	0.000	0.333EXP(	4.314	
10	2	0.599EXP(	3.142	0.293EXP(	0.000	0.955EXP(	0.000	0.191EXP(	4.314	
10	3	0.359EXP(	3.142	0.138EXP(	0.000	0.353EXP(	0.000	0.128EXP(	4.314	
10	4	0.281EXP(	3.142	0.141EXP(	0.000	0.141EXP(	0.000	0.097EXP(	4.314	2.033
11	0	0.317EXP(	3.142	0.143EXP(	0.000	0.307EXP(	0.000	0.119EXP(	5.393	
11	1	0.411EXP(	3.142	0.139EXP(	0.000	0.916EXP(	0.000	0.333EXP(	5.393	
11	2	0.599EXP(	3.142	0.293EXP(	0.000	0.955EXP(	0.000	0.191EXP(	5.393	
11	3	0.359EXP(	3.142	0.138EXP(	0.000	0.353EXP(	0.000	0.128EXP(	5.393	
11	4	0.281EXP(	3.142	0.141EXP(	0.000	0.141EXP(	0.000	0.097EXP(	5.393	2.481

Final Component Coefficients for Iteration # 3 :

Point #	Comp Freq#	Signal Vert.	Signal Pol.	Signal Horiz.	Signal Pol.	Filter Vert.	Filter Pol.	Filter Horiz	Filter Pol.	SIR
Opt	0	0.317EXP(	3.142	0.143EXP(	0.000	0.307EXP(	0.000	0.119EXP(	0.000	
Opt	1	0.411EXP(	3.142	0.139EXP(	0.000	0.916EXP(	0.000	0.333EXP(	0.000	
Opt	2	0.599EXP(	3.142	0.293EXP(	0.000	0.955EXP(	0.000	0.191EXP(	0.000	
Opt	3	0.359EXP(	3.142	0.138EXP(	0.000	0.353EXP(	0.000	0.128EXP(	0.000	
Opt	4	0.281EXP(	3.142	0.141EXP(	0.000	0.141EXP(	0.000	0.097EXP(	0.000	2.697

TABLE B6

MAXIMIZING SIR BY VARYING ONLY SIGNAL PHASE

Starting Component Coefficients for Iteration # 1 :

Point #	Comp. Freq#	Signal Vert. Pol.	Signal Horiz. Pol.	Filter Vert. Pol.	Filter Horiz. Pol.	SIR
1	0	0.316EXP(0.000	0.316EXP(0.000	0.316EXP(0.000	0.316EXP(0.000	
1	1	0.316EXP(0.000	0.316EXP(0.000	0.316EXP(0.000	0.316EXP(0.000	
1	2	0.316EXP(0.000	0.316EXP(0.000	0.316EXP(0.000	0.316EXP(0.000	
1	3	0.316EXP(0.000	0.316EXP(0.000	0.316EXP(0.000	0.316EXP(0.000	
1	4	0.316EXP(0.000	0.316EXP(0.000	0.316EXP(0.000	0.316EXP(0.000	0.648
2	0	0.316EXP(1.047	0.316EXP(0.000	0.316EXP(0.000	0.316EXP(0.000	
2	1	0.316EXP(1.047	0.316EXP(0.000	0.316EXP(0.000	0.316EXP(0.000	
2	2	0.316EXP(1.047	0.316EXP(0.000	0.316EXP(0.000	0.316EXP(0.000	
2	3	0.316EXP(1.047	0.316EXP(0.000	0.316EXP(0.000	0.316EXP(0.000	
2	4	0.316EXP(1.047	0.316EXP(0.000	0.316EXP(0.000	0.316EXP(0.000	0.756
3	0	0.316EXP(2.094	0.316EXP(0.000	0.316EXP(0.000	0.316EXP(0.000	
3	1	0.316EXP(2.094	0.316EXP(0.000	0.316EXP(0.000	0.316EXP(0.000	
3	2	0.316EXP(2.094	0.316EXP(0.000	0.316EXP(0.000	0.316EXP(0.000	
3	3	0.316EXP(2.094	0.316EXP(0.000	0.316EXP(0.000	0.316EXP(0.000	
3	4	0.316EXP(2.094	0.316EXP(0.000	0.316EXP(0.000	0.316EXP(0.000	1.132
4	0	0.316EXP(3.142	0.316EXP(0.000	0.316EXP(0.000	0.316EXP(0.000	
4	1	0.316EXP(3.142	0.316EXP(0.000	0.316EXP(0.000	0.316EXP(0.000	
4	2	0.316EXP(3.142	0.316EXP(0.000	0.316EXP(0.000	0.316EXP(0.000	
4	3	0.316EXP(3.142	0.316EXP(0.000	0.316EXP(0.000	0.316EXP(0.000	
4	4	0.316EXP(3.142	0.316EXP(0.000	0.316EXP(0.000	0.316EXP(0.000	1.507
5	0	0.316EXP(4.189	0.316EXP(0.000	0.316EXP(0.000	0.316EXP(0.000	
5	1	0.316EXP(4.189	0.316EXP(0.000	0.316EXP(0.000	0.316EXP(0.000	
5	2	0.316EXP(4.189	0.316EXP(0.000	0.316EXP(0.000	0.316EXP(0.000	
5	3	0.316EXP(4.189	0.316EXP(0.000	0.316EXP(0.000	0.316EXP(0.000	
5	4	0.316EXP(4.189	0.316EXP(0.000	0.316EXP(0.000	0.316EXP(0.000	1.132
6	0	0.316EXP(5.236	0.316EXP(0.000	0.316EXP(0.000	0.316EXP(0.000	
6	1	0.316EXP(5.236	0.316EXP(0.000	0.316EXP(0.000	0.316EXP(0.000	
6	2	0.316EXP(5.236	0.316EXP(0.000	0.316EXP(0.000	0.316EXP(0.000	
6	3	0.316EXP(5.236	0.316EXP(0.000	0.316EXP(0.000	0.316EXP(0.000	
6	4	0.316EXP(5.236	0.316EXP(0.000	0.316EXP(0.000	0.316EXP(0.000	0.756
7	0	0.316EXP(0.000	0.316EXP(1.079	0.316EXP(0.000	0.316EXP(0.000	
7	1	0.316EXP(0.000	0.316EXP(1.079	0.316EXP(0.000	0.316EXP(0.000	
7	2	0.316EXP(0.000	0.316EXP(1.079	0.316EXP(0.000	0.316EXP(0.000	
7	3	0.316EXP(0.000	0.316EXP(1.079	0.316EXP(0.000	0.316EXP(0.000	
7	4	0.316EXP(0.000	0.316EXP(1.079	0.316EXP(0.000	0.316EXP(0.000	0.763
8	0	0.316EXP(0.000	0.316EXP(2.197	0.316EXP(0.000	0.316EXP(0.000	
8	1	0.316EXP(0.000	0.316EXP(2.197	0.316EXP(0.000	0.316EXP(0.000	
8	2	0.316EXP(0.000	0.316EXP(2.197	0.316EXP(0.000	0.316EXP(0.000	
8	3	0.316EXP(0.000	0.316EXP(2.197	0.316EXP(0.000	0.316EXP(0.000	
8	4	0.316EXP(0.000	0.316EXP(2.197	0.316EXP(0.000	0.316EXP(0.000	1.163
9	0	0.316EXP(0.000	0.316EXP(3.236	0.316EXP(0.000	0.316EXP(0.000	
9	1	0.316EXP(0.000	0.316EXP(3.236	0.316EXP(0.000	0.316EXP(0.000	
9	2	0.316EXP(0.000	0.316EXP(3.236	0.316EXP(0.000	0.316EXP(0.000	
9	3	0.316EXP(0.000	0.316EXP(3.236	0.316EXP(0.000	0.316EXP(0.000	
9	4	0.316EXP(0.000	0.316EXP(3.236	0.316EXP(0.000	0.316EXP(0.000	1.503
10	0	0.316EXP(0.000	0.316EXP(4.314	0.316EXP(0.000	0.316EXP(0.000	
10	1	0.316EXP(0.000	0.316EXP(4.314	0.316EXP(0.000	0.316EXP(0.000	
10	2	0.316EXP(0.000	0.316EXP(4.314	0.316EXP(0.000	0.316EXP(0.000	
10	3	0.316EXP(0.000	0.316EXP(4.314	0.316EXP(0.000	0.316EXP(0.000	
10	4	0.316EXP(0.000	0.316EXP(4.314	0.316EXP(0.000	0.316EXP(0.000	1.072
11	0	0.316EXP(0.000	0.316EXP(5.393	0.316EXP(0.000	0.316EXP(0.000	
11	1	0.316EXP(0.000	0.316EXP(5.393	0.316EXP(0.000	0.316EXP(0.000	
11	2	0.316EXP(0.000	0.316EXP(5.393	0.316EXP(0.000	0.316EXP(0.000	
11	3	0.316EXP(0.000	0.316EXP(5.393	0.316EXP(0.000	0.316EXP(0.000	
11	4	0.316EXP(0.000	0.316EXP(5.393	0.316EXP(0.000	0.316EXP(0.000	0.739

Final Component Coefficients for Iteration # 1 .

Point #	Comp Freq#	Signal Vert Pol	Signal Horiz Pol.	Filter Vert Pol	Filter Horiz Pol.	SIR
Opt	0	0.316EXP(3.142	0.316EXP(0.000	0.316EXP(0.000	0.316EXP(0.000	
Opt	1	0.316EXP(3.142	0.316EXP(0.000	0.316EXP(0.000	0.316EXP(0.000	
Opt	2	0.316EXP(3.142	0.316EXP(0.000	0.316EXP(0.000	0.316EXP(0.000	
Opt	3	0.316EXP(3.142	0.316EXP(0.000	0.316EXP(0.000	0.316EXP(0.000	
Opt	4	0.316EXP(3.142	0.316EXP(0.000	0.316EXP(0.000	0.316EXP(0.000	1.507

TABLE B7

MAXIMIZING SIR BY VARYING FILTER MAGNITUDE

Starting Component Coefficients for Iteration # 3 :

Point #	Comp. Freq#	Signal Vert.	Signal Pol.	Signal Horiz.	Signal Pol.	Filter Vert.	Filter Pol.	Filter Horiz.	Filter Pol.	SIR
1	0	0.304EXP	3.142	0.170EXP	0.000	0.305EXP	0.000	0.08CEXP	0.000	
1	1	0.410EXP	3.142	0.094EXP	0.000	0.416EXP	0.000	0.08CEXP	0.000	
1	2	0.623EXP	3.142	0.296EXP	0.000	0.621EXP	0.000	0.296EXP	0.000	
1	3	0.392EXP	3.142	0.092EXP	0.000	0.442EXP	0.000	0.09CEXP	0.000	
1	4	0.264EXP	3.142	0.157EXP	0.000	0.267EXP	0.000	0.08CEXP	0.000	2.680
2	0	0.304EXP	3.142	0.170EXP	0.000	0.000EXP	0.000	0.333EXP	0.000	
2	1	0.410EXP	3.142	0.094EXP	0.000	0.333EXP	0.000	0.333EXP	0.000	
2	2	0.623EXP	3.142	0.296EXP	0.000	0.333EXP	0.000	0.333EXP	0.000	
2	3	0.392EXP	3.142	0.092EXP	0.000	0.333EXP	0.000	0.333EXP	0.000	
2	4	0.264EXP	3.142	0.157EXP	0.000	0.333EXP	0.000	0.333EXP	0.000	2.009
3	0	0.304EXP	3.142	0.170EXP	0.000	0.333EXP	0.000	0.333EXP	0.000	
3	1	0.410EXP	3.142	0.094EXP	0.000	0.003EXP	0.000	0.333EXP	0.000	
3	2	0.623EXP	3.142	0.296EXP	0.000	0.333EXP	0.000	0.333EXP	0.000	
3	3	0.392EXP	3.142	0.092EXP	0.000	0.333EXP	0.000	0.333EXP	0.000	
3	4	0.264EXP	3.142	0.157EXP	0.000	0.333EXP	0.000	0.333EXP	0.000	1.939
4	0	0.304EXP	3.142	0.170EXP	0.000	0.333EXP	0.000	0.333EXP	0.000	
4	1	0.410EXP	3.142	0.094EXP	0.000	0.333EXP	0.000	0.333EXP	0.000	
4	2	0.623EXP	3.142	0.296EXP	0.000	0.000EXP	0.000	0.333EXP	0.000	
4	3	0.392EXP	3.142	0.092EXP	0.000	0.333EXP	0.000	0.333EXP	0.000	
4	4	0.264EXP	3.142	0.157EXP	0.000	0.333EXP	0.000	0.333EXP	0.000	1.900
5	0	0.304EXP	3.142	0.170EXP	0.000	0.333EXP	0.000	0.333EXP	0.000	
5	1	0.410EXP	3.142	0.094EXP	0.000	0.333EXP	0.000	0.333EXP	0.000	
5	2	0.623EXP	3.142	0.296EXP	0.000	0.333EXP	0.000	0.333EXP	0.000	
5	3	0.392EXP	3.142	0.092EXP	0.000	0.000EXP	0.000	0.333EXP	0.000	
5	4	0.264EXP	3.142	0.157EXP	0.000	0.333EXP	0.000	0.333EXP	0.000	1.950
6	0	0.304EXP	3.142	0.170EXP	0.000	0.333EXP	0.000	0.333EXP	0.000	
6	1	0.410EXP	3.142	0.094EXP	0.000	0.333EXP	0.000	0.333EXP	0.000	
6	2	0.623EXP	3.142	0.296EXP	0.000	0.333EXP	0.000	0.333EXP	0.000	
6	3	0.392EXP	3.142	0.092EXP	0.000	0.333EXP	0.000	0.333EXP	0.000	
6	4	0.264EXP	3.142	0.157EXP	0.000	0.000EXP	0.000	0.333EXP	0.000	2.037
7	0	0.304EXP	3.142	0.170EXP	0.000	0.333EXP	0.000	0.00CEXP	0.000	
7	1	0.410EXP	3.142	0.094EXP	0.000	0.333EXP	0.000	0.333EXP	0.000	
7	2	0.623EXP	3.142	0.296EXP	0.000	0.333EXP	0.000	0.333EXP	0.000	
7	3	0.392EXP	3.142	0.092EXP	0.000	0.333EXP	0.000	0.333EXP	0.000	
7	4	0.264EXP	3.142	0.157EXP	0.000	0.333EXP	0.000	0.333EXP	0.000	2.163
8	0	0.304EXP	3.142	0.170EXP	0.000	0.333EXP	0.000	0.333EXP	0.000	
8	1	0.410EXP	3.142	0.094EXP	0.000	0.333EXP	0.000	0.00CEXP	0.000	
8	2	0.623EXP	3.142	0.296EXP	0.000	0.333EXP	0.000	0.333EXP	0.000	
8	3	0.392EXP	3.142	0.092EXP	0.000	0.333EXP	0.000	0.333EXP	0.000	
8	4	0.264EXP	3.142	0.157EXP	0.000	0.333EXP	0.000	0.333EXP	0.000	2.163
9	0	0.304EXP	3.142	0.170EXP	0.000	0.333EXP	0.000	0.333EXP	0.000	
9	1	0.410EXP	3.142	0.094EXP	0.000	0.333EXP	0.000	0.333EXP	0.000	
9	2	0.623EXP	3.142	0.296EXP	0.000	0.333EXP	0.000	0.00CEXP	0.000	
9	3	0.392EXP	3.142	0.092EXP	0.000	0.333EXP	0.000	0.333EXP	0.000	
9	4	0.264EXP	3.142	0.157EXP	0.000	0.333EXP	0.000	0.333EXP	0.000	2.162
10	0	0.304EXP	3.142	0.170EXP	0.000	0.333EXP	0.000	0.333EXP	0.000	
10	1	0.410EXP	3.142	0.094EXP	0.000	0.333EXP	0.000	0.333EXP	0.000	
10	2	0.623EXP	3.142	0.296EXP	0.000	0.333EXP	0.000	0.333EXP	0.000	
10	3	0.392EXP	3.142	0.092EXP	0.000	0.333EXP	0.000	0.00CEXP	0.000	
10	4	0.264EXP	3.142	0.157EXP	0.000	0.333EXP	0.000	0.333EXP	0.000	2.166
11	0	0.304EXP	3.142	0.170EXP	0.000	0.333EXP	0.000	0.333EXP	0.000	
11	1	0.410EXP	3.142	0.094EXP	0.000	0.333EXP	0.000	0.333EXP	0.000	
11	2	0.623EXP	3.142	0.296EXP	0.000	0.333EXP	0.000	0.333EXP	0.000	
11	3	0.392EXP	3.142	0.092EXP	0.000	0.333EXP	0.000	0.333EXP	0.000	
11	4	0.264EXP	3.142	0.157EXP	0.000	0.333EXP	0.000	0.000EXP	0.000	2.164

Final Component Coefficients for Iteration # 3

Point #	Comp Freq#	Signal Vert	Signal Pol	Signal Horiz	Signal Pol	Filter Vert	Filter Pol	Filter Horiz	Filter Pol	SIR
Opt.	0	0.304EXP	3.142	0.170EXP	0.000	0.305EXP	0.000	0.08CEXP	0.000	
Opt.	1	0.410EXP	3.142	0.094EXP	0.000	0.416EXP	0.000	0.08CEXP	0.000	
Opt.	2	0.623EXP	3.142	0.296EXP	0.000	0.621EXP	0.000	0.296EXP	0.000	
Opt.	3	0.392EXP	3.142	0.092EXP	0.000	0.442EXP	0.000	0.09CEXP	0.000	
Opt.	4	0.264EXP	3.142	0.157EXP	0.000	0.267EXP	0.000	0.08CEXP	0.000	2.680

APPENDIX C

ON MULTI-CHANNEL DETECTION OF RANDOM SIGNAL IN GAUSSIAN NOISE

ON MULTI-CHANNEL DETECTION OF RANDOM SIGNALS IN GAUSSIAN NOISE

1. INTRODUCTION.

In the classical books Van Trees [1], [2] has presented the single channel detection theory when signals are deterministic or have random parameters. Extension of these works to multi-channels case has received little attention. An earlier reference is [3] in which Lindsey derived the optimum receiver and its performance for independent Rician fading multi-channels.

Vannicola [4] introduced a natural extension of the above single channel model for the two-channel radar detection problems. In his model, Vannicola used the scatter matrix B to describe the characteristics of each channel and the correlations between two channels. These models are important for both radar detection and communication problems. Our revisit to Vannicola's model reveals that, for some of the important detection problems, the extension of single channel results to multi-channel situations is not straightforward and requires additional techniques to yield desired expression for the optimum receiver.

In this paper, we consider one of the important cases of such multi-channels problems, i.e., the slowly fluctuating point target model when the noise is white or colored. Using the maximum likelihood criterion, orthonormalizing procedure, and eigen value–eigen vector approach, we have derived the optimum receiver for the two-channels case. Extension of these results to more than two channels is straightforward.

2. OPTIMUM RECEIVER FOR SINGLE CHANNEL CASE.

This section contains a brief summary of single-channel detection results. These results are well known and most conveniently available in Van Trees. The reason to reproduce some of these results here in that it allows an easy reference as well as a comparison with multi-channel results derived in the remaining sections.

For the detection of slowly fluctuating point targets in the presence of additive white Gaussian noise, Van Trees derived the statistical model as

$$\tilde{r}(t) = \sqrt{E_t}\,\tilde{b}\tilde{f}(t) + \tilde{w}(t) \quad 0 \le t \le T : H_1 \tag{2.1}$$

$$\tilde{r}(t) = \tilde{w}(t) \quad 0 \le t \le T : H_0 \tag{2.2}$$

where $\tilde{r}(t)$ is the complex envelope of the received wave form, $\tilde{b}$ is a zero-mean complex Gaussian random variable which satisfies

$$E(|\tilde{b}|^2) = E(\tilde{b}\tilde{b}^*) = 2\sigma_b^2, \tag{2.3}$$

$\tilde{f}(t)$ is the complex envelope of the transmitted signal with unit energy, i.e.,

$$\int |f(t)|^2 dt = \int f(t) f^*(t) dt = 1, \tag{2.4}$$

$\tilde{w}(t)$ is a zero-mean complex Gaussian white noise process which is independent of $\tilde{b}$ and satisfies

$$E[\tilde{w}(t)\tilde{w}^*(u)] = N_0\delta(t-u). \tag{2.5}$$

The optimum receiver is constructed by using the complete orthonormal (C. O. N.) set expansion, and by finding the sufficient statistic. It turns out that this sufficient statistic has the form

$$r_1 = \int_0^T \tilde{f}(t)\tilde{r}^*(t)dt. \tag{2.6}$$

The optimum receiver computes $|\tilde{R}_1|^2$ and decides acceptance or rejection of H_1 depending upon

$$|\tilde{R}_1|^2 \underset{H_0}{\overset{H_1}{\gtrless}} r^* \tag{2.7}$$

where r^* is called the threshold. This structure of the optimum receiver is graphically presented in Figure 1 below:

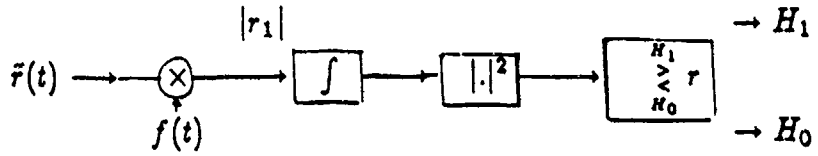

Figure 1. Optimum receiver of Single-Channel Case.

3. OPTIMUM RECEIVER FOR MULTI-CHANNEL MODEL. WHITE NOISE CASE.

For the multi-channel model derivation of the optimum receiver is relatively complicated. For simplicity in presentation we consider the two-channel case first.

The statistical model for two-channel case can be formulated as follows:

$$\underline{r}(t) = \underline{b}\underline{f}(t) + \underline{w}(t) \qquad 0 \le t \le T \;:\; H_1 \tag{3.1}$$

$$\underline{r}(t) = \underline{w}(t) \qquad 0 \le t \le T \;:\; H_0 \tag{3.2}$$

where the vectors $\underline{r}$, $\underline{f}$ and $\underline{w}$ and matrix $\underline{b}$ can be expressed in terms of their components as follows:

$$\begin{aligned} \underline{\tilde{r}}(t) &= \begin{bmatrix} r_1(t) \\ r_2(t) \end{bmatrix}, \quad \underline{\tilde{f}}(t) = \begin{bmatrix} f_1(t) \\ f_2(t) \end{bmatrix}, \\ \underline{\tilde{w}}(t) &= \begin{bmatrix} w_1(t) \\ w_2(t) \end{bmatrix}, \quad \underline{\tilde{b}} = \begin{bmatrix} b_{11} & b_{12} \\ b_{21} & b_{22} \end{bmatrix}. \end{aligned} \tag{3.3}$$

The vector $\tilde{\underline{r}}(t)$ is the convex envelope of the received wave forms, $\tilde{\underline{b}}$ is the scatter matrix of the target, $\tilde{\underline{f}}(t)$ is the convex envelope of the transmitted signals and its energy equals:

$$E = \int_0^T [\underline{f}(t)]^T [\underline{f}(t)]^* dt = \int_0^T |f_1(t)|^2 dt + \int_0^T |f_2(t)|^2 dt$$
$$= E_1 + E_2 \tag{3.4}$$

where E_1 and E_2 are the integrals of $|f_1(t)|^2$ and $|f_2(t)|^2$ and represent energies in channel 1 and 2, respectively. (For amplitude-modulated signals actual transmitted energy equals $E/2$). The zero-mean vector white noise process $\tilde{\underline{w}}(t)$ is independent of the scatter matrix $\tilde{\underline{b}}$ and the two components of the vector $\tilde{\underline{w}}(t)$ are independent of each other. Moreover, it is assumed that the two components have equal spectral densities in the two channels, i.e.,

$$E[\tilde{\underline{w}}(t)\tilde{\underline{w}}^\dagger(t)] = N_0 \begin{bmatrix} \delta(t-u) & 0 \\ 0 & \delta(t-u) \end{bmatrix}$$
$$= N_0 \delta(t-u) I. \tag{3.5}$$

Following the procedure of deriving the optimum receiver for the single-channel model, we define a vector C. O. N. set $\{\underline{\phi}_i(t)\}_{i=1}^{\infty}$. Since this is a C. O. N. set, the elements $\underline{\phi}_i(t)$ satisfy

$$\underline{\phi}_i(t) = \begin{bmatrix} \phi_{1i}(t) \\ \phi_{2i}(t) \end{bmatrix}$$

and

$$\int_0^T \underline{\phi}_i^T(t) \quad \underline{\phi}_j^*(t) dt = \int_0^T \underline{\phi}_j^\dagger(t) \phi_i(t) dt = \delta_{ij} \tag{3.6}$$

where † denotes complex conjugate and matrix transpose. In terms of $\underline{\phi}_i(t)$'s the received vector $\underline{\tilde{r}}(t)$ can be written as

$$\underline{\tilde{r}}(t) = \lim_{k\to\infty} \sum_{i=1}^{k} \tilde{r}_i \underline{\phi}_i(t) \tag{3.7}$$

where

$$\tilde{r}_i = \int_0^T \underline{\tilde{r}}^T(t)\underline{\phi}_i^*(t)dt = \int_0^T \underline{\phi}^\dagger(t)\underline{\tilde{r}}(t)dt \tag{3.8}$$

From the assumptions, made earlier, on the process $\underline{\tilde{r}}(t)$ it is easily observed that the coefficients $\tilde{r}_i$'s are zero-mean complex Gaussian random variables. If we can choose the C. O. N. set such that only k of the coefficients are dependent on which hypothesis is true and if these k coefficients are statistically independent of the other coefficients, collectively they will give us a k-dimensional sufficient statistic. The coefficients $\tilde{r}_i$'s will satisfy the independence condition if

$$E[\tilde{r}_i\tilde{r}_j^*|H_l] = 0 \quad \text{for } l = 0,1 \quad \text{and for all } i \neq j \tag{3.9}$$

On H_0 the desired condition is satisfied due to the fact that $\tilde{r}_i$'s depend only on the white noise process. On H_1, the correlation between $\tilde{r}_i$'s can be written as:

$$E[\tilde{r}_i\tilde{r}_j^*|H_1] = \iint \underline{\tilde{\phi}}_i^\dagger(t)\underline{\tilde{K}}_s(t,u)\underline{\tilde{\phi}}_j(u)dt\,du + N_0\delta_{ij} \tag{3.10}$$

where

$$\underline{\tilde{K}}_s(t,u) = E[\underline{\tilde{b}}\,\underline{\tilde{f}}(t)\underline{\tilde{f}}^*(u)\underline{\tilde{b}}^\dagger] \tag{3.11}$$

is the kernel of received signal components. This kernel is known provided all statistics of the scatter matrix $\underline{\tilde{b}}$ are known and the transmitted signal

wave form $\underline{\tilde{f}}(t)$ are given. From (3.10), $\tilde{r}_i$'s are uncorrelated if and only if the functions in the C. O. N. set satisfy the integral equation

$$\iint \underline{\tilde{\phi}}_i^{\dagger}(t)\underline{\tilde{K}}_s(t,u)\underline{\tilde{\phi}}_j(u)dt\,du = \lambda_i\delta_{ij},$$

or equivalently

$$\int \underline{\tilde{K}}_s(t,u)\underline{\tilde{\phi}}_i(u)du = \lambda_i\underline{\tilde{\phi}}_i(t). \tag{3.12}$$

This last expression shows that if the eigen functions $\tilde{\phi}_i(t)$'s and eigen values λ_i's can be solved, then the construction of the likelihood ratio test is straightforward. In other words, the likelihood ratio is given by

$$\Lambda(R) = \lim_{k\to\infty} \frac{P[\underline{\tilde{R}}_k|H_1]}{P[\underline{\tilde{R}}_k|H_0]} = \lim_{k\to\infty} \frac{\prod_{i=1}^{k} P[\tilde{R}_i|H_1]}{\prod_{i=1}^{k} P[\tilde{R}_i|H_0]} \underset{H_0}{\overset{H_1}{\gtrless}} \eta. \tag{3.13}$$

The probablility density functions of the complex Gaussian variables as appears in (3.13) are given by

$$\begin{aligned} P[\tilde{R}_i|H_1] &= \{\pi(N_0+\lambda_i)\}^{-1}exp\{-|R_i|^2/(N_0+\lambda_i)\} \\ P[\tilde{R}_i|H_0] &= \{\pi N_0\}^{-1}exp\{-|R_i|^2/N_0\}. \end{aligned} \tag{3.14}$$

Substitution of (3.14) in (3.13) and then taking its logarithm and further simplification results in the following log likelihood ratio test

$$l_R = \lim_{k\to\infty} \sum_{i=1}^{k} \frac{\lambda_i}{N_0(N_0+\lambda_i)}|R_i|^2 \underset{H_0}{\overset{H_1}{\gtrless}} \gamma \tag{3.15}$$

where $\gamma = \ln\eta + \sum \ln\{(N_0+\lambda_i)/N_0\}$ is the decision threshold. If the number of nonzero λ_i's is infinite, then construction of the optimum receiver according to (3.15) is impractical, and instead we must find its closed form representation. For the single-channel model it was straightforward to solve

(3.12) because the function $\underline{f}(u)$ can be separated from the kernel, i.e., in the single-channel case

$$K_s(t,u) = E[\tilde{b}\tilde{f}(t)f(u)\tilde{b}^*] = E(|\tilde{b}|^2)\tilde{f}(t)\tilde{f}^*(u). \tag{3.16}$$

Due to this simplification the integral equation (3.12) can be written as

$$E(|\tilde{b}|^2)\tilde{f}(t)\int_0^T \tilde{f}^*(u)\phi_i(u)du = \lambda_i\phi_i(t). \tag{3.17}$$

It follows that a solution of (3.17) is given by $\phi_1(t) = \tilde{f}(t)/\sqrt{e_t}$ and the associated eigen value $\lambda_1 = e_t E(|\tilde{b}|^2) = 2\sigma_b^2 e_t = e_r$. Any other function $\tilde{\phi}_i(t), i = 2,3,\ldots$ which is orthogonal to $\tilde{\phi}_1(t)$ is a solution of (3.17) with zero eigen value. Thus, in brief, the single-channel case is straightforward due to aforementioned simplification and the corresponding log likelihood ratio statistic is

$$l_R = \frac{e_r}{N_0(N_0+e_r)}|R_1|^2$$

which can also be written as (2.7).

For the multi-channel case, in general, the kernel $\underline{\tilde{K}}(t,u)$ cannot be written in the form of (3.16). Hence we cannot derive the sufficient statistics in the same way as in the single-channel case. In this paper, we first consider some special cases which lend themselves to easier solutions. Our next goal is to show that it is possible to extend the results so obtained to a general setting and thus obtain the optimum detector of Gaussian signal in the presence of white or colored noise.

CASE I. Identical Signal Envelopes.

Suppose that the two transmitted signals, in two different channels, have identical envelopes and may differ only in their energies and phases, i.e.,

$$\underline{\tilde{f}}(t) = \begin{bmatrix} \tilde{f}_1(t) \\ \tilde{f}_2(t) \end{bmatrix} = \begin{bmatrix} A_1 \\ A_2 \end{bmatrix} \tilde{s}(t) = \begin{bmatrix} \sqrt{E_1} & e^{j\theta_1} \\ \sqrt{E_2} & e^{j\theta_2} \end{bmatrix} \tilde{s}(t) = \underline{A}\tilde{s}(t) \qquad (3.18)$$

where E_1 and E_2 are the energies and θ_1 and θ_2 are the phases of $\tilde{f}_1(t)$ and $\tilde{f}_2(t)$, respectively, and $s(t)$ is a real valved function with unit energy. Thus,

$$E_l = \int_0^T |\tilde{f}_l(t)|^2 dt \quad l = 0, 1$$

and (3.19)

$$\int_0^T s^2(t)dt = 1.$$

The signal components in received wave forms can be written as

$$\underline{b}\underline{\tilde{f}}(t) = \begin{bmatrix} b_{11} & b_{12} \\ b_{11} & b_{12} \end{bmatrix} \begin{bmatrix} \sqrt{E_1} & e^{j\theta} \\ \sqrt{E_1} & e^{j\theta} \end{bmatrix} s(t) = x_1\underline{\phi}_1(t) + x_2\underline{\phi}_2(t) \qquad (3.20)$$

where

$$\underline{\phi}_1(t) = \begin{bmatrix} s(t) \\ 0 \end{bmatrix}, \quad \underline{\phi}_2(t) = \begin{bmatrix} 0 \\ s(t) \end{bmatrix},$$

$$x_1 = b_{11}\sqrt{E_1}e^{j\theta_1} + b_{12}\sqrt{E_2}e^{j\theta_2} = \underline{b}_1^T A = A^T\underline{b}_1$$

$$x_2 = b_{21}\sqrt{E_1}e^{j\theta_1} + b_{22}\sqrt{E_2}e^{j\theta_2} = \underline{b}_2^T A = A^T\underline{b}_2$$

$$\underline{b}_1 = \begin{bmatrix} b_{11} \\ b_{12} \end{bmatrix} \quad \text{and} \quad \underline{b}_2 = \begin{bmatrix} b_{21} \\ b_{22} \end{bmatrix}.$$

We observe that $\underline{\phi}_1(t)$ and $\underline{\phi}_2(t)$ are orthonormal functions, the signal process $\underline{b}\underline{\tilde{f}}(t)$ is a two-dimensional vector in $\underline{\phi}_1$, and $\underline{\phi}_2$ plane, and its components

x_1 and x_2 are random variables. These two functions, $\underline{\phi}_1(t)$, $\underline{\phi}_2(t)$, can be augmented into a C. O. N. set. In summary, it is possible to expand $\underline{\tilde{r}}(t)$ as

$$\underline{\tilde{r}}(t) = \begin{cases} \sum_{i=1}^{\infty} \tilde{r}_i \underline{\phi}_i(t) = \sum_{i=1}^{2} \tilde{r}_i \underline{\phi}_i(t) + \sum_{i=3}^{\infty} \tilde{w}_i \underline{\phi}_i(t) : H_1 & (3.21) \\ \sum_{i=1}^{\infty} \tilde{r}_i \underline{\phi}_i(t) = \sum_{i=1}^{\infty} \tilde{w}_i \underline{\phi}_i(t) \quad : H_0 & (3.22) \end{cases}$$

where it is important to note that for $i > 3$, all r_i's are independent of the hypotheses H_1 and H_0. Because of the independence between $\tilde{b}$ and $\underline{\tilde{w}}(t)$ the first two coefficients r_1 and r_2 are independent of the remaining coefficients $r_i = w_i$, $i > 2$. But r_1 and r_2 are not necessarily independent of each other. In any case, this does not prevent us from obtaining the likelihood function

$$\Lambda(R) = \frac{P[R|H_1]}{P[R|H_0]} = \frac{P[R_1, R_2|H_1]}{P[R_1, R_2|H_0]}. \tag{3.21}$$

The joint covariance matrix of r_1, r_2 can be derived as follows:

$$\begin{aligned} E[r_i r_j^*|H_0] &= E[\iint_0^T \underline{\phi}_i^\dagger(t)\underline{w}(t)\underline{w}^\dagger(u)\underline{\phi}_j(u)dt\,du] \\ &= \iint_0^T \underline{\phi}_i^\dagger(t)[N_0\delta(t-u)]\underline{\phi}_j(u)dt\,du \\ &= N_0 \int_0^T \underline{\phi}_i^\dagger(t)\underline{\phi}_j(t)dt = N_0\delta_{ij} \quad i,j = 1,2. \end{aligned} \tag{3.22}$$

In a similar manner and due to independence of x_i and w_j, $i,j = 1,2$ it is observed that

$$\begin{aligned} E[r_i r_j^*|H_1] &= E[x_i x_j^*] + E[w_i w_j^*] \\ &= E[\underline{b}_i^T A A^\dagger \underline{b}_j^*] + N_0\delta_{ij}. \end{aligned} \tag{3.23}$$

Thus, $\underline{R} = (R_1, R_2)^T$ is a zero-mean Gaussian random vector whose covariance matrices are given by

$$\underline{K}_0 = E[\underline{R}\underline{R}^\dagger | H_0] = N_0 I \tag{3.24}$$

and

$$\begin{aligned} \underline{K}_1 = E[\underline{R}\underline{R}^\dagger | H_1] &= E[\underline{b}\underline{A}\underline{A}^\dagger \underline{b}^\dagger] + N_0 I \\ &= \underline{K}_s + N_0 I, \end{aligned} \tag{3.25}$$

where $\underline{K}_s = E[\underline{b}\underline{A}\underline{A}^\dagger \underline{b}^\dagger]$ is the covariance matrix of the received signal components.

The matrix $\underline{K}_s$ may be diagonalized by a unitary transformation T, i.e.,

$$\underline{T}^\dagger \underline{K}_s \underline{T} = \begin{bmatrix} \mu_1 & 0 \\ 0 & \mu_2 \end{bmatrix} \tag{3.26}$$

where $\underline{T} = [\underline{C}_1 \vdots \underline{C}_2]$ is a 2×2 unitary transformation, μ_1 and μ_2 are eigen values of $\underline{K}_s$, and $\underline{C}_1$ and $\underline{C}_2$ are the corresponding eigen vectors. Using the fundamental theorem of linear algebra we then expand $\underline{K}_s$, $\underline{K}_0$ and $\underline{K}_1$, in terms of eigen values and vectors as shown below.

$$\begin{aligned} \underline{K}_s &= \mu_1 \underline{C}_1 \underline{C}_1^\dagger + \mu_2 \underline{C}_2 C_2^\dagger \\ \underline{K}_0 &= N_0 \underline{C}_1 \underline{C}_1^\dagger + N_0 \underline{C}_2 \underline{C}_2^\dagger = N_0 T I T^\dagger \\ \underline{K}_1 &= \underline{K}_s + \underline{K}_0 = (\mu_1 + N_0)\underline{C}_1 \underline{C}_1^\dagger + (\mu_2 + N_0)\underline{C}_2 \underline{C}_2^\dagger \\ &= T \begin{bmatrix} \mu_1 + N_0 & 0 \\ 0 & \mu_2 + N_0 \end{bmatrix} T^\dagger \end{aligned} \tag{3.27}$$

The above results also allow us to write the inverses

$$\underline{K}_0^{-1} = T \begin{bmatrix} \frac{1}{N_0} & 0 \\ 0 & \frac{1}{N_0} \end{bmatrix} T^\dagger, \qquad \underline{K}_1^{-1} = T \begin{bmatrix} \frac{1}{N_0 + \mu_1} & 0 \\ 0 & \frac{1}{N_0 + \mu_2} \end{bmatrix} T^\dagger. \tag{3.28}$$

Substitution of the joint Gaussian probability density functions

$$P[R_1 R_2 | H_l] = (2\pi)^{-2} |K_l|^{-1/2} exp(-\underline{R}^\dagger K_l^{-1} \underline{R}), l = 0, 1$$

in (3.21) and simplification of its logarithm gives the two-channel log likelihood ratio

$$l_R = \underline{R}^\dagger(\underline{K}_0^{-1} - K_1^{-1})\underline{R} = (R^\dagger T)\begin{bmatrix} \frac{\mu_1}{(\mu_1+N_0)N_0} & 0 \\ 0 & \frac{\mu_2}{(\mu_2+N_0)N_0} \end{bmatrix}(T^\dagger R)$$

$$= \sum_{i=1}^{2} \frac{\mu_i}{(\mu_i + N_0)N_0}|Y_i|^2 \tag{3.29}$$

where

$$\underline{Y} = \underline{T}^\dagger \underline{R} = [\underline{C}_1 \ \vdots \ \underline{C}_2]^\dagger \underline{R} = \begin{bmatrix} \underline{C}_1^\dagger & \underline{R} \\ \underline{C}_2^\dagger & \underline{R} \end{bmatrix}. \tag{3.30}$$

The $\underline{R}$ vector is derived by correlating the received waveform with the transmitted signal $s(t)$, i.e.,

$$\underline{R} = (r_1, r_2)^T = [\int_0^T \phi_1^T(t)\underline{r}(t)dt \quad \int_0^T \phi_2^T(t)\underline{r}(t)dt]^T$$

$$= \int_0^T s(t)\underline{r}(t)dt. \tag{3.31}$$

Hence, the optimum receiver for the identical envelope case has the form given in figure 2 below.

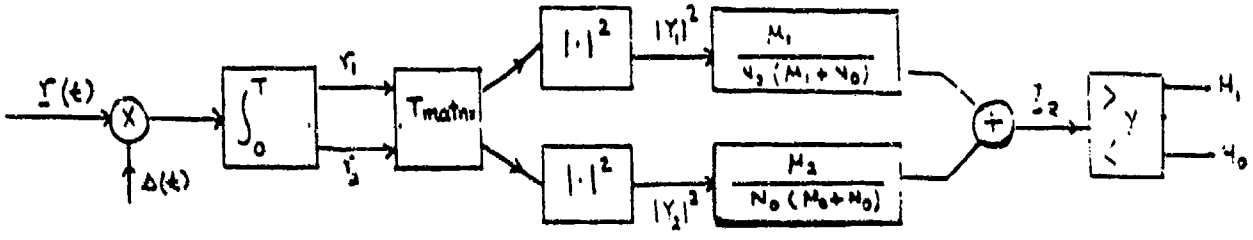

Figure 2. Optimum Receiver for Identical Envelope Case

Using the new orthonormal functions

$$\underline{\psi}_l(t) = \underline{C}_l s(t), \quad l = 0, 1$$

gives

$$Y_l = \int_0^T \underline{\psi}_l^\dagger(t)\underline{r}(t)dt \quad l = 0, 1$$

and consequently the optimum receiver has the form

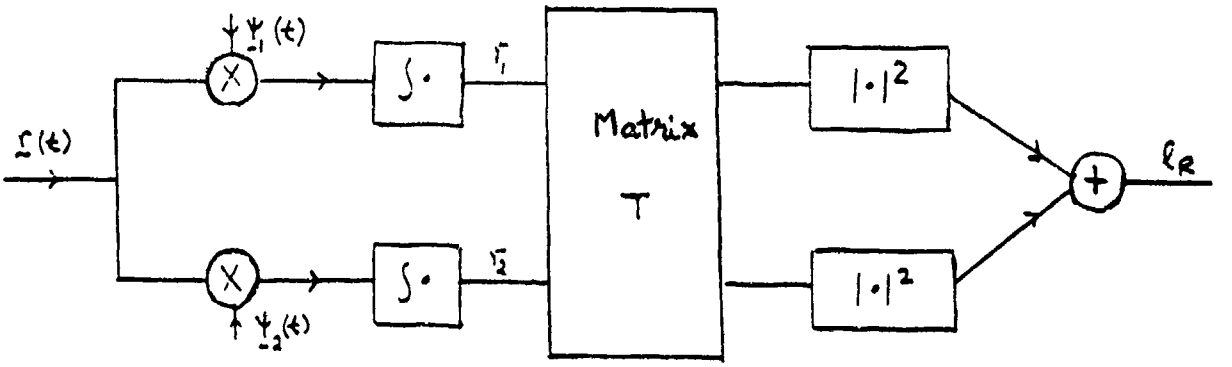

Figure 3. Another Form of Optimum Receiver for Identical Envelope Case

CASE II. The Orthogonal Envelopes Case.

This is another extreme situation in which we assume that the transmitted signals in the two channels are orthogonal. This implies that

$$\int_0^T f_1(t)f_2^*(t)dt = 0$$

Hence the signal comonents of the received waveform can be written as

$$\begin{aligned}
\underline{bf}(t) &= \begin{bmatrix} b_{11} & b_{12} \\ b_{21} & b_{22} \end{bmatrix} \begin{bmatrix} f_1(t) \\ f_2(t) \end{bmatrix} \\
&= b_{11} \begin{bmatrix} f_1(t) \\ 0 \end{bmatrix} + b_{21} \begin{bmatrix} 0 \\ f_1(t) \end{bmatrix} + b_{12} \begin{bmatrix} f_2(t) \\ 0 \end{bmatrix} + b_{22} \begin{bmatrix} 0 \\ f_2(t) \end{bmatrix} \\
&= b_{11}\sqrt{E_1}\underline{\phi}_1(t) + b_{21}\sqrt{E_1}\underline{\phi}_2(t) + b_{12}\sqrt{E_2}\underline{\phi}_3(t) + b_{12}\sqrt{E_2}\underline{\phi}_4(t)
\end{aligned}$$

where

$$\underline{\phi}_1(t) = \frac{1}{\sqrt{E_1}} \begin{bmatrix} f_1(t) \\ 0 \end{bmatrix}, \underline{\phi}_2(t) = \frac{1}{\sqrt{E_1}} \begin{bmatrix} 0 \\ f_1(t) \end{bmatrix}, \underline{\phi}_3(t) = \frac{1}{\sqrt{E_2}} \begin{bmatrix} f_2(t) \\ 0 \end{bmatrix},$$

$$\underline{\phi}_4(t) = \frac{1}{\sqrt{E_2}} \begin{bmatrix} 0 \\ f_2(t) \end{bmatrix}$$

It is easy to verify that $\underline{\phi}_1(t), \underline{\phi}_2(t), \underline{\phi}_3(t)$, and $\underline{\phi}_4(t)$ form a set of orthonormal functions. They can be augmented to a C.O.N. set. Using this C.O.N. set, it is possible to expand $\underline{r}(t)$ and then verify that the coefficients r_i's are statistically independent random variables for $i \geq 5$, and that they are independent of the hypotheses H_1 or H_0. As for the coefficients r_1, r_2, r_3, and r_4 it can be seen that they are statistically independent of r_i's $i \geq 5$, and constitute a four-dimensional sufficient statistic.

Let $\underline{R} = (r_1, r_2, r_3, r_4)^T$. Then the logarithmic likelihood ratio can be written as

$$l_R = \underline{R}^\dagger (\underline{K}_0^{-1} - \underline{K}_1^{-1}) \underline{R} \underset{H_0}{\overset{H_1}{\gtrless}} \gamma$$

where, in this case, both $\underline{K}_0$ and $\underline{K}_1$ are 4×4 matrices and

$$\underline{K}_0 = N_0 \underline{I}, \qquad \underline{K}_1 = \underline{K}_s + \underline{K}_0 = E[\underline{X}\,\underline{X}^T] + N_0 \underline{I}$$

$$\underline{X} = (b_{11}\sqrt{E_1}, \quad b_{21}\sqrt{E_1}, \quad b_{12}\sqrt{E_2}, \quad b_{22}\sqrt{E_2}).$$

As in case I, the statistic l_R can be written as

$$l_R = \underline{Y}^\dagger \text{diagonal}\left[\frac{\mu_1}{(\mu_1 + N_0)N_0}, \frac{\mu_2}{(\mu_2 + N_0)N_0}, \frac{\mu_3}{(\mu_3 + N_0)N_0}, \frac{\mu_4}{(\mu_4 + N_0)N_0}\right] \underline{Y}$$

$$= \sum_{i=1}^{4} \frac{\mu_i}{(\mu_i + N_0)N_0} |Y_i|^2$$

where

$$\underline{Y} = \underline{T}^\dagger \underline{R} = [\underline{C}_1 \underline{C}_2 \underline{C}_3 \underline{C}_4]^\dagger \underline{R} = (Y_1, Y_2, Y_3, Y_4)^T,$$

Here, as in the previous case, μ_i's denote the eigen values and C_i's denote the corresponding eigen vectors of the $\underline{K}_s$ matrix. The optimum receiver for this case has the form given in figure 4, where $\alpha_i = \mu_i / \{(\mu_i + N_0)N_0\}, i = 1, \ldots, 4$.

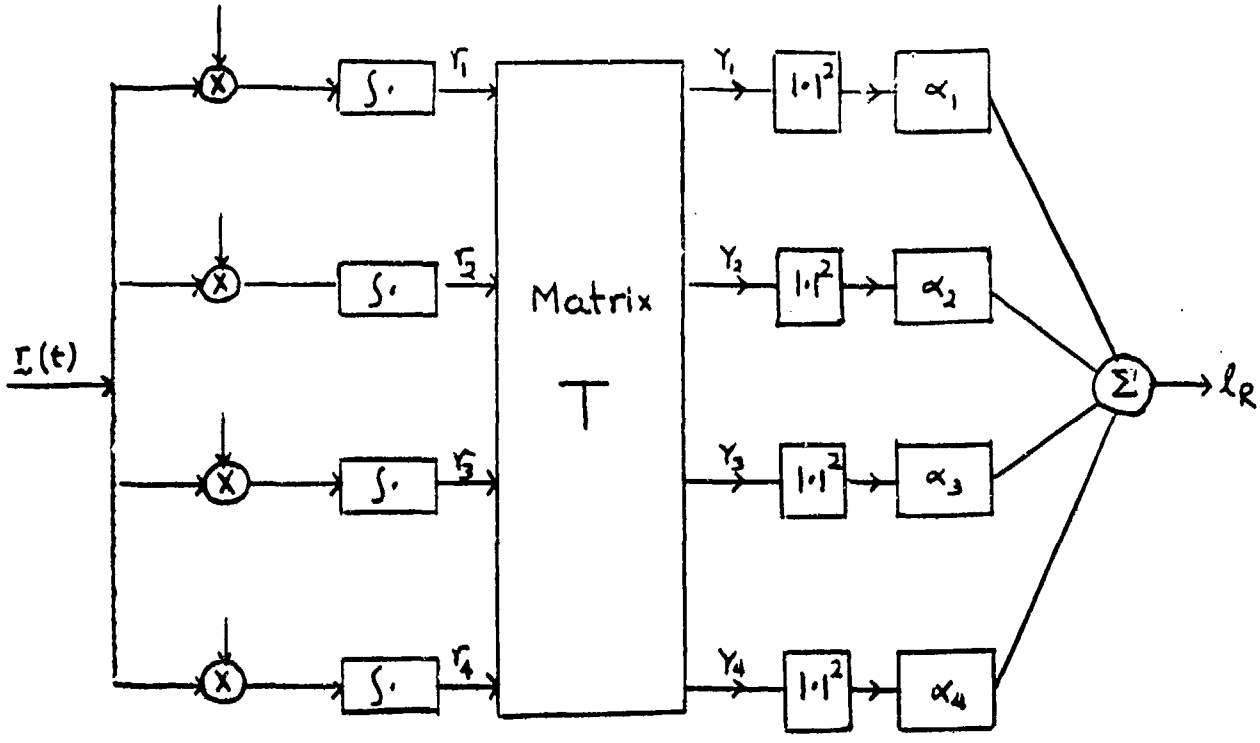

Figure 4. Optimum Receiver for the Orthonormal Envelopes

It is useful to note that unlike the identical envelope case, here we have a four dimensional sufficient statistic. Both cases give correlation receivers. As long as all statistics of the scatter matrix $\underline{b}$ and the energies of the transmitting signals are known, it is easy to derive the structure of the optimum receiver which requires solution of some matrix eigen values problem.

Knowledge gained in this case can now be employed to obtain the optimum receiver in the general situation. This case is considered below.

CASE III. The General Model.

In general the signal components in returned waveforms can be expressed as

$$\underline{b}\underline{f}(t) = b_{11}\begin{bmatrix} f_1(t) \\ 0 \end{bmatrix} + b_{21}\begin{bmatrix} 0 \\ f_1(t) \end{bmatrix} + b_{12}\begin{bmatrix} f_1(t) \\ 0 \end{bmatrix} + b_{22}\begin{bmatrix} 0 \\ f_2(t) \end{bmatrix}.$$

Whenever the additive noise is colored, a possible solution is obtained by first applying a whitening filter and then using the results known for the white noise case. We follow the above approach to solve the problem in the multi-channel model also. More specifically, let the model for slowly fluctuating point target in the presence of colored noise be given as follows:

$$\underline{r}(t) = \begin{cases} \underline{b}\underline{f}(t) + \underline{n}_c(t) + \underline{w}(t) = \underline{b}f(t) + \underline{n}(t) : H_1 \\ \underline{n}_c(t) + \underline{w}(t) = \underline{n}(t) : H_0 \end{cases}$$

Then, we can design a whitening filter $h_w(t,u)$ such that after passing through this filter, the noise $\underline{n}(t)$ will become a white noise process with a height of spectral density 1. Thus, if

$$\underline{n}_*(t) = \int \underline{h}_w(t,u)\underline{n}(u)du$$

then

$$E(\underline{n}_*(t)\underline{n}_*^\dagger(u)) = \delta(t-u)\underline{I}.$$

After passing through the whitening filter $h_w(t,u)$, the received waveform $\underline{r}(t)$ becomes $\underline{r}_*(t)$ where

$$\underline{r}_*(t) = \begin{cases} \underline{b}f_*(t) + n_*(t) : H_1 \\ n_*(t) : H_0 \end{cases}$$

and

$$f_*(t) = \int h_w(t,u)\underline{f}(u)du.$$

Results of Case III, when applied to $r_*(t)$, given above, give us the desired optimum receiver. The optimum receiver has exactly the same form as given in figure 4 except that all expressions are replaced by their starred versions which identifies that we are dealing with the filtered process. The whitening filter $h_w(t,u)$ is obtained by solving a matrix eigen value problem that

depends on the statistics of the $\underline{n}_c(t)$ process. Hence, the colored noise case can be handled only if statistics of the colored noise are known. The nature of the equation to obtain $h_w(t,u)$ remains the same as for the single- channel case.

4. CONCLUSIONS.

In this paper we have developed the construction of optimum receiver for the slowly fluctuating point target in the presence of white or colored noise. It is concluded that, in general, in the case of the n-channels model, n^2 matched filters (or correlations) are required to obtain the receiver. The matching is done with the orthogonalized signals instead of the transmitted signals. The optimum receiver computes the weighted sum of the outputs of matched filter. These weights are such that the risk in detection is minimized. We do not evaluate the performance measures of these optimum detectors. However, it follows from the distributional properties of the summands that these measures can be derived in terms of weighted sum of chi-squares. When the number of channels, n, is large these performance measures can be approximated by normal. In general, approaches discussed in [1] and [2] are applicable.

References.

[1] H. L. Van Trees. *Detection, Estimation and Modulation Theory, Part I.* John Wiley and Sons, Inc.

[2] Van Trees. *Detection, Estimation and Modulation Theory, Part III.*

[3] W. Lindsey. "Error Probabililities for Rician Coding Channel Reception of Binary and M-ary Signals." *IEEE Trans. Information Theory.* Oct., 1964.

[4] V. Vannicola, "On the Theory of Radar Polarization Processing for clutter Suppression," *Proceedings of the Workshop on Polarimetric Radar Technolgy, U. S. Army Missile Command, Redstone Arsenal, Alabama,* 25-26 June, 1980, GACIA PR-81-02.

MISSION
of
Rome Air Development Center

RADC plans and executes research, development, test and selected acquisition programs in support of Command, Control, Communications and Intelligence (C^3I) activities. Technical and engineering support within areas of competence is provided to ESD Program Offices (POs) and other ESD elements to perform effective acquisition of C^3I systems. The areas of technical competence include communications, command and control, battle management, information processing, surveillance sensors, intelligence data collection and handling, solid state sciences, electromagnetics, and propagation, and electronic, maintainability, and compatibility.